BNL 19947

DAS

DEPARTMENT of APPLIED SCIENCE

AN ANALYSIS OF STEADY-STATE AND PULSED OPERATING REGIMES FOR CONTROLLED THERMONUCLEAR REACTORS WITH VERY LARGE POWER RATINGS

John L. Usher and James R. Powell

March 1975

BROOKHAVEN NATIONAL LABORATORY
UPTON, NEW YORK 11973

INFORMAL REPORT

BNL AUI

BNL 19947

AN ANALYSIS OF STEADY-STATE AND PULSED OPERATING REGIMES FOR CONTROLLED THERMONUCLEAR REACTORS WITH VERY LARGE POWER RATINGS

John L. Usher and James R. Powell

Department of Applied Science
Brookhaven National Laboratory
Upton, New York 11973

March 1975

Work performed under the auspices of the U.S. Energy Research and Development Administration.

TABLE OF CONTENTS

ABSTRACT

Controlled thermonuclear reactors (CTR's) have been primarily considered for central station generation of electricity where maximum power ratings are typically 5000 MW (th). Multipurpose CTR's (electricity, H_2 production, process heat, etc.) can have much larger ratings and still be compatible with existing power grids. The economic advantages of operation at very high power ratings [12.5 GW(th) to 50 GW(th)] have been discussed in a previous report.[1] The purpose of the present research is to determine the operating regimes of these large CTR's. These regimes are identified and examined for cases of steady-state and pulsed operation. Several technological benefits of these large reactors are determined: 1) low maximum magnetic field strength requirements (25 to 50% less than for 5000 MW(th) reactors), 2) high $n\tau$ products (10^{15} to 10^{17} sec/cm^3) with associated high burn-up fractions (10 to 50%), 3) relatively little problem with impurity build-up, and 4) long confinement times (50 to 500 seconds). The advantages of

pulsed operation are also discussed: 1) smaller problem with impurities than in the steady-state case, 2) alleviation of any possible fueling difficulties, and 3) no problem with control of temperature in the pulsed reactor based on a simple control function model incorporating a finite delay time.

Chapter 1

INTRODUCTION

The purpose of this research is the determination of the plasma and engineering parameters which represent the operating regimes of very large CTR's. The computations are based on a circular cross section tokamak configuration. The D-T fuel cycle is used and trapped-ion confinement scaling is assumed. Two possible operating schemes are to be examined as well as two separate fueling models. The first operating mode to be examined is that of steady-state operation and based upon these results a long-pulsed operating mode will also be examined. The fueling models to be investigated are: 1) pellet fueling with beam heating and 2) beam fueling only. In the pellet-fueling case the total fuel source is the sum of pellet and beam sources, and the beam also serves to supplementally heat the plasma. In the case of beam fueling only, the beam is the sole fuel source as well as again providing supplemental heating. In the examination of the pulsed operation mode only the pellet-fueling with beam-heating case is investigated due to the need for beam control of temperature excursions.

Chapter 2 contains a development of the plasma and engineering model to be used in the calculations for all cases. The plasma and engineering parameter equations are presented and the approximations upon which they are based are discussed. A four-species plasma is considered--fuel ions, alpha particles, impurity ions (argon), and electrons are all accounted for. Loss of energetic beam and alpha particles is accounted for in terms of energy loss only. The energetics model is also presented in Chapter 2. Also presented is a beam-plasma interaction model which is included in the calculations.

Chapter 3 contains a breakdown of the various equations of Chapter 2 into terms corresponding to the steady-state and the pulsed examples to be considered. The reduction of the system of equations to a workable level is completed. A computer code is described which calculates the plasma and engineering properties for the steady-state case. A computational model is also developed for the pulsed example including a control function and a fueling procedure. The computer code which is developed to solve for the temporal values of the reactor parameters is also discussed.

Chapter 4 presents the results of the computations performed using the codes developed in Chapter 3. The absolute

values of the steady-state variables are presented as well as a discussion of the variations of the parameters with other reactor properties. A detailed analysis of two pulsed examples is performed and these results are presented and discussed. The most significant portion of the research is contained in Section III of Chapter 4. The basic conclusions drawn from the results of the first two sections of Chapter 4 are presented in Section III.

As an additional aid to the reader a separate section of tables listing the complete results calculated herein is contained in the Appendix. A nomenclature explaining the terms used throughout this report precedes the Appendix.

Chapter 2

PLASMA AND ENGINEERING MODEL

In order to establish a model for these investigations it is first essential to decide what approximations are necessary to reduce the system of variables to a workable level and, as well, to verify that these approximations are valid ones. Two types of variables are to be examined in this report--1) plasma properties: temperatures, densities, source strengths and energies, confinement times, and energy properties; and 2) engineering parameters: magnetic field strengths, plasma current, physical reactor dimensions, first wall loading and thermal power levels. There are also other properties involved which interconnect these sets of variables, e.g., plasma beta and safety factor.

The first set of equations comprise the plasma model. These equations are simply plasma particle and energy conservation equations. The first conservation equation is for the fuel ions which are assumed to be a 50% deuterium-50% tritium mixture:

$$\frac{dn_f}{dt} = S_t - \frac{n_f}{\tau} - \frac{n_f^2}{2} \langle \sigma v \rangle \quad , \qquad (1)$$

where S_t is the total external source rate of fuel ions, τ is the particle confinement time and $\langle\sigma v\rangle$ is the velocity-averaged reaction probability per unit time. Alpha particles and neutrons are created in the D-T fusion reactions; the neutrons are ignored in the plasma calculations because they escape so rapidly from the plasma region. The alpha particle conservation is represented in the following manner:

$$\frac{dn_\alpha}{dt} = \frac{n_f^2}{4}\langle\sigma v\rangle - \frac{n_\alpha}{\tau} + S_b f_{TCT} \quad , \tag{2}$$

where S_b represents the beam source strength and f_{TCT} is the probability per beam particle per unit time of undergoing a beam-plasma fusion encounter while slowing down. The electron density is represented by utilizing the charge neutrality condition:

$$n_e = n_f + 2n_\alpha + Z_I n_I \quad , \tag{3}$$

where Z_I and n_I are the electronic charge and species density, respectively, of the impurity ions. The respresentation of the impurity ion density will be outlined in the next chapter. The next step is to develop energy conservation equations for the plasma. It is at this point where the first really significant approximations come into play. It is assumed that all ion species relax to the ion

temperature so rapidly that particle losses during slowing-down may be neglected, however, since the average energy of a slowing particle is so much larger than the average energy of a thermalized particle, energy losses while slowing down are not neglected. These assumptions result in the following equations for ion and electron energy densities:

$$\frac{d}{dt}\frac{3}{2}n_iT_i = \frac{n_f^2}{4}\langle\sigma v\rangle Q_\alpha U_{\alpha i} + S_b V_b U_{bi} + S_b f_{TCT} Q_\alpha U_{\alpha i} + W_{ei} - \frac{3}{2}\frac{n_iT_i}{\tau_E} - \frac{n_b\bar{E}_b}{\tau_E}U_{bi} - \frac{n_\alpha}{\tau_E}\frac{\tau_{SD}^\alpha}{\tau}\bar{E}_\alpha U_{\alpha i} \quad (4)$$

and

$$\frac{d}{dt}\frac{3}{2}n_eT_e = \frac{n_f^2}{4}\langle\sigma v\rangle Q_\alpha(1-U_{\alpha i}) + S_b V_b(1-U_{\alpha i}) + S_b f_{TCT} Q_\alpha(1-U_{\alpha i}) - W_{ei} - \frac{3}{2}\frac{n_eT_e}{\tau_E} - P_b - P_s \quad (5)$$
$$\frac{-n_b\bar{E}_b}{\tau_E}(1-U_{bi}) \quad \frac{-n_\alpha}{\tau_E}\frac{\tau_{SD}^\alpha}{\tau}\bar{E}_\alpha(1-U_{\alpha i})$$

$U_{\alpha i}$ and U_{bi} represent the fractions of alpha particle and beam energies transferred to the ion species during slowing down, and W_{ei} represents the energy transfer rate between the electrons and ions including the ions which have now thermalized. The S_bV_b term accounts for supplemental heating; V_b is the beam energy. τ_E is the energy confinement time and f_{TCT} again represents the contribution to the

energy balance from beam-plasma fusion reactions. P_b and P_s represent energy loss rates due to bremsstrahlung and synchrotron radiation, respectively. $\bar{E}_b$ and $\bar{E}_\alpha$ are average energies of beam particles and slowing-down alpha particles, respectively; τ_{SD}^{α} is the slowing-down time for alpha particles. The final term in the representation of the plasma model is the poloidal plasma beta:

$$\beta_\theta = \frac{8\pi}{B_p^2} \left(n_i T_i + n_e T_e + \frac{2}{3} n_\alpha \frac{\tau_{SD}^{\alpha}}{\tau} \bar{E}_\alpha + \frac{2}{3} n_b \bar{E}_b\right) \quad . \qquad (6)$$

B_p is the poloidal magnetic field strength. This quantity represents the ratio of total plasma kinetic pressure to poloidal magnetic pressure. The plasma beta and the synchrotron radiation term both contain explicit values of magnetic field strengths; in this manner these equations tend to couple the plasma parameters to the engineering properties of the reactor model.

The first two engineering property equations to be discussed also couple the plasma properties to the engineering parameters. The expression for total reactor thermal power and total first wall loading are given by

$$P_t = \frac{n_f^2}{4} \langle \sigma v \rangle E_{fus} 2\pi^2 R a^2 \quad , \qquad (7)$$

and

$$p_w = \frac{n_f^2 \langle \sigma v \rangle}{4} E_{fus} \frac{1}{2} \frac{a^2}{r_w} \quad . \tag{8}$$

E_{fus} represents the total energy released in a fusion reaction including any blanket reactions. Figure 1 illustrates the reactor geometry utilized in these calculations. R and a are the major and minor radii of the plasma, respectively, and r_w is the first wall radius. The effect of TCT reactions has been ignored in the calculations of power factors although Eqs. (7) and (8) may be modified to include these effects simply by increasing E_{fus}. Another useful engineering parameter relates the toroidal and poloidal magnetic field components; this relationship defines the plasma safety factor,

$$q = \frac{a}{R} \frac{B_t}{B_p} \quad . \tag{9}$$

Finally, the plasma current is given by the following relationship:

$$I = c\, B_p\, a \quad , \tag{10}$$

where c is a unit constant. This set of ten non-linear equations completes the initial formulation of the model used in the calculations which follow.

It is now necessary to break down further the many terms involving radiation, energy properties and confinement times

in order to completely specify the final model to be used in the calculations. Bremsstrahlung and synchrotron radiation are modeled by simple expressions:[2,3]

$$P_b = b\, n_e^2\, Z_{eff}\, T_e^{1/2} \quad , \tag{11}$$

and

$$P_s = k_s\, n_e^{1/2}\, T_e^2\, B_t^{5/2} \left(\frac{1-r_f}{R}\right)^{1/2} \quad , \tag{12}$$

where Z_{eff} is the effective plasma charge and r_f is the reflection coefficient of the system for synchrotron radiation. b and k_s are unit constants for bremsstrahlung and synchrotron radiation, respectively. Recombination and line radiation have been neglected in these calculations. The slowing-down and energy partition model to be utilized is one reported by Houlberg.[4] The two most important terms in the energy calculations are the energy partition between electrons and ions, represented by U_{Ti} and the average energy of a slowing-down test particle, $\bar{E}_T$:

$$U_{Ti} = \frac{1}{3}\frac{E_{crit}^T}{E_{To}}\left\{ln\left[\frac{E_{crit}^T - E_{crit}^{T\,1/2} E_{To}^{1/2} + E_{To}}{E_{crit}^T + 2E_{crit}^{T\,1/2} E_{To}^{1/2} + E_{To}}\right]\right.$$

$$\left. + 2\sqrt{3}\ \tan^{-1}\left(\frac{2E_{To}^{1/2} - E_{crit}^{T\,1/2}}{\sqrt{3}\ E_{crit}^{T\,1/2}}\right) + \frac{\pi}{\sqrt{3}}\right\} \quad , \tag{13}$$

and

$$\overline{E}_T = \frac{3}{2} \frac{(E_{To} - T_i)(1 - U_{Ti})}{\ell n \left[1 + \left(\frac{E_{To}}{E^T_{crit}} \right)^{3/2} \right]} \quad , \tag{14}$$

where T is a subscript identifying properties to be associated with the test ion. E_{To} is the initial energy of the test particle. E^T_{crit} is a term known as the critical energy, which represents the point in the energy history of the test particle at which energy transfer rates to plasma ions and electrons are equal:

$$E^T_{crit} = 14.8\, A_T T_e \left(\frac{1}{n_e \ell n \Lambda_e} \left[\sum_i \frac{Z_i^2 n_i \ell n\, \Lambda_i}{A_i} \right] \right)^{2/3} \quad , \tag{15}$$

where the A_i are the atomic mass numbers of the respective ion species. The $\ell n\, \Lambda$ terms represent the coulomb logarithms of the various plasma species:

$$\Lambda_e^2 = c_e T_e \left[\frac{n_e}{T_e} + \sum_i \frac{Z_i^2\, n_i}{T_i} \right]^{-1} \quad , \tag{16}$$

and

$$\Lambda_i^2 = c_i \frac{E_T A_T A_i^2}{(A_T + A_i)^2} \left[\frac{n_e}{T_e} + \sum_i \frac{Z_i^2 n_i}{T_i} \right]^{-1} \quad , \tag{17}$$

where again the T subscripts refer to the test particle properties and the i subscripts refer to the plasma ion

species. The c-factors are unit constants. Another important property associated with the plasma energetics is the slowing-down time of test particles,

$$\tau_{SD}^{T} = \tau_{T}^{\prime} \ln \frac{E_{To}^{3/2} + E_{crit}^{T\ 3/2}}{T_i^{3/2} + E_{crit}^{T\ 3/2}} \quad , \tag{18}$$

where T_i represents the ion temperature, which is assumed to be the final energy of the test particle, and

$$\frac{1}{\tau_T^{\prime}} = c \frac{Z_T^2}{A_T} \frac{n_e \ln \Lambda_e}{T_e^{3/2}} \tag{19}$$

is a numerical factor necessary to the calculation of slowing-down time. Z_T is the electronic charge of the test particle. The lone remaining term in the energetics model is the energy transfer rate between electrons and ions,

$$W_{ei} = c \frac{n_e n_i (T_e - T_i)}{T_e^{3/2}} \quad . \tag{20}$$

One remaining factor in the completion of the reactor model is the establishment of particle and energy confinement approximations. For purposes of this report trapped-ion scaling[5,6] is presumed. The expression defining this confinement model follows:

$$\tau = c_\tau K \frac{I^4 b_t^2 \beta_{pe}^2 Z_{eff} A'^{5/2}}{n_e T_e^{11/2}} \left(1 + \frac{T_e}{T_i}\right)^2 , \qquad (21)$$

where A' is the reduced aspect ratio, A/3, and b_t is the reduced toroidal magnetic field strength, $B_t/50$ kilogauss. c_τ is a factor determining what fraction of trapped-ion scaling is actually utilized in the calculations. I is the plasma current and β_{pe} is the poloidal electron beta:

$$\beta_{pe} = \frac{8\pi}{B_p^2} n_e T_e . \qquad (22)$$

In using the trapped-ion scaling approximation, it is inherently assumed that the particle and energy confinement times are equal. There is some numerical discrepancy involved in using the value of τ from reference 6, page 41. On repeating the calculations necessary to express τ in this form, a numerical factor of 0.2 was found to be missing in the expression calculated by Dean et al.[6] This factor of 0.2 is included in the calculations which follow.

A few words are also necessary here concerning the model to be used for the beam-plasma fusion interactions. For the purposes of these calculations the simple model of Dawson et al.[7] is sufficient. F is defined by Dawson as the fusion energy gain divided by the beam particle energy

on a per-particle basis. The quantity f_{TCT} is defined by the following relationship:

$$F = f_{TCT} \frac{E_{fus}}{V_b} \quad , \tag{23}$$

where E_{fus} is the total energy released per fusion reaction (22.4 MeV in Dawson's calculations) and V_b is the beam particle energy. f_{TCT} represents the probability that a beam particle will undergo a fusion reaction with a plasma ion while slowing down. The F-values from the Dawson reference for 10 keV electron temperature are used in the calculations which follow, with the following alteration: Dawson assumes a deuterium beam slowing down in a tritium plasma, while the model used here assumes a 50-50 D-T mixture in both beam and plasma. Therefore, ignoring DD and TT beam-plasma interactions, the f_{TCT} value will be one-half of the value calculated directly from the Dawson data.

This essentially concludes the derivation of the plasma and engineering system model which is to be utilized in the following computations. The subject of the next chapter in the development of a computational model based on the determinations of this chapter. The validity of this model and the approximations comprising it will be discussed.

Chapter 3

COMPUTATIONAL MODEL

Once the equations and relationships which comprise the reactor model have been established, the problem solving proceeds to the next phase--establishing a workable computational scheme for solution. First, the problem of determining the variables which specify the steady-state reactor operating regime will be examined. Once these steady-state parameters have been calculated, they will be utilized in the examination of a pulsed operation mode example. The previous chapter indicates a set of 23 non-linear equations which comprise the reactor model. In order to expect realistically to solve for reactor parameters this set of equations must be reduced to a workable level before attempting computer solution. Certain restrictions imposed upon some of the problem variables aid in the reduction of the system of equations. These restrictions will be explained as they apply in the discussion which follows.

In order to establish the parameters which specify the steady-state operating regime, one particular value is specified initially for each of the following variables: P_t, p_w, q, β_θ, and c_τ. Values for T_i and E_{fus} are also specified for

the reactor model. In addition to these restrictions, the value of the plasma aspect ratio,

$$A = R/a \quad , \tag{24}$$

is also specified. The final restriction necessary to begin initial computation is the following:

$$r_w = a + 1.0 \text{ m} \quad , \tag{25}$$

which specifies the first-wall radius in terms of the plasma radius, a. The equations for total power,

$$P_t = \frac{n_f^2}{4} \langle \sigma v \rangle \, E_{fus} \, 2\pi^2 \, Ra^2 \quad , \tag{26}$$

and wall loading,

$$p_w = \frac{n_f^2}{4} \langle \sigma v \rangle \, E_{fus} \, \frac{1}{2} \frac{a^2}{r_w} \quad , \tag{27}$$

together with the aspect ratio and the expression for r_w are utilized to determine R, the major plasma radius; a, r_w, and n_f, the fuel ion density, required for each total power level and each wall loading. These values are presented in the discussion of the results in the next chapter. Note that these parameters (R, a, r_w, and n_f) are independent of all plasma parameters except P_t, p_w, A, T_i, and E_{fus}. The assumption has been made that the TCT component of fusion power does not contribute significantly to the expression for P_t or p_w.

The next step in the reduction of the system of equations is to establish steady-state versions of Equations (1), (2), (4), and (5) by setting the temporal derivatives equal to zero:

$$S_t = \frac{n_f}{\tau} + \frac{n_f^2}{2} \langle \sigma v \rangle \quad , \tag{28}$$

$$n_\alpha = \tau \left(\frac{n_f^2}{4} \langle \sigma v \rangle + S_b \, f_{TCT} \right) \quad , \tag{29}$$

$$\frac{3}{2} \frac{n_i T_i}{\tau} = \frac{n_f^2}{4} \langle \sigma v \rangle \, Q_\alpha \, U_{\alpha i} + S_b \, V_b \, U_{bi}$$

$$+ S_b \, f_{TCT} \, Q_\alpha \, U_{\alpha i} + W_{ei} - \frac{n_b \bar{E}_b}{\tau} \, U_{bi} - n_\alpha \frac{\tau_{SD}^\alpha}{\tau^2} \bar{E}_\alpha \, U_{\alpha i}, \tag{30}$$

$$\frac{3}{2} \frac{n_e T_e}{\tau} = \frac{n_f^2}{4} \langle \sigma v \rangle \, Q_\alpha \, (1-U_{\alpha i}) + S_b \, V_b \, (1-U_{bi})$$

$$+ S_b \, f_{TCT} \, Q_\alpha \, (1-U_{\alpha i}) - W_{ei} - P_b - P_s \quad . \tag{31}$$

$$\frac{-n_b \bar{E}_b}{\tau} (1-U_{bi}) - n_\alpha \frac{\tau_{SD}^\alpha}{\tau^2} \bar{E}_\alpha \, (1 - U_{\alpha i})$$

For the case of pellet fueling with beam heating $S_t = S + S_b$, where S_b is the beam source rate (energetic injection) and S is the pellet source rate (non-energetic), but for the case of beam fueling, $S_t = S_b$. It can then be seen that in the pellet case S and n_α may be expressed as functions of τ and S_b; while in the beam-fueling case, S_b and n_α may be expressed as functions of τ only. All this assumes preknowledge of n_f and $\langle \sigma v \rangle$, which is a function of T_i only. The next step

in the process is to utilize the conditions of plasma neutrality,

$$n_e = n_f + 2n_\alpha + Z_I\, n_I \quad , \tag{32}$$

and the ratio of bremsstrahlung radiation to alpha particle heating,

$$P_b = 1.2\, \frac{n_f^2}{4}\, \langle \sigma v \rangle\, Q_\alpha \quad , \tag{33}$$

together with the previously given relationship for P_b (Equation (11)) to calculate expressions for n_e and n_I. The calculations assume that there is a specified impurity present within the plasma with a known electronic charge, e.g., Z_I = 18 for argon, which is considered here. Combining Equations (11), (32), and (33) produces values for n_e and n_I which are functions of S, S_b, τ, T_e (and n_f and $\langle \sigma v \rangle$) which again may be related specifically back to being functions of τ, S_b, and T_e only.

In order to relate the above discussed plasma parameters to the engineering properties of the model, use is made of the relationship for plasma beta,

$$\beta_\theta = \frac{8\pi}{B_p^2} \left(n_i T_i + n_e T_e + \frac{2}{3}\, n_b \bar{E}_b + \frac{2}{3}\, n_\alpha\, \frac{\tau_{SD}^{\alpha}}{\tau}\, \bar{E}_\alpha \right) \quad , \tag{34}$$

and Equation (12) for synchrotron radiation. In order to determine magnetic field strength from Equation (34), it is first

necessary to examine the energetics model for the plasma. If a simple approximation is made in the calculation of the argument of the coulomb logarithm,

$$\Lambda_i^2 = c_i \frac{E_T A_T A_i^2}{(A_T+A_i)^2}\left[\frac{n_e}{T_e} + \sum_i \frac{Z_i^2 n_i}{T_i}\right]^{-1} , \qquad (35)$$

namely by substituting a value equal to $E_{To}/2$ into the calculation replacing E_T, the expressions become quite simplified. Actually in the calculations which follow, a value of $V_b/2$ is substituted for the beam particle energy, while a value of $Q_\alpha/3$ was found to be more accurate for the alpha particle energy. This approximation is quite valid in view of the fact that Λ_i^2 enters the calculations only as $\ell n\, \Lambda_i$ in certain expressions. This simplification eliminates the need for any iterative calculations within the energetics model itself. All the properties associated with the energetics model (Equations (13) through (20)) may now be expressed as functions of the plasma independent variables τ, S_b, T_e, and V_b, the beam energy. The expression for β_θ may now be utilized since the number of alpha particles and beam ions in the process of slowing down may be calculated via knowledge of the associated slowing-down times:

$$n_b = S_b \tau_{SD}^b , \qquad (36a)$$

and

$$n'_\alpha = \frac{n_\alpha}{\tau}\,\tau^\alpha_{SD} \quad . \tag{36b}$$

B_p, poloidal magnetic field strength, may now be calculated from Equation (34) and again related to the independent plasma variables, τ, S_b, T_e, and V_b. Definitions of the safety factor, q, and plasma current, I, may now be used to calculate B_t, toroidal magnetic field strength, and I. The reactor model is now essentially complete and all reactor plasma and engineering properties may be calculated from the basic set of independent plasma parameters: τ, S_b, T_e, and V_b.

In summary of this section, three equations are essentially left to be solved for three plasma independent variables in each of the two fueling models to be discussed. The first two of these, Equations (30) and (31), were derived from the temporal energy conservation equations for the plasma. The third equation is the relationship used to represent the type of diffusion model (trapped-ion scaling) assumed to be present in the plasma:

$$\tau = c_\tau K \frac{I^4 b_t^2 \beta_{pe}^2 Z_{eff} A'^{5/2}}{n_e T_e^{11/2}} \left(1+\frac{T_e}{T_i}\right)^2 \quad . \tag{37}$$

Specifically, for the case of pellet fueling, the independent variables are τ, S_b, and T_e. V_b is given as an initial restriction of the model and is varied parametrically. For the

case of beam fueling, the independent variables are τ, T_e, and V_b. In this case S_b is determined via Equation (28) as a function of τ and the given parameters. Essentially the problem is then reduced to a case of three variable unknowns which are to be determined from a set of three non-linear algebraic equations.

In addition to the models already discussed, one further case will be considered, and that is the case of fixed burn-up. The fractional burn-up is defined as the ratio of the plasma fuel burned in fusion reactions to the total fuel source rate:

$$f_b = \frac{\frac{n_f^2}{2}\langle\sigma v\rangle}{\frac{n_f}{\tau} + \frac{n_f^2}{2}\langle\sigma v\rangle} \quad , \tag{38}$$

which reduces to

$$f_b = \frac{1}{1 + \frac{2}{\langle\sigma v\rangle}\frac{1}{n_f\tau}} \quad . \tag{39}$$

It can readily be seen that the effect of fixing the fractional burn-up is equivalent to fixing the confinement time since fuel density and fusion reactivity are already specified. τ is no longer a variable for the purposes of computation and is replaced as a variable by c_τ, the coefficient

of trapped-ion scaling. Calculations for the two fueling models are still performed as before with only the simple variable change from τ to c_τ.

There are various numerical methods available for the solution of a set of simultaneous non-linear equations. One of the most basic of these is a successive-substitution method whereby better and better approximations to the actual solution vector may be found by repeated substitution of values of τ, T_e, and S_b or V_b into Equations (30), (31), and (37). New values for the variables may be calculated directly from the equations since they may all be expressed in the form

$$X_i = F(X_i, X_j, X_k) \quad , \tag{40}$$

where the X's are the variables to be determined. This method is somewhat restrictive in that it requires that the initial approximation to the solution vector lie within a specific region known as the "region of convergence"[8] in order for the method to generate the correct solution. For this reason this method was rejected here in favor of a somewhat less restrictive least-squares minimization technique which is described below. Basically, the least-squares program used here searches for the values of the plasma properties which will minimize the quantity

$$Q = \sum_i (z_i - \tilde{z}_i)^2 \tag{41}$$

where Z_i is the known value of a fixed plasma parameter and $\tilde{Z}_i$ is the value of that parameter generated from one of the three equations in question. In order to make sure that the equations were all given equal statistical weight in these calculations, it was decided to make all the Z_i equal. For the purposes of this problem the Z_i chosen was n_f, the fuel ion density, which is specified totally by R, a, P_t, p_w, and T_i as mentioned previously. n_f is chosen because it is explicitly contained in each of Equations (30), (31), and (37). The specific quantity to be minimized in this research is then

$$Q = \sum_{i=1}^{3} (n_f - \tilde{n}_{fi})^2 , \qquad (42)$$

where the $\tilde{n}_{fi}$ are generated from the three equations. The specific program utilized in these calculations is not reproduced in this report. There are many versions of least-squares programs commonly used in curve-fitting problems which are readily adaptable to research of this nature. The remainder of the plasma and engineering parameters which specify the operating regime are determined directly from the three plasma variables which are the output of the program.

Once the steady-state regime has been completely identified for these large CTR's, the second of the operating regimes--pulsed operation--is now examined. A very simple model is chosen to illustrate pulsed operation. Since a complete

set of reactor parameters is generated by the steady-state model, these parameters will be utilized as initial conditions in the pulsed cycle. The basic difference in the pulsed and steady-state models is in the fueling mechanism: steady-state assumes continual fueling while in the pulsed case, fuel is injected only at the initiation of the cycle. Owing to the fact that the initial fueling amount is a large fraction (typically 25% or greater) of the steady-state fuel ion density, the density perturbation will cause the onset of the thermal instability described by Ohta et al.[9] at the low operating temperature. For this reason it will be necessary to control the reactor in order to diminish the thermal excursions. Feedback control of the beam source strength is one possible means of control and necessitates the use of the pellet-fueling with beam-heating model. Now that the general requirements for the model have been outlined, the next step is the establishment of the particulars of the computational model.

Most of the components of the pulsed model have been outlined in the explanation of the steady-state model. There are two essential differences: 1) Equations (1), (2), (4), (5), and

$$\frac{dn_I}{dt} = -\frac{n_I}{\tau} \tag{43}$$

are utilized since the pulsed case, i.e., time dependent, is now being analyzed and 2) S_b is now a time and temperature dependent property which is used to control plasma thermal excursions. The second of the above conditions necessitates the rewriting of Equations (4) and (5):

$$\frac{d}{dt}\frac{3}{2} n_i T_i = \frac{n_f^2}{4} \langle\sigma v\rangle Q_\alpha U_{\alpha i} + S_b(t,T)[V_b U_{bi} + f_{TCT} Q_\alpha U_{\alpha i}] + W_{ei} - \frac{3}{2}\frac{n_i T_i}{\tau} - \frac{n_b \bar{E}_b}{\tau} U_{bi} - n_\alpha \frac{\tau_{SD}^\alpha}{\tau^2} \bar{E}_\alpha U_{\alpha i}, \tag{44}$$

and

$$\frac{d}{dt}\frac{3}{2} n_e T_e = \frac{n_f^2}{4} \langle\sigma v\rangle Q_\alpha (1-U_{\alpha i}) + S_b(t,T)[V_b(1-U_{bi}) + f_{TCT} Q_\alpha (1-U_{\alpha i})] - W_{ei} - \frac{3}{2}\frac{n_e T_e}{\tau} - P_b - P_s , \tag{45}$$

$$\frac{-n_b \bar{E}_b}{\tau} (1-U_{bi}) \quad \frac{-n_\alpha \tau_{SD}^\alpha}{\tau^2} \bar{E}_\alpha (1-U_{\alpha i})$$

where

$$S_b(t,T) = S_{bo} + S'(t,T) \quad . \tag{46}$$

S_{bo} is the steady-state value of the beam source strength and S' is the control function which depends on both departures from design operating temperature and the delay time associated with the acquisition of this information in the feedback circuit. The model chosen for S' was first used by Ohta et al., who demonstrated its effectiveness in thermal instability control:

$$S' = \alpha\, n_{fo}\, \frac{T(t-\Delta t) - T_o}{T_o} \quad , \tag{47}$$

where α is a numerical constant, n_{fo} is the steady-state fuel ion density, $T(t-\Delta t)$ is the operating temperature at time $t-\Delta t$, Δt is the delay time, and T_o is the design operating temperature. Note that T and T_o may refer to either electron or ion temperature values. In performing a parametric study of the effectiveness of this control Δt is varied. The remainder of the computational model consists of Equations (3) and (6) through (23) where now all of the plasma properties are time dependent.

Essentially, the computer solution of this problem involves specifically a numerical approximation to the solution of the system of non-linear differential Equations (1), (2), (43), (44), and (45). There are numerous techniques available to solve these types of systems, and the one chosen here is a fourth-order predictor-corrector technique known as Hamming's method.[8] Basically the procedure consists of the following steps. First, the initial conditions are used to establish approximations to the densities and temperatures at three equally spaced points in time, the derivatives of these quantities are readily calculable from the five-equation system. The initial three points are calculated usually

via use of the Runge-Kutta method. Hamming's method is then applied to predict the fifth point in time using the Milne predictor:

$$y^{o}_{j,4} = y_{j,o} + \frac{4}{3} h(2 f_{j,3} - f_{j,2} + 2 f_{j,1}) \quad , \qquad (48)$$

where the y_j represent the densities and temperatures which are being solved for and the f_j are the temporal derivatives of these quantities. The predicted solutions are modified using estimates of the local truncation errors:

$$y^{*}_{j,4} = y^{o}_{j,4} + \frac{112}{9} e_{j,3} \quad , \qquad (49)$$

where $e_{j,3}$ represents the truncation error estimated at the previous point in time,

$$e_{j,3} = \frac{9}{121} (y'_{j,3} - y^{o}_{j,3}) \quad . \qquad (50)$$

y' is the estimate of the solution calculated using the corrector portion of Hamming's method,

$$y'_{j,4} = \frac{1}{8} [9 y_{j,3} - y_{j,1} + 3h(f^{*}_{j,4} + 2f_{j,3} - f_{j,2})] \quad , \qquad (51)$$

where f^{*}_{j} is calculated using the values of y^{*}_{j} which were determined in Equation (49). Points y_5, etc. may then be calculated using the previous approximation determined in the above manner. The computer code used in these calculations is essentially that available on pp. 400 of the reference.[8]

Only two features remain to be modeled to complete the

description of the computational procedure: 1) the fueling model and 2) the incorporation of the delay time. Fueling is modeled as a delta function assuming injection at t=0. The initial plasma fuel ion density is then given as

$$n_f = n_{fo} + C_p\, t_p\, S \quad . \tag{52}$$

n_{fo} is the steady-state fuel density, t_p is the pulse length, S is the steady-state pellet fuel injection rate and C_p is a numerical factor which is varied to determine the average thermal power output over the cycle time. The desired value of C_p is calculated iteratively over a series of runs. Use of this given value for n_f affects the values of the other plasma properties and they are automatically adjusted by the program. The question of delay time is a rather simple one: values of either T_e or T_i are stored at each time step and then the program will call on a particular value of T for use in Equation (47) dependent upon the delay time desired. This completes the description of the computational models used in the calculations and leads to a presentation and discussion of results thereby calculated.

Chapter 4

REACTOR REGIMES

Using the computational procedures outlined in the previous chapter, the operating regimes of the large CTR's under consideration are determined. As mentioned previously, the initial step in the reduction of the system of non-linear equations developed in Chapter 2 is the establishment of a set of restrictive conditions on certain of the plasma variables, some of which are then to be varied parametrically. These restrictive conditions are enumerated in Table 1. All of these values, with the exception of the beam energies, apply for both fueling models. As mentioned previously, when considering the fixed burn-up case, the values for c_τ given in Table 1 do not apply due to the fact that c_τ replaces τ as a variable in the calculations. All other restrictions apply to the fixed burn-up case.

I. Steady-State Results

The initial values to be determined following the procedure of Chapter 3 are the torus dimensions and the plasma fuel density. These values are listed in Table 2. Fuel densities vary from 0.3 to 2.0 x 10^{14} ions/cm^3 while plasma major and minor radii vary from 10 to 56 meters and from 4

to 21 meters, respectively. Fuel density increases with larger wall loadings but decreases as total reactor power levels increase. Physical reactor dimensions decrease with rising wall loads but become larger as power levels are increased. These parameters are all determined independent of plasma β, q, or fueling model and apply to each of the various cases which follow.

The results of the parameter survey for the pellet-fueling with beam-heating model are listed in Tables A1 through A12 in the appendix. The separate tables each represent the results found utilizing different values for wall loading and beam energy. In each table values are listed according to power level, plasma q, and poloidal beta. In order to further facilitate data interpretation, values of total plasma beta;

$$\beta = \frac{8\pi}{B_t^2}\left(n_i T_i + n_e T_e + \frac{2}{3} n_b \bar{E}_b + \frac{2}{3} n_\alpha \frac{\tau_{SD}^{\alpha}}{\tau} \bar{E}_\alpha\right) , \qquad (53)$$

are listed in Table 3 as functions of q and β_θ according to the additional relationship,

$$\beta = \frac{\beta_\theta}{q^2 A^2} . \qquad (54)$$

Results found do not cover the full range of input variables indicated in Table 1. For cases of too-small confinement

time, insufficient energy is retained in the plasma to permit adequate heating to maintain 10 keV ion temperature. For the case of too-long confinement time either too much energy is retained in the plasma (requiring a negative beam strength) or alpha particle accumulation causes bremsstrahlung radiation to become too large (requiring negative impurity concentration). Almost all of the results for the pellet-fueling with beam-heating model fall into the numerical ranges indicated below. The species densities are all related to the fuel ion densities given in Table 2: the electron density varies from 1.2 to 2.0 times fuel ion density while alpha particle density is 15 to 40% of fuel density and impurity (argon) density is typically 1 to 2% or less of the steady-state fuel concentration. Confinement times range largely between 50 and 500 seconds with corresponding fractional burn-ups of 10 to 50%. Pellet and beam source strengths are typically 10^{11} to 4 x 10^{12} ions/cm^3/second. Plasma current ranges from 30 to 70 megamperes. Magnetic field strengths are strongly dependent upon wall loading and their variations may be illustrated by utilizing the maximum magnetic field strength, B_{max}, which is the maximum value of the toroidal B-field present at the magnetic superconductor:

$$B_{max} = B_t \frac{R}{R-(a+3)} , \qquad (55)$$

with the radii given in meters. B_{max} ranges from 30 to 80 kilogauss for 1.0 MW/m^2 wall load; from 50 to 130 kG for 3.0 MW/m^2 and from 100 to 225 kG for 6.0 MW/m^2. This paragraph summarized the absolute values of the variations found in the pellet-fueling with beam-heating case.

The second interesting facet of these steady-state results is their variation as a function of the other plasma and engineering parameters. In the discussion which follows it is assumed that when considering the variations mentioned as a function of one particular property, the other parameters are held constant. Once again for the case of pellet-fueling with beam-heating, the variations of plasma and engineering variables are summarized below. The first effect to be considered is that of reactor thermal power rating. As the rating increases, electron temperature increases slightly, while alpha particle concentration, fractional burn-up and confinement time each increase markedly. This increase promotes a decrease in both electron and impurity densities. Pellet, beam and total source strengths all decrease as the power rating rises. As for the engineering properties, plasma current increases and, significantly, magnetic field strengths

decrease with increasing power level. The effect of increasing wall loading is to raise slightly the electron temperature while electron, impurity, and alpha particle densities all increase more markedly. Higher wall loadings decrease confinement times but increase fractional burn-ups due to the increased fuel density values. The source strength terms are all increased with larger wall loads, as are magnetic field requirements, while plasma current is decreased.

Certain of the internal plasma parameters also have marked effects on the remaining plasma and engineering properties. The effect of increasing plasma beta is to decrease electron temperature and density, along with alpha particle concentrations, confinement times, and fractional burn-ups. Impurity density is increased with larger plasma beta. Source strength values are all raised by increasing beta, while plasma current and magnetic field strengths are lowered. The effect of plasma safety factor, q, is exactly the opposite of plasma beta. Increasing q raises electron temperature and density, alpha particle concentration, confinement time, and fractional burn-up. Impurity concentration is lowered as q increases. Source strengths are lowered by increased q, and plasma current and magnetic field strengths are elevated. Increasing

c_τ raises electron temperature and density, alpha particle density and fractional burn-up while lowering impurity concentration. The source strengths are each decreased by higher c_τ values, and plasma current and field strengths rise with higher c_τ. The effect of injection energy is essentially negligible except when considering source strengths. Increasing beam energy decreases the beam source strength while increasing the pellet source rate; the total source rate increases slightly with higher beam energy. This essentially completes the qualitiative summary of variations of reactor properties in the pellet-fueling with beam-heating model.

Plotted summaries of some of the results are presented in Figures 2 through 9 for the case of pellet-fueling with beam heating assuming a value of c_τ equal to 0.1. Figures 2 and 3 present the variation of the confinement time as a function of reactor power level. Figure 2 illustrates the variation of τ with plasma beta and Figure 3 shows the variation of τ with first wall loading. Figures 4 and 5 illustrate the variation of the fractional burn-up; again, plasma beta and wall loading effects are illustrated parametrically. Figures 6 and 7 show the variations of the toroidal magnetic field strength while Figures 8 and 9 illustrate the variation of the maximum B-field strength. Figures 6 and 8 indicate the magnetic field

dependences on beta, and Figures 7 and 9 show the dramatic variation of B-field strength with first wall loading.

Tables A13, A14, and A15 contain the results of the steady-state calculations for the beam-fueling model. In these tables there is only one value for source strength corresponding to the beam source, and in addition V_b is now entered as a system variable rather than as an initial restriction. The range of parameters is very similar to that discussed for the pellet-fueling case. The variation of V_b covers the range from 50 to 250 keV in most cases. In addition to the restrictions imposed on the operating regime by too-short or too-long confinement times as in the pellet-fueled case, an additional restriction is imposed when the value of V_b is less than 10 keV. In this regime ($V_b < T_i$) the energetics model of Chapter 2 breaks down and the results are discounted. Mention is also made of the fact that for beam energies less than 100 keV, the beam probably would not penetrate sufficiently into the plasma to provide the type of uniform heating which the model presumes. For this reason regimes wherein the beam energy is less than 100 keV may not be physically realistic, and the accuracy of these results is not guaranteed. The variations of the plasma and engineering properties with the parameters

discussed previously is essentially identical to the variations discussed for the pellet-fueling case. However, the inclusion of V_b as a system variable does need to be qualitatively examined. The beam energy increases with rising power level and wall loading. V_b also increases with increasing q and c_τ and decreases with larger plasma beta. Figures 10 through 17 indicate the variations of τ, f_B, B_t, and B_{max} again as functions of power level, plasma beta and wall loading. A value of c_τ equal to 0.1 has again been presumed in the calculations.

The remainder of the results for the steady-state case presumes a fixed fractional burn-up of 20%. As mentioned previously, fixing f_B fixes the confinement time for given values of power level and wall loading and introduces c_τ into the calculations as a variable replacing τ. Tables A16 through A27 present the variables calculated for the pellet-fueling model. Tables A28, A29, and A30 represent the beam-fueling results. Again, the same restrictions (Table 1) apply here that applied to the previous discussion. The restrictions on operating regimes are also the same. The variable range is essentially the same as for the previous cases, except that here

the values of c_τ range from 0.02 to 0.5 in most cases. Variations of the reactor properties are also identical with those previously discussed. c_τ decreases with increasing power level and decreases as wall loading rises. c_τ increases as beta rises but decreases as q is raised. Increasing the injection energy raises the value of c_τ slightly. Figures 18 and 19 depict the c_τ variation with power level, plasma beta and wall loading for the pellet-fueling example. Figures 20 through 23 illustrate the B-field variations for the fixed burn-up pellet-fueling case. Figures 24 and 25 show the c_τ variation for the beam-fueling case with fixed burn-up and Figures 26 through 29 illustrate the corresponding B-field fluctuations. This concludes the presentation of results for the steady-state models. The most important features of this study will be discussed in the conclusions which follow at the end of this chapter.

II. Pulsed Operation Results

The next model to be examined is the quasi-steady-state or long pulse operation scheme. As mentioned previously the pellet-fueling model is utilized for these computations. The requirement of a pulse time which is shorter than the particle confinement time and yet is still on the order of a few minutes limits the choices of reactor regime somewhat.

Table 4 presents the steady-state reactor model chosen. The confinement time of 240 seconds is to conform with a pulse length of 200 seconds. It is assumed that Table 4 shows the plasma parameters prior to the initiation of the power pulse. Once the pulse is underway the fuel density will be altered as modeled in Equation (52):

$$n_f = n_{fo} + c_p \, t_p \, S \quad ,$$

where S is given as 0.95×10^{11} ions/cm^3/second. c_p is to be determined dependent upon the averaged power output desired over the power producing cycle. This change in the value of n_f also produces changes in the values of the other species densities as well as in the value of plasma beta. These parameters will vary throughout the power cycle and their variations will be plotted and discussed.

In the initial computations it is assumed that the desired average power output over the 200 second cycle is 12.5 gigawatts, the same as the steady-state power rating. For this model c_p is determined to be 0.65, which produces an initial density perturbation of 1.2×10^{13} ions/cm^3 or 25% of the steady-state fuel density. This large density perturbation drives the plasma ion temperature to zero in 14 seconds via the thermal instability mechanism[9] previously discussed. It is thus necessary to implement the thermal control mechanism modeled

by Equations (46) and (47). In the calculations a value of $\alpha = 1$ is assumed along with a delay time of 0.5 second. This control function effectively controls the plasma ion temperature within the bounds of 9.9 keV and 10.1 keV, i.e., an rms variation of 1%. The variations of the plasma parameters n_f, β_θ, and τ are shown in Figures 30, 31, and 32. The behavior is essentially the same in all cases--a monotonic decrease from the initially perturbed values. n_f varies from a maximum of 6.1×10^{13} ions/cm^3 to a minimum of 2.7×10^{13} ion/cm^3. The dashed line on the figures represents the steady-state value of the particular plasma parameter taken from Table 4. β_θ varies from a maximum of 1.4 to a minimum of 0.7 while τ varies from 245 seconds to 90 seconds. Other plasma species densities are observed to exhibit exactly the same monotonically decreasing behavior. The average value of the control portion of the beam source throughout the cycle is found to be -0.064×10^{11} ions/cm^3/second. The control fraction is negative due to the fact that the ion temperature fluctuations tend to be more positive for this case. The average beam source rate throughout the power cycle is then 2.32×10^{11} ions/cm^3/second. The ratio of injected power to total thermal power is found to be 0.036 when averaged over the cycle. The control function is determined to be -2.7% of the beam value.

The effect of increased delay time in the implementation of the control function was also analyzed as a part of these studies. The range of variation of the ion temperature is 9.9 to 10.1 keV for 0.5 second delay, 9.9 to 10.3 keV for 0.7 second delay and 9.8 to 10.8 keV for 1.0 second delay time. All of these variations are quite small and result in the use of only small fractions of available power for control purposes. For the case of the 200 second power pulse, the beam power is only about 3.5% of the total reactor power rating regardless of the delay time chosen. The control becomes more and more negative as a function of increasing delay time. For 0.5 second delay the control strength is -2.7% of the beam strength; for 0.7 second delay the control is -5.6%; and for 1.0 second delay time the control is -20.2% of the beam strength.

The final case to be examined is the case of a 200 second power pulse followed by a 100 second dead time wherein the plasma parameters are assumed to be returned to the values given in Table 4 prior to beginning a second power pulse. In this case the averaged power rating over the power cycle is to be 1.5 times the steady-state value of 12.5 GWatts. In this case c_p is determined to be 1.05. The density perturbation in this example is 2.0×10^{13} ions/cm^3, which

represents a 41% perturbation and the ion temperature drops to zero in 11 seconds if the thermal instability is not controlled. The variation of the plasma properties is essentially the same as in Figures 30, 31 and 32 although the numerical values are somewhat larger. Fuel density varies from 6.8×10^{13} to 4.0×10^{13} ions/cm^3. β_θ ranges from 1.6 to 1.04, and τ varies between 255 seconds and 140 seconds. This time the average control fraction of the beam source is found to be $+0.95 \times 10^{11}$ ions/cm^3/second, which is approximately 34% of the steady-state beam source strength. The average beam power throughout the power cycle is 3.4% of the total thermal power, which is 18.75 GWatts in this example. For this more physically-realistic case (allowing for a dead time), the fraction of power needed to control the thermal instability is only about 1% of the total reactor thermal power rating.

III. Conclusions

The original purpose of this research was to identify the reactor operating regimes for CTR's with thermal power ratings between 12.5 and 50 GW(th). This research was to aid in the selection of particular reactor models for the purposes of a complete system design study. Several favorable combinations of variables were observed which will aid in the pursuit of this eventual goal:

1. Low β_e and low q combinations are desirable. Low β_e (relative to A, the aspect ratio) results in no problems with MHD instabilities and produces large burn-up fractions. Low q results in reduced magnetic field strength requirements and high burn-up also.

2. Injection energies should be kept in the low range (200 to 350 keV) to produce lower total source strength requirements and lower beam source power levels. Optimal beam heating profiles tend to occur also in this range of beam energies.

3. A median range of power level and wall loading will need to be utilized to achieve an optimal design. Increased power rating increases the physical reactor dimensions while decreasing the magnetic field requirements. The effect of increased wall loading is just the opposite. Increased power levels also decrease significantly the pellet and beam source rates.

These factors will all need to be considered when a reactor model is chosen for a system analysis.

The results of the parameter survey of operating regimes of CTR's with very large thermal power ratings have been presented in a previous section of this chapter. In addition a particular set of these parameters representing a possible

pulsed reactor model has also been examined in depth. Certain overall conclusions have been reached regarding both the steady-state and pulsed operating regimes:

1. Maximum magnetic field strengths are between 25 and 50% less for these large CTR's than in the case of 5000 MW (th) reactors which have been the subject of previous design analysis.

2. These large CTR's represent a regime of high $n_e \tau_E$ product (typically 10^{15} to 10^{17} sec/cm^3) with associated high burn-up fractions (10 to 50%) which indicate excellent power production capabilities as well as efficient fuel use.

3. There is relatively little problem with impurity build-up and this problem may be further alleviated via use of the pulsed reactor concept modeled herein.

4. Long confinement times (50 to 500 seconds) are found throughout most of the reactor regime.

5. While fueling using the pellet concept may present some difficulties, this is alleviated via use of the pulsed operation scheme.

6. The effectiveness of the control mechanism for thermal instability has been shown to be most effective while not consuming a significant fraction of the energy produced by the reactor operating in the pulsed mode. Typically, the fraction of power utilized for control is 1% or less of the total reactor thermal power rating.

In addition to the technological advantages of operation at these very large power ratings covered in the above analysis, a previous report[1] has indicated economic and environmental advantages associated with these very large CTR's when they are used in conjunction with synthetic fuels production and process heat generation in addition to electricity production. It is this last factor which is perhaps most significant because it indicates the mechanism whereby these very large CTR's can be used in conjunction with existing power grids.

REFERENCES

1. J. Powell et al., BNL 18430 (1973).

2. S. Glasstone and R. H. Lovberg, Controlled Thermonuclear Reactions, D. Van Nostrand Company, Inc., Princeton, New Jersey, p. 31 (1960).

3. M. N. Rosenbluth, Nuclear Fusion 10, 340 (1970).

4. W. A. Houlberg, "Thermalization of an Energetic Heavy Ion in a Multispecies Plasma," Report UWFDM-103, Madison, Wisconsin (1974).

5. B. B. Kadomtsev and O. P. Pogutse, Nuclear Fusion 11, 67 (1971).

6. S. O. Dean et al., WASH-1295 (1974).

7. J. M. Dawson et al., Phys. Rev. Letters 26, 1156 (1971).

8. B. Carnahan et al., Applied Numerical Methods, John Wiley and Sons, Inc., New York, New York, p. 390 (1969).

9. M. Ohta et al., Plasma Physics and Controlled Thermonuclear Fusion Research, Vol. 3, IAEA, p. 432 (1971).

Table 1

RESTRICTIVE CONDITIONS

Power - GW(th)		
12.5	25.0	50.0
Wall Load - MW/m^2		
1.0	3.0	6.0
q: 1.5	2.0	2.5
β_θ: 1.0	1.5	2.0
c_T: 0.1	1.0	10.0

E_f = 20 MeV

T_i = 10 keV

A = 2.6

For Beam and Pellet Case Only

V_b - keV			
200	350	500	1000

Table 2

POWER-RESTRICTED PARAMETERS

Wall Load (MW/m^2)	Power (GW)	Fuel Density (10^{13} cm^{-3})	a (m)	R (m)
1.0	12.5	4.8	10.6	27.4
	25.0	4.0	15.1	39.2
	50.0	3.3	21.6	56.0
3.0	12.5	11.5	5.9	15.3
	25.0	9.4	8.5	22.1
	50.0	6.5	13.7	35.6
6.0	12.5	20.2	4.0	10.5
	25.0	16.0	6.0	15.3
	50.0	13.0	8.5	22.0

Table 3

TOTAL PLASMA BETA

q	β_e	β
1.5	1.0	0.066
	1.5	0.099
	2.0	0.132
2.0	1.0	0.037
	1.5	0.056
	2.0	0.074
2.5	1.0	0.024
	1.5	0.036
	2.0	0.048

Table 4

OPERATING PARAMETERS AT PULSE INITIATION

Power = 12.5 GW(th)

Wall Load = 1 MW/m^2

$q = 1.5$ $\beta_\theta = 1.0$

$\tau = 240$ sec. $f_B = 39\%$

Temperatures

Ion	:	10.0 keV
Electron	:	9.1 keV

Densities

Fuel	:	4.8×10^{13} cm^{-3}
Electrons	:	9.1×10^{13} cm^{-3}
Alphas	:	1.6×10^{13} cm^{-3}
Impurities	:	5.9×10^{11} cm^{-3}

Sources

Pellet	:	0.95×10^{11} cm^{-3} sec^{-1}
Beam	:	2.40×10^{11} cm^{-3} sec^{-1}
Beam Energy	:	200 keV

Fields

Toroidal	:	30 kilogauss
Maximum	:	60 kilogauss

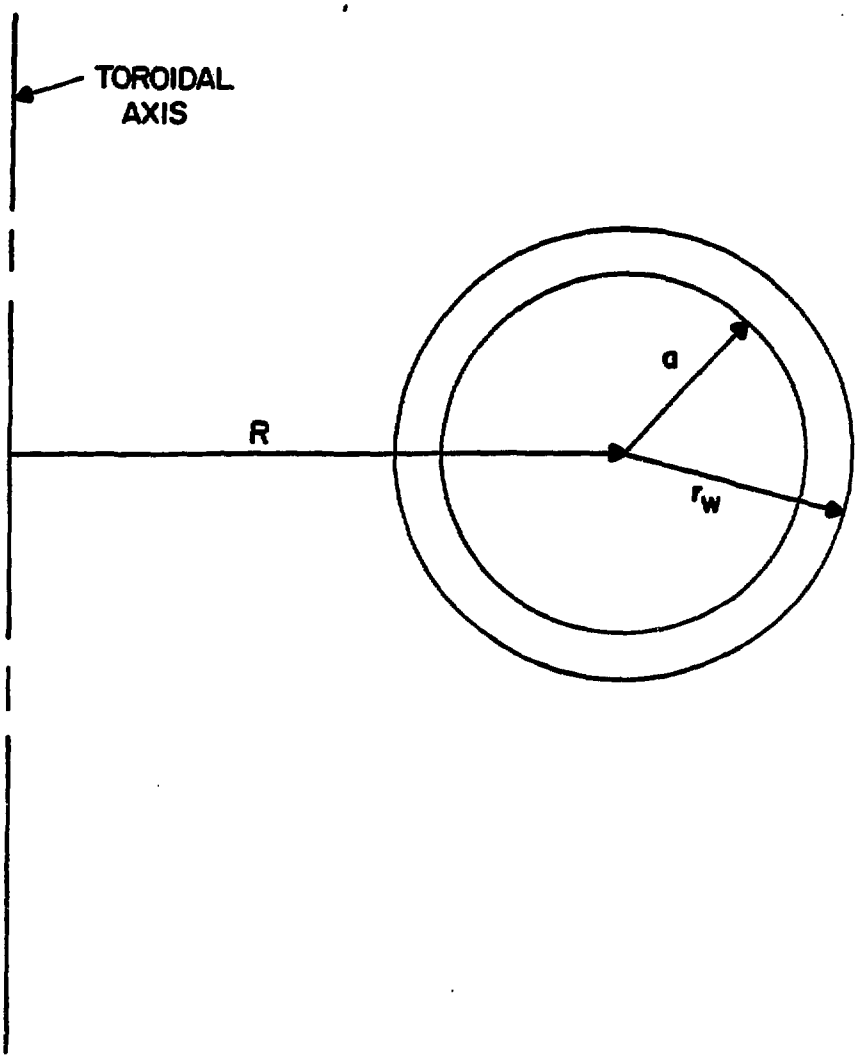

TOKAMAK REACTOR GEOMETRY

FIGURE 1

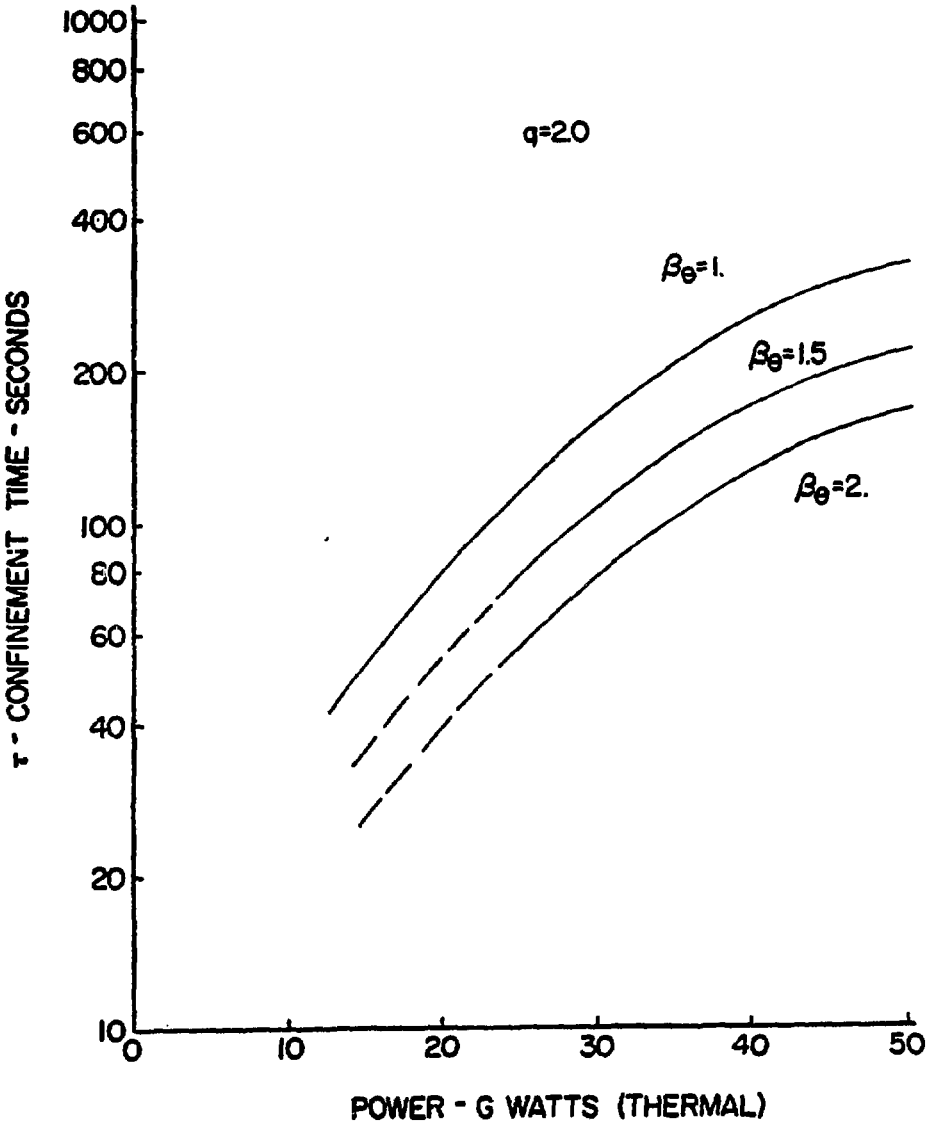

PELLET-FUELING (V_b=500 keV)

P_w=1.0 MW/m^2

FIGURE 2

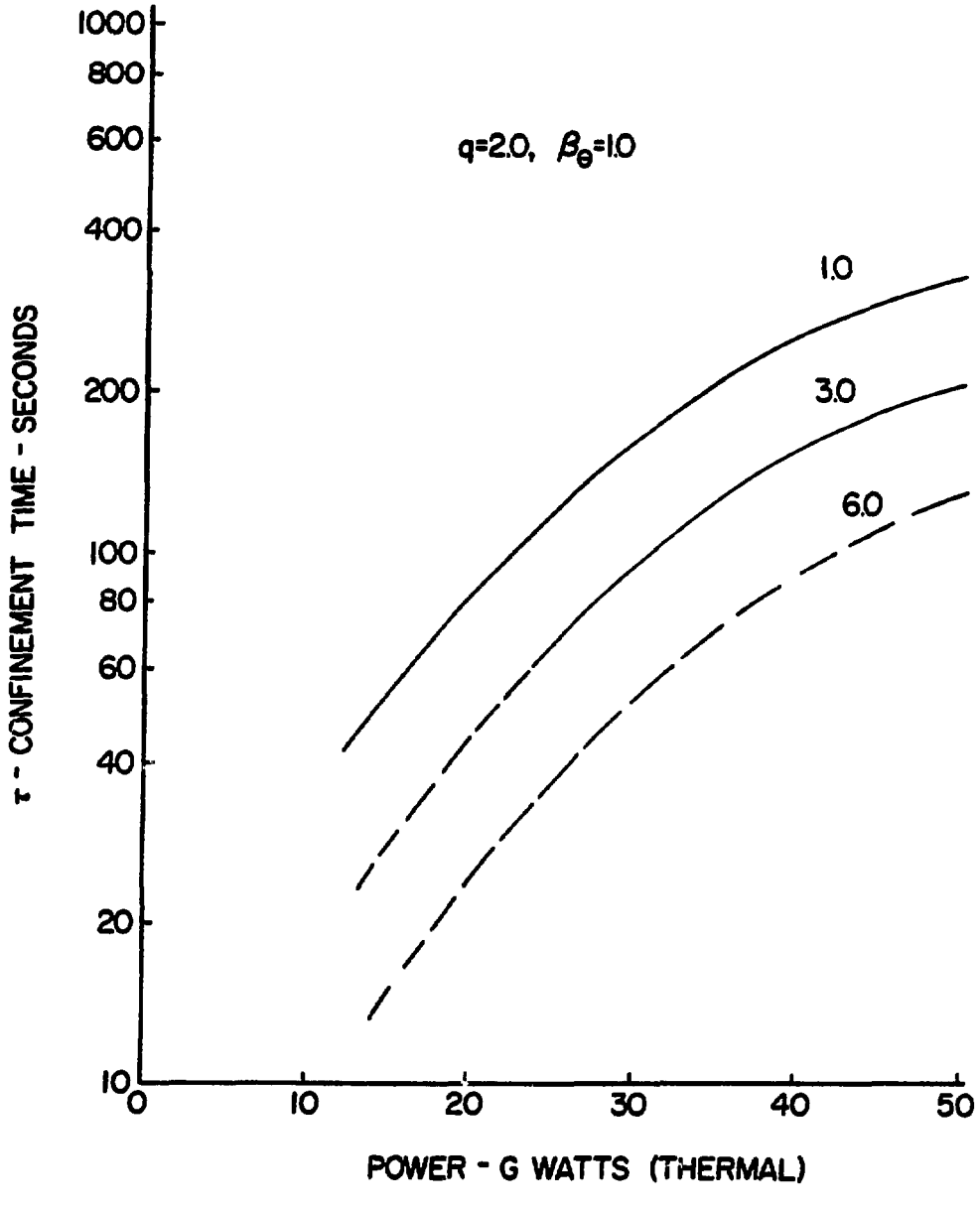

PELLET-FUELING (V_b=500 keV)
P_w VARIATION

FIGURE 3

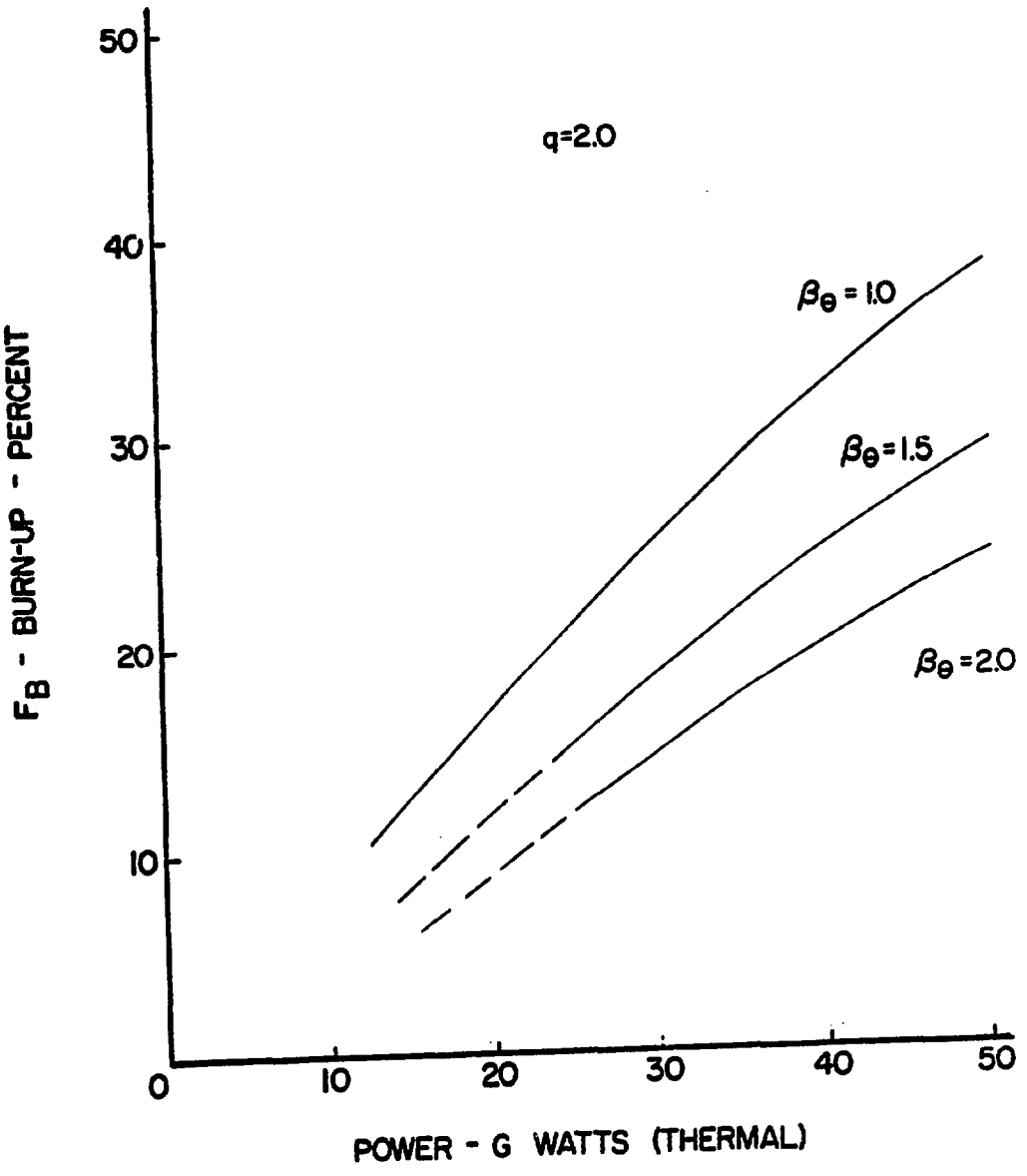

PELLET-FUELING (V_b=500 keV)

P_W=1.0 MW/m^2

FIGURE 4

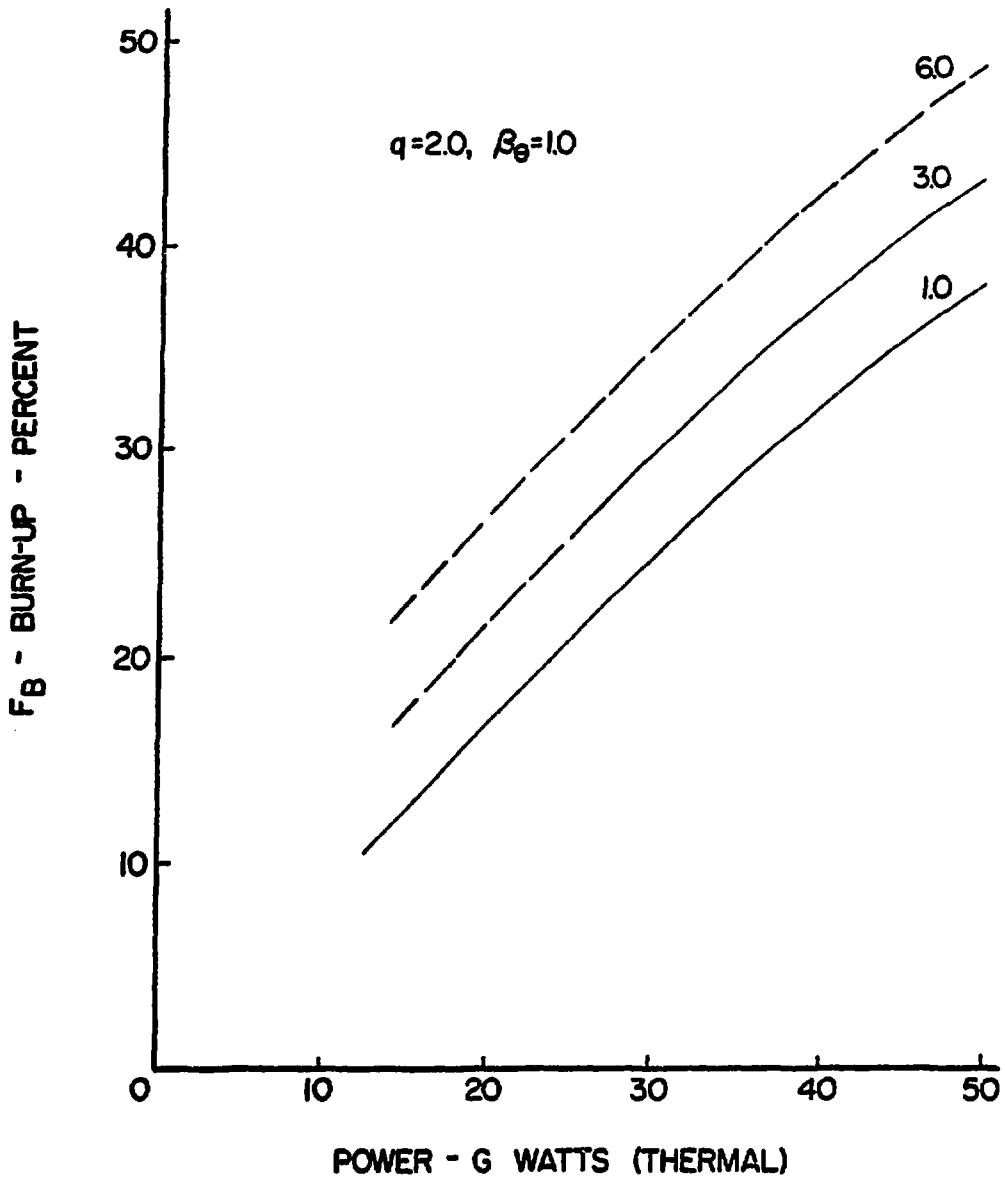

PELLET-FUELING (V_b=500 keV)
P_W VARIATION

FIGURE 5

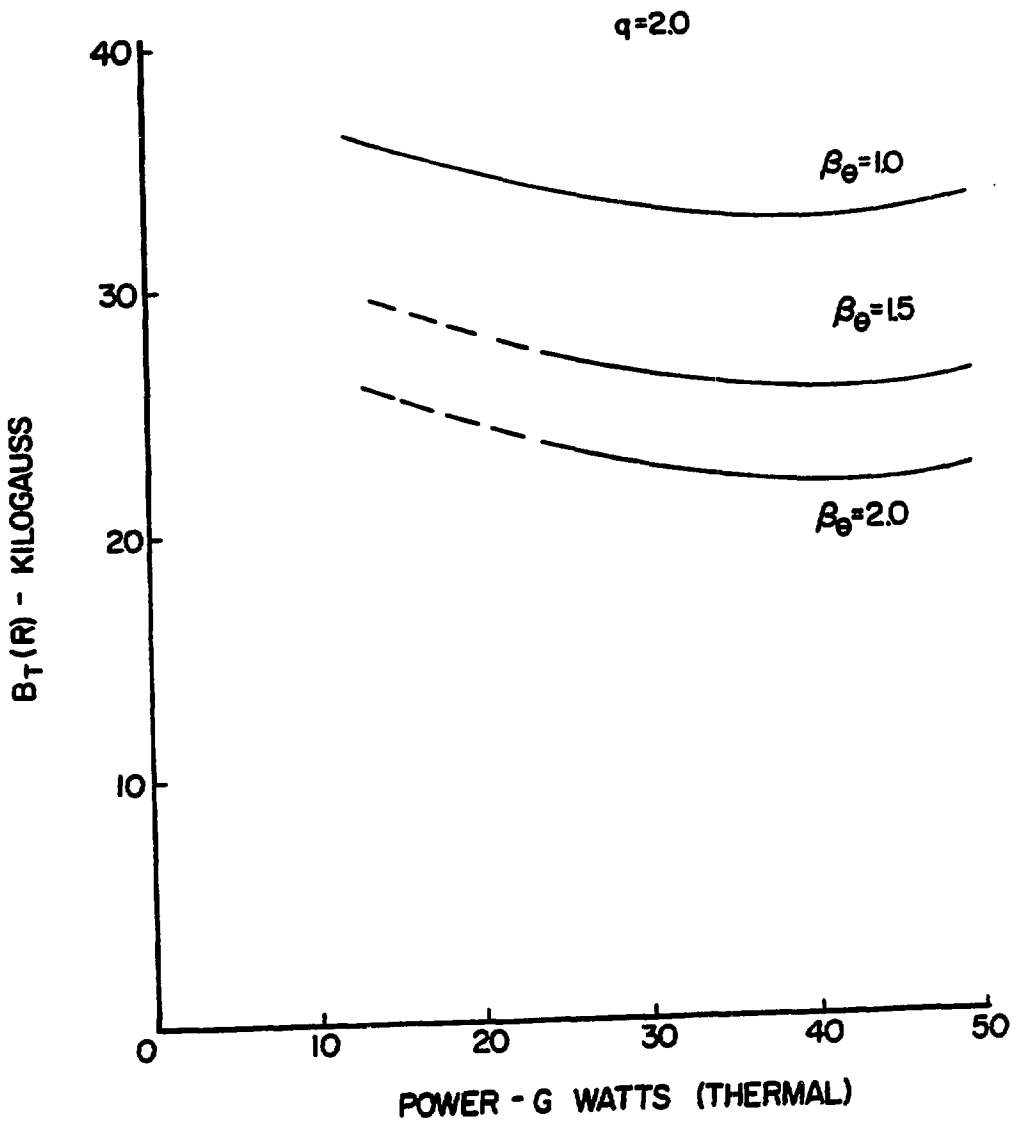

PELLET-FUELING (V_b=500 keV)

P_w = 1.0 MW/m^2

FIGURE 6

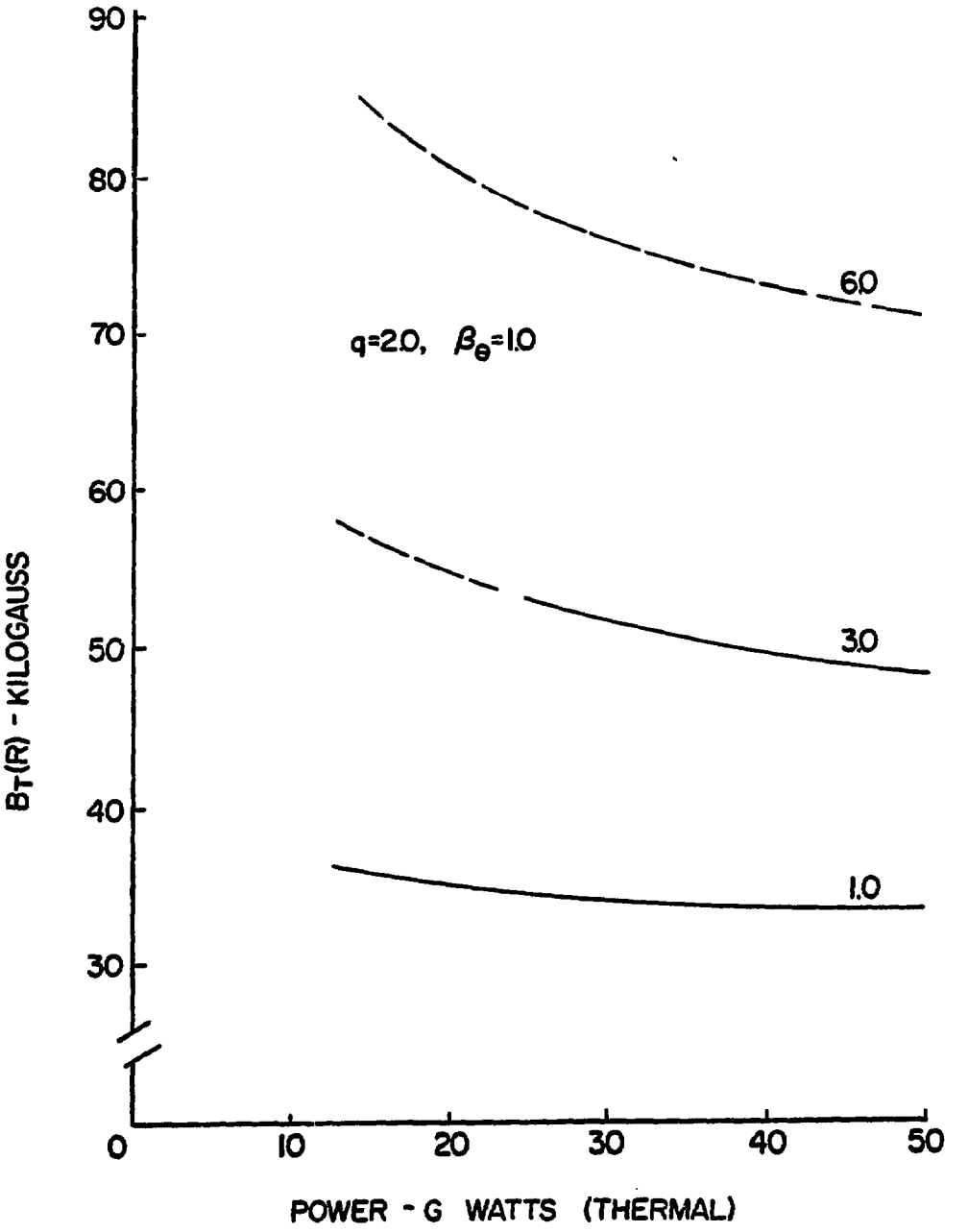

PELLET-FUELING (V_b=500 keV)
P_w VARIATION

FIGURE 7

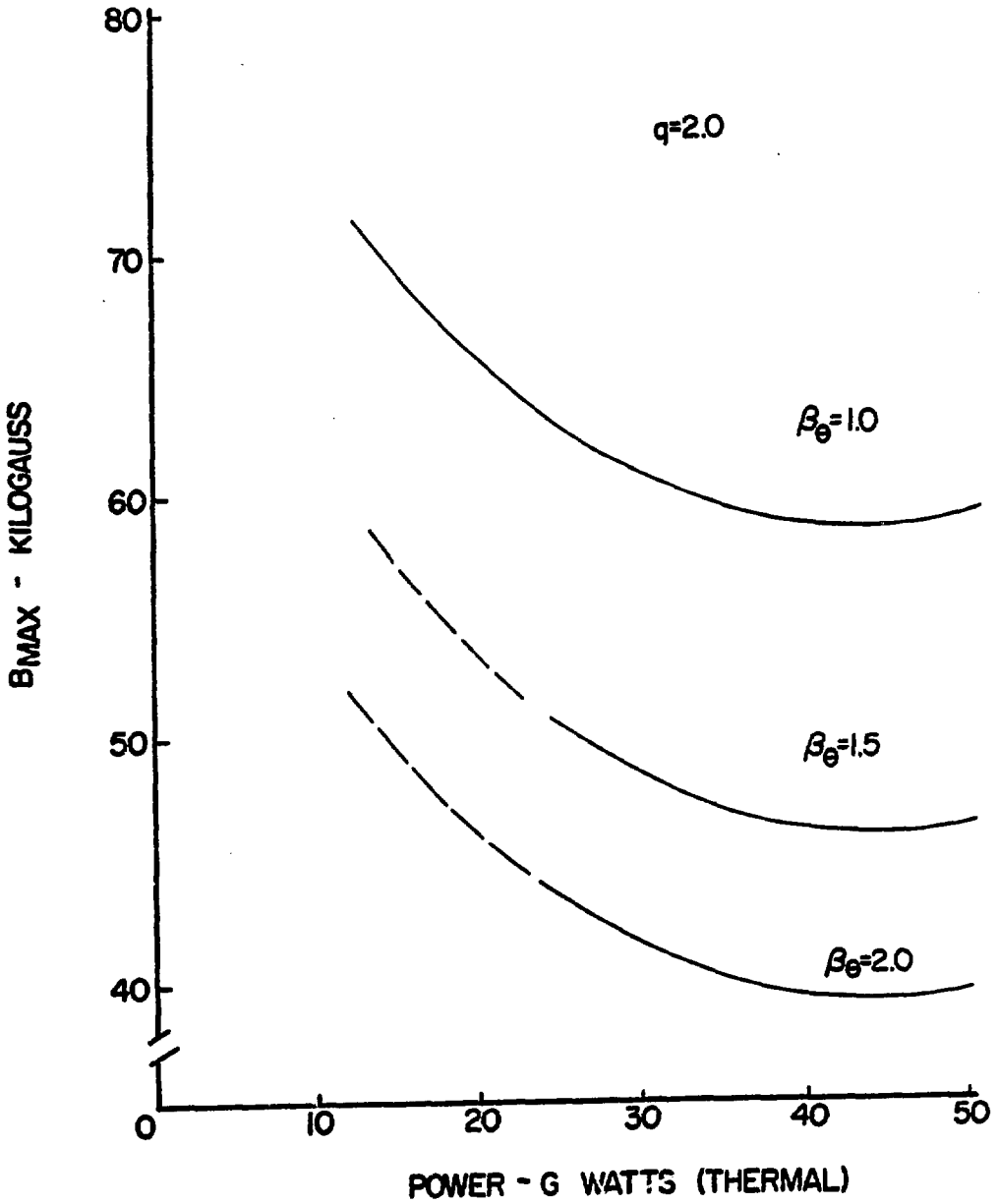

PELLET-FUELING (V_b=500 keV)

P_w=1.0 MW/m^2

FIGURE 8

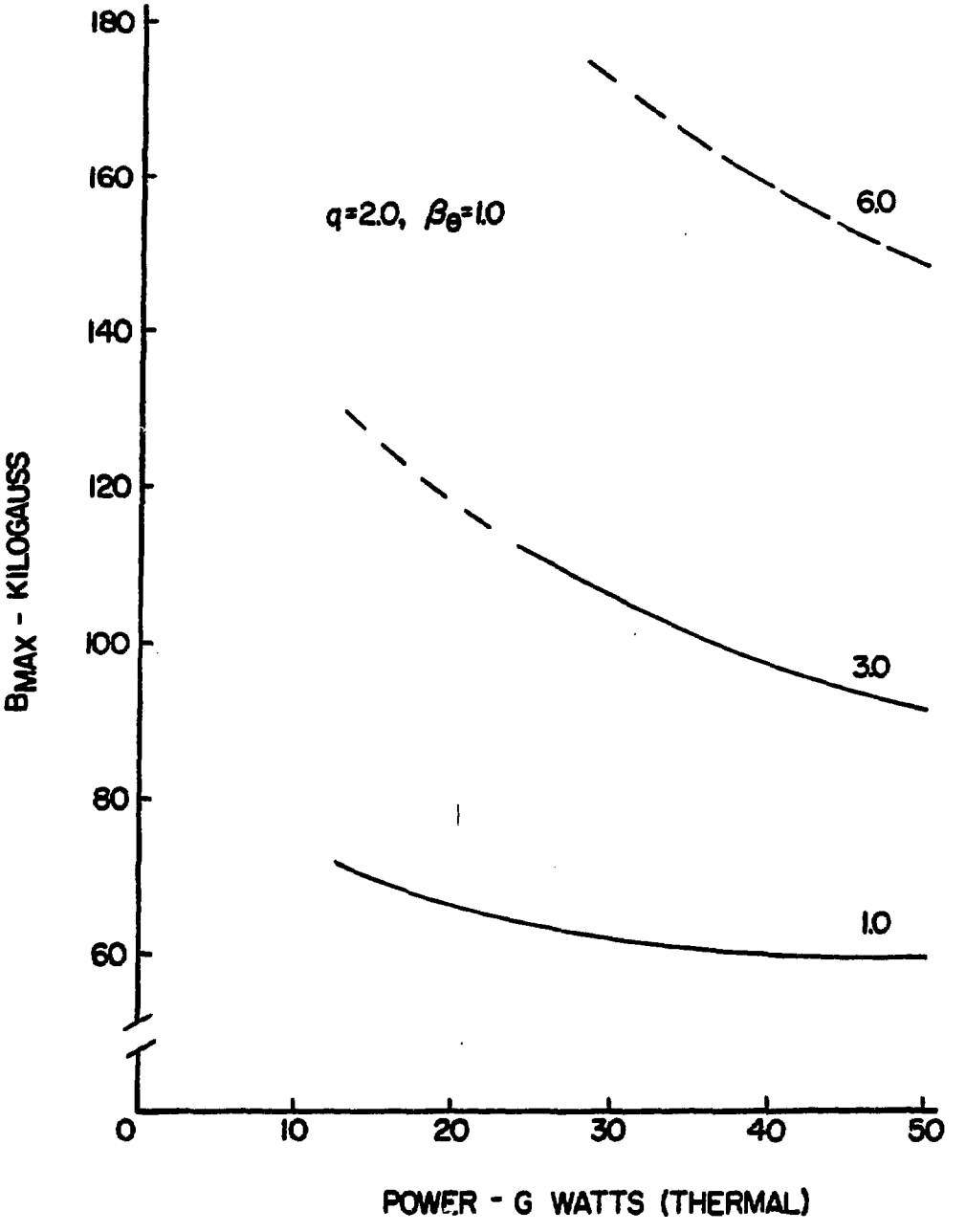

PELLET-FUELING (V_b=500 keV)
P_w VARIATION

FIGURE 9

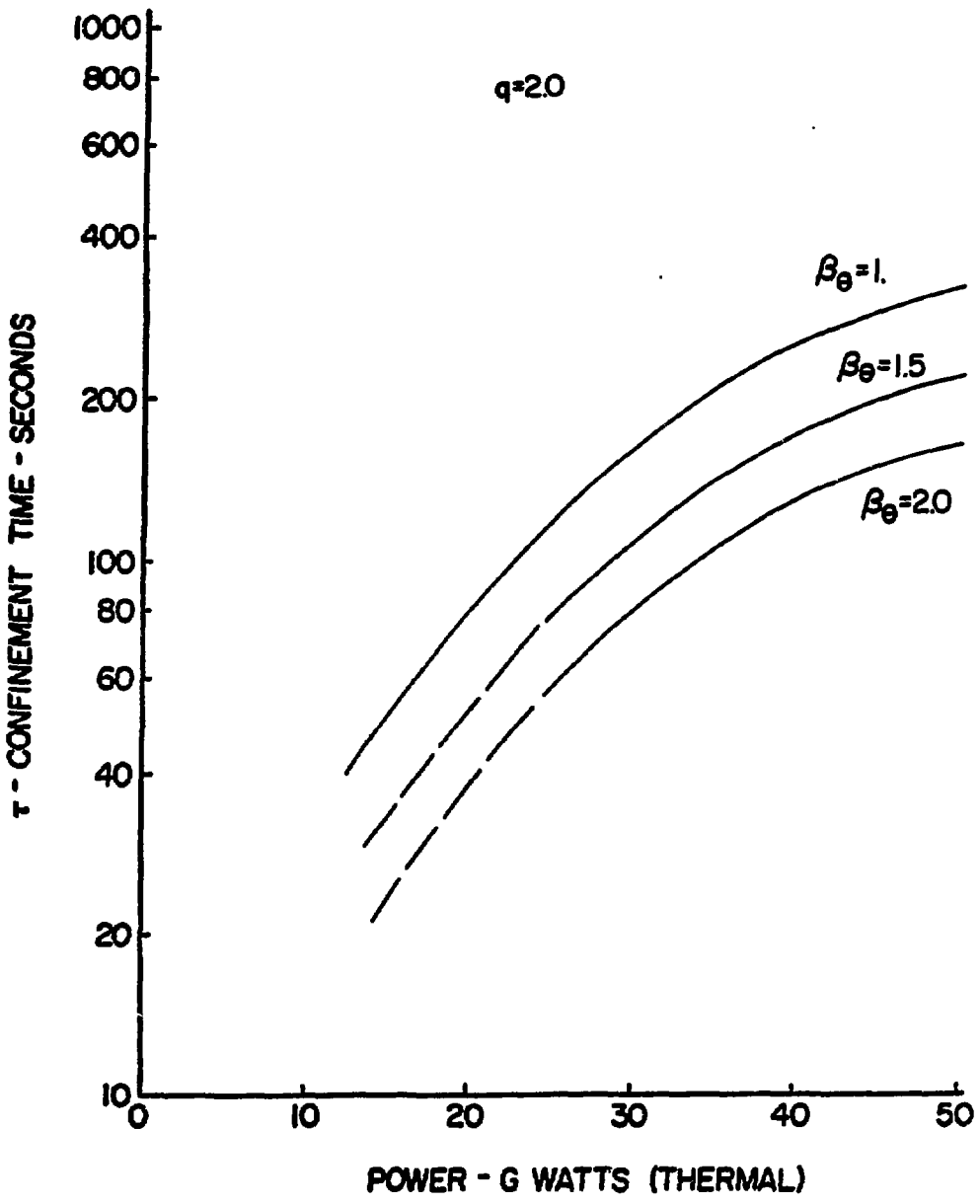

BEAM-FUELING
P_w=1.0 MW/m^2

FIGURE 10

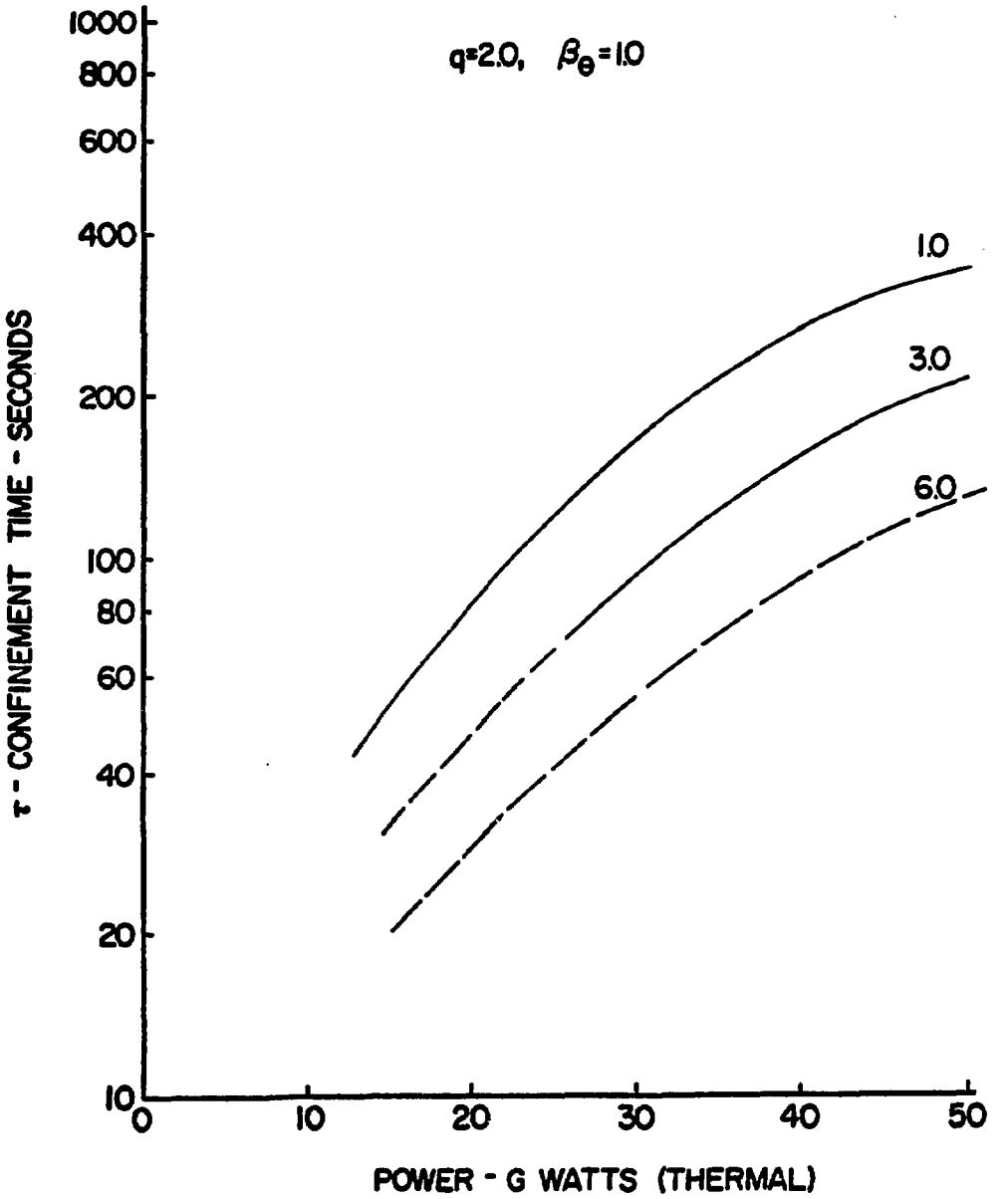

BEAM - FUELING
P_w VARIATION

FIGURE 11

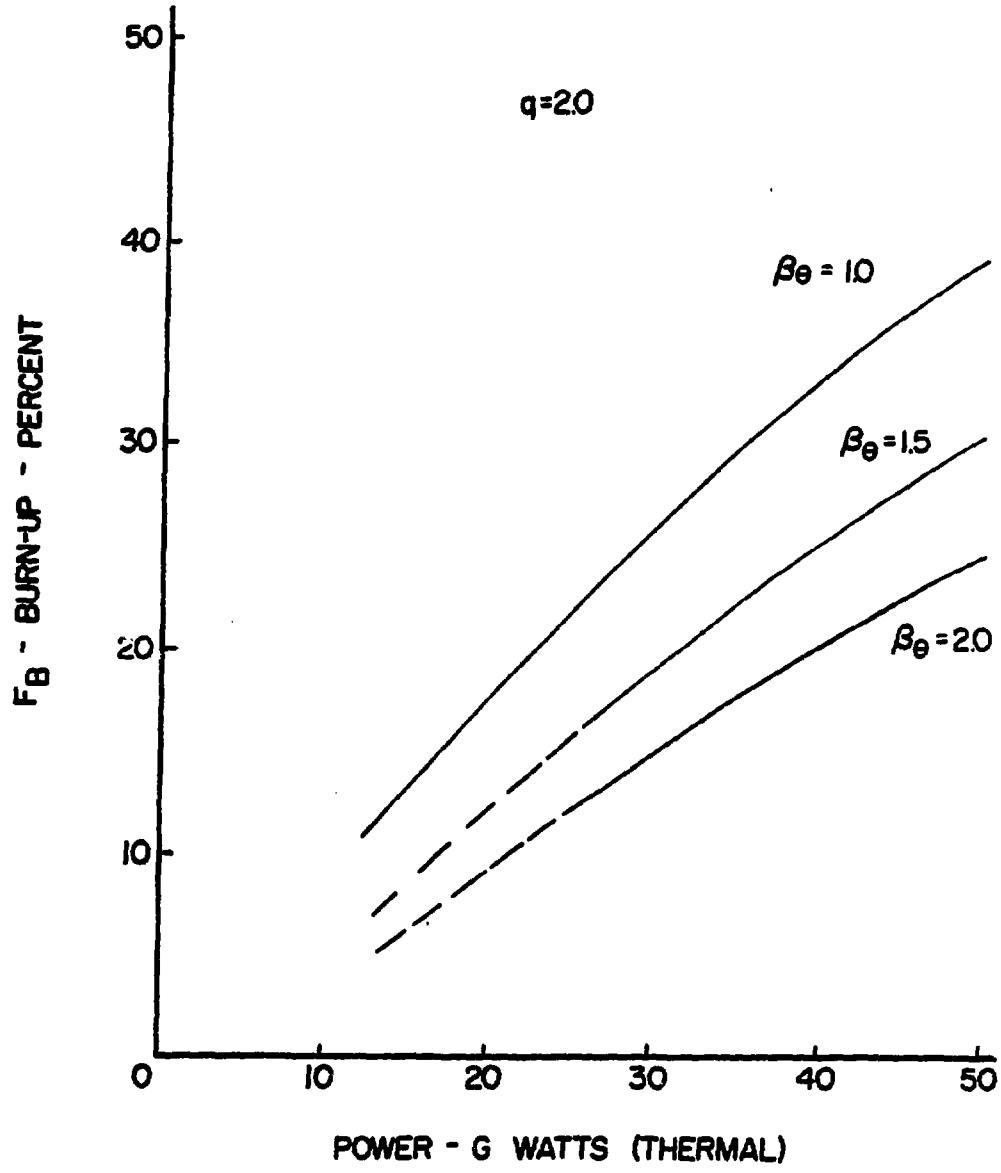

BEAM-FUELING
P_W=1.0 MW/m^2

FIGURE 12

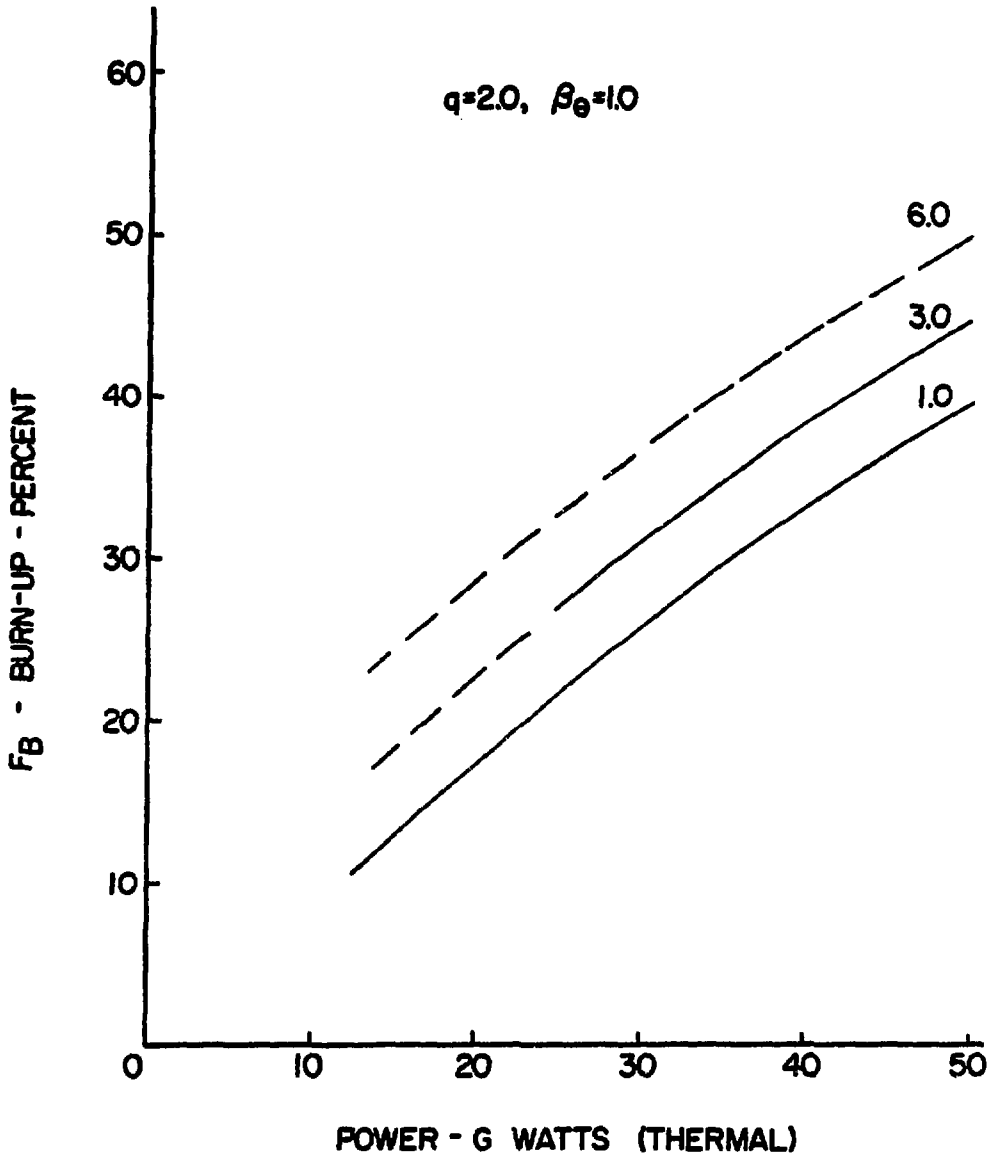

BEAM-FUELING
P_W VARIATION

FIGURE 13

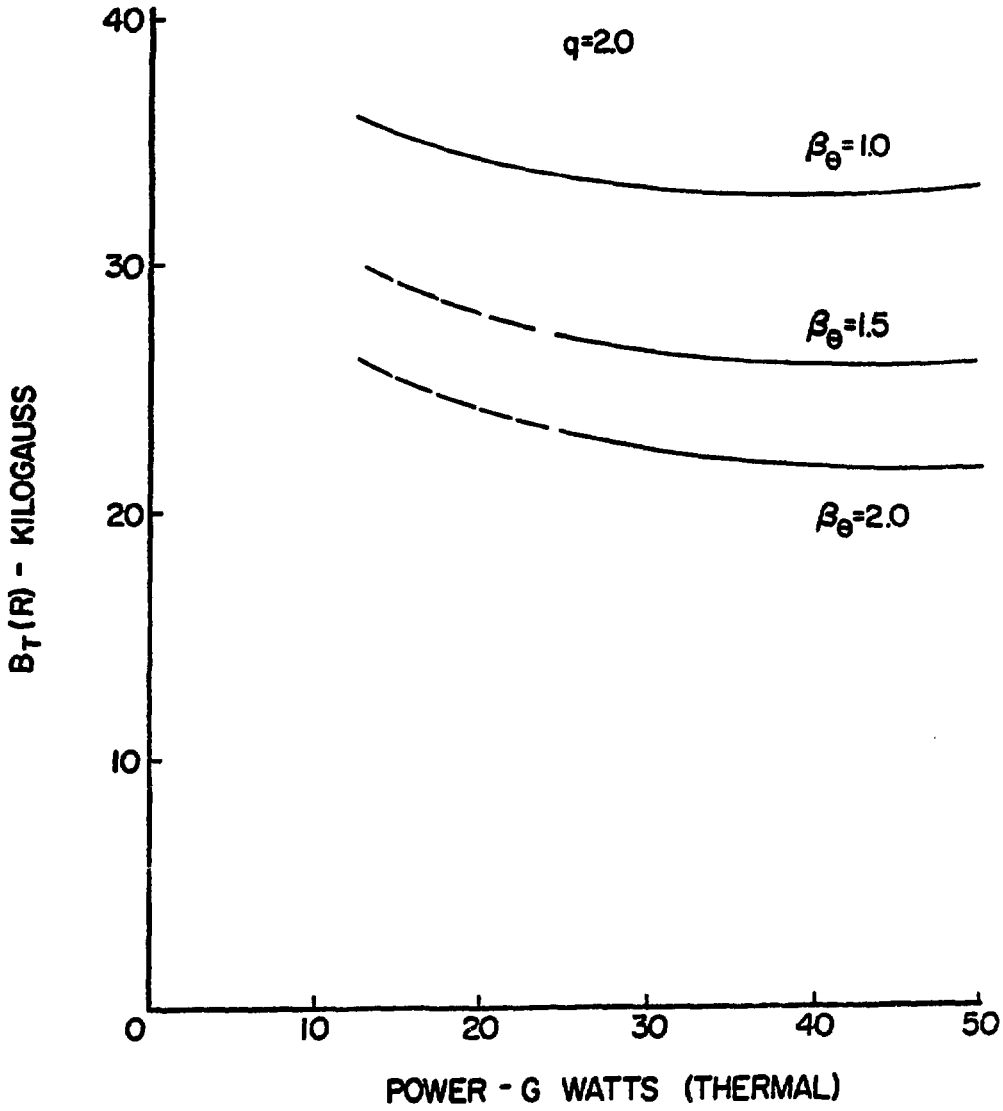

BEAM-FUELING
P_W=1.0 MW/m^2

FIGURE 14

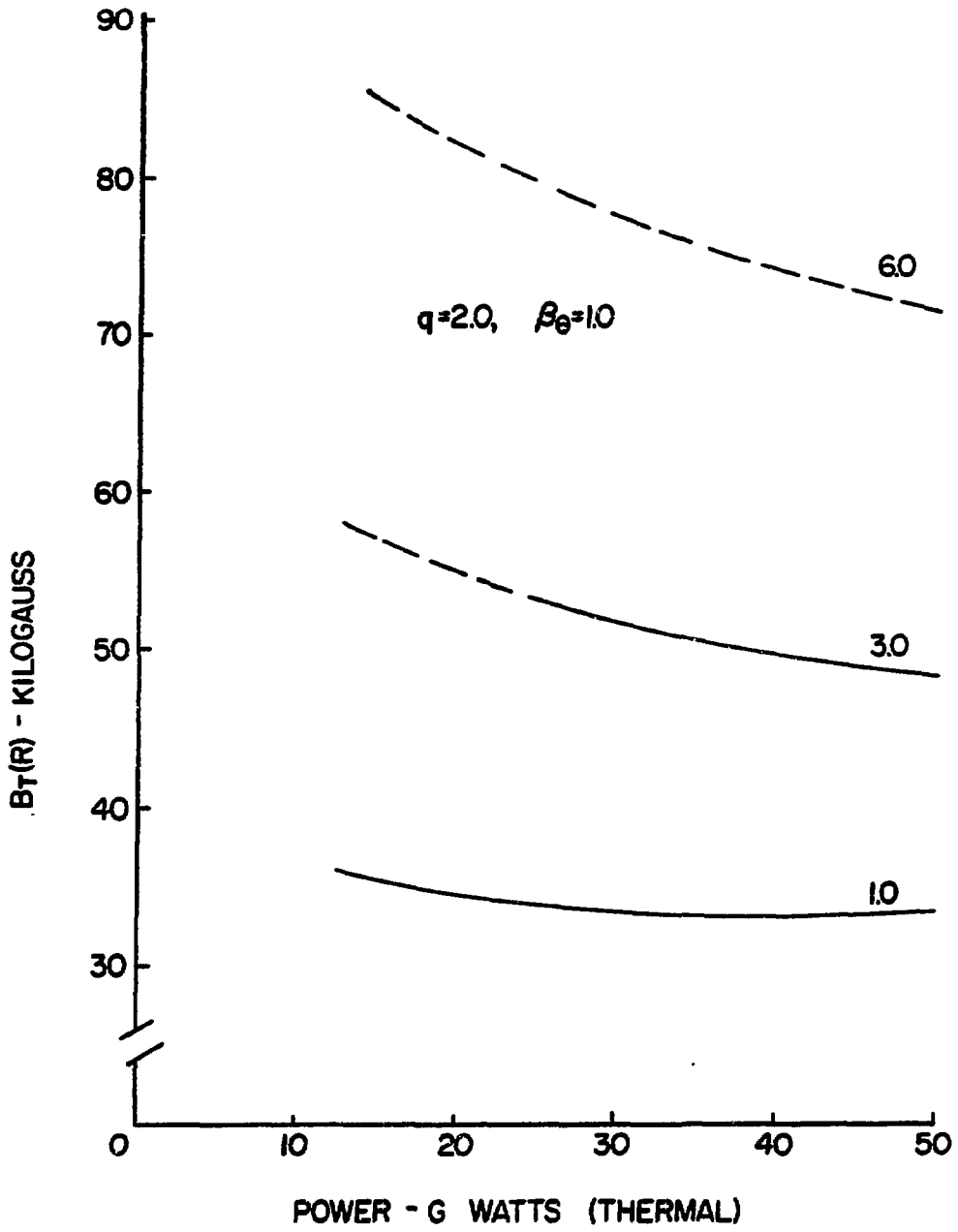

BEAM-FUELING
P_W VARIATION

FIGURE 15

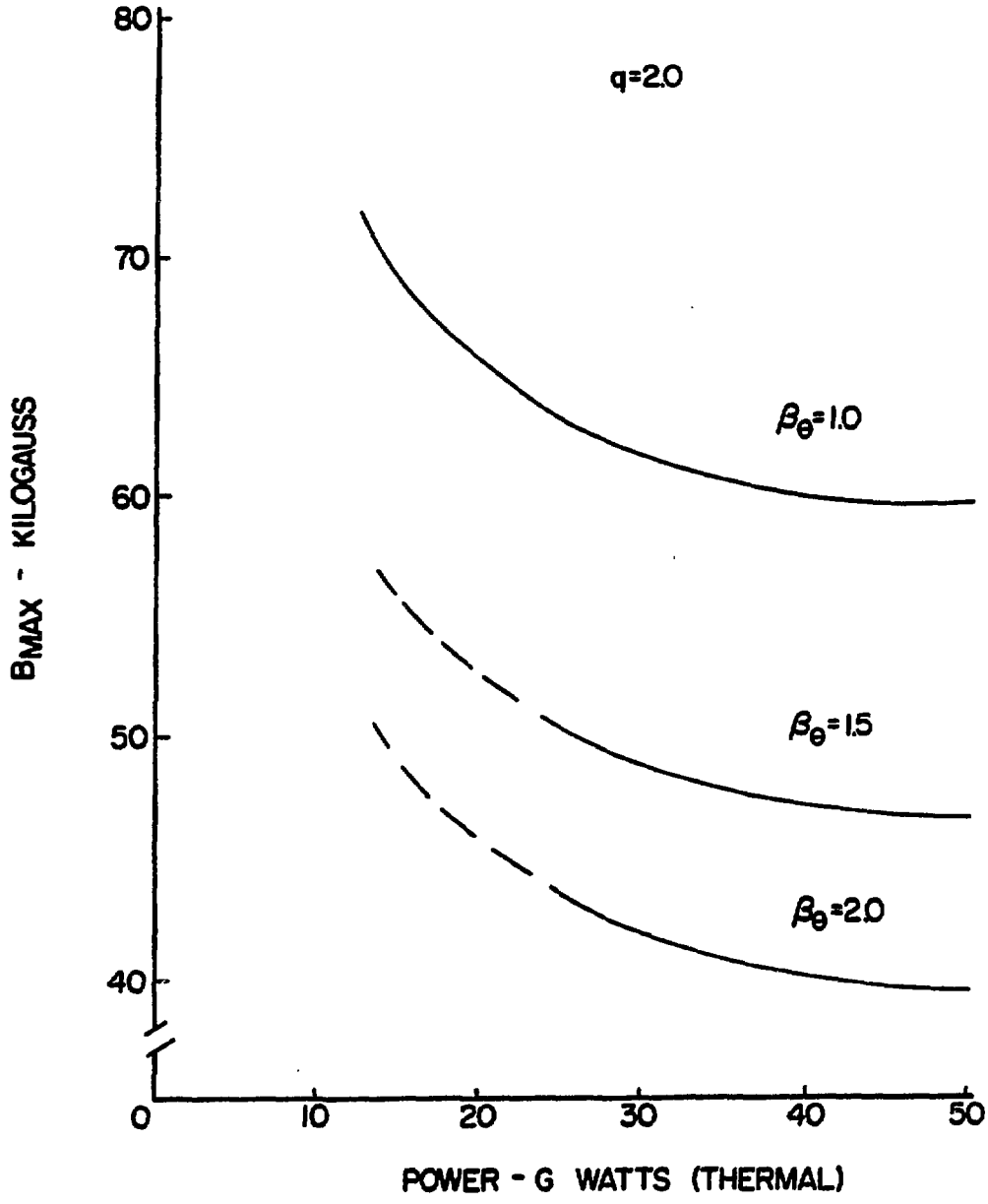

BEAM-FUELING
P_W=1.0 MW/m^2

FIGURE 16

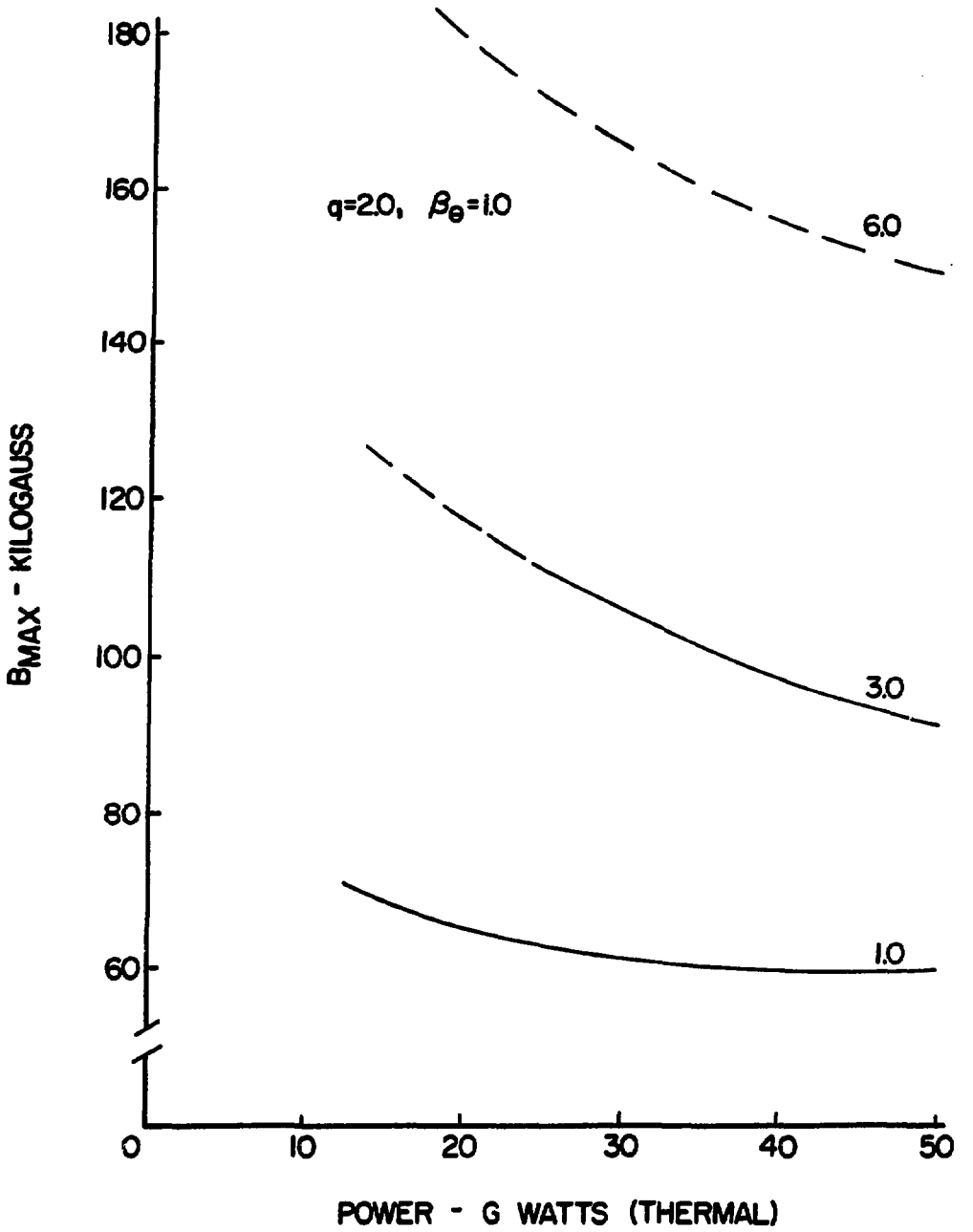

BEAM-FUELING
P_W VARIATION

FIGURE 17

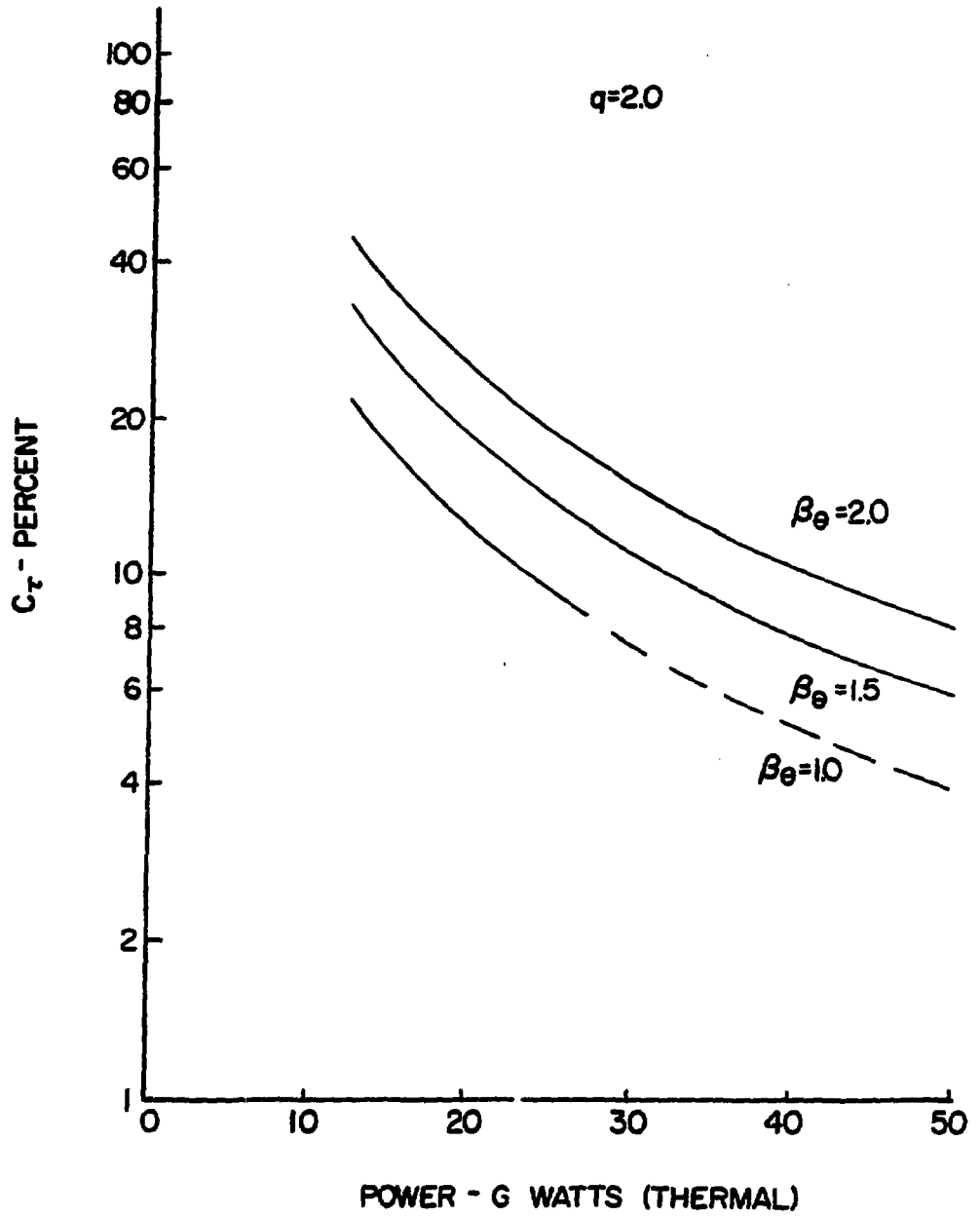

PELLET - FUELING (V_b=500 keV)

P_w=1.0 MW/m^2, F_b=20%

FIGURE 18

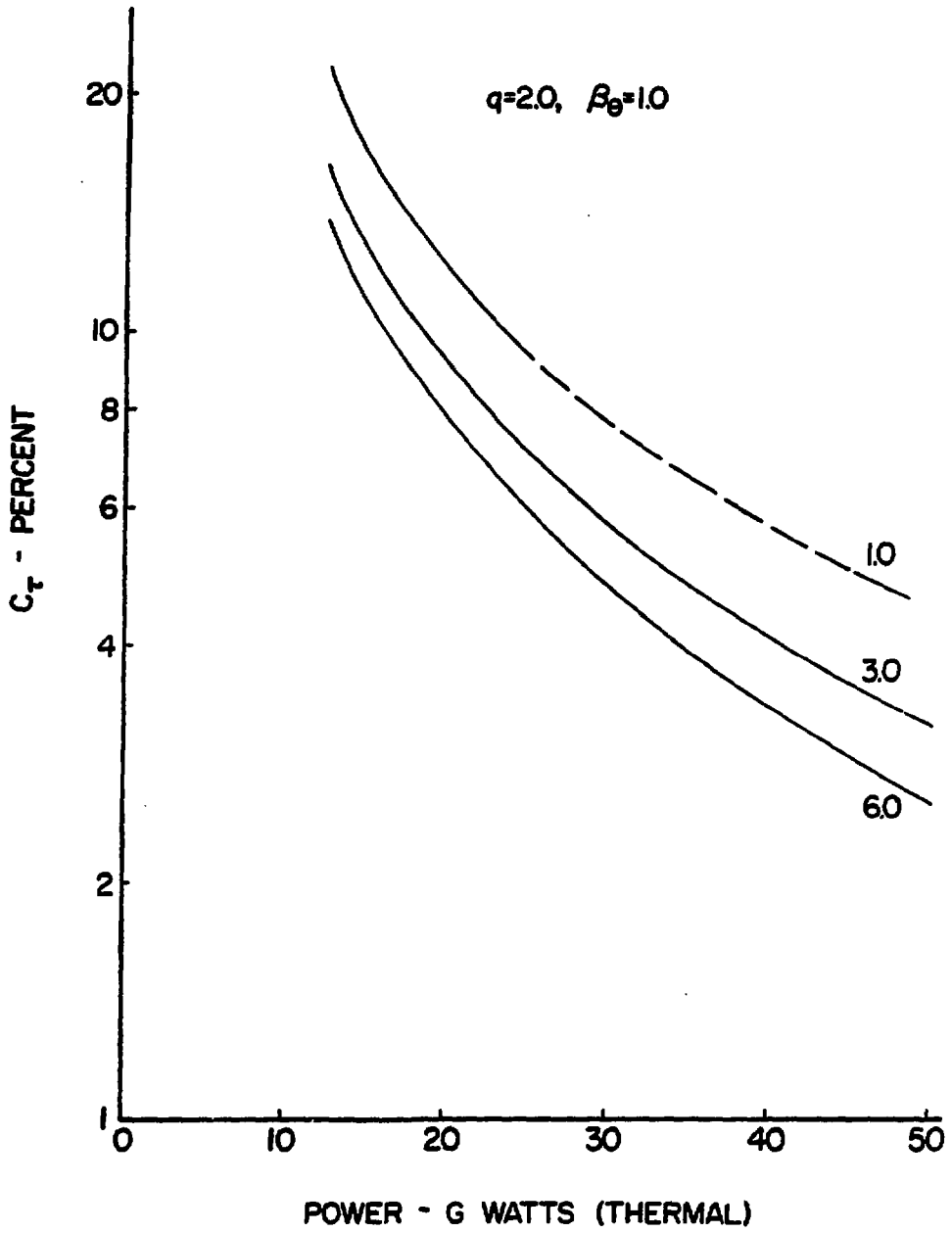

PELLET - FUELING (V_b=500 keV)
P_w VARIATION, F_b=20%

FIGURE 19

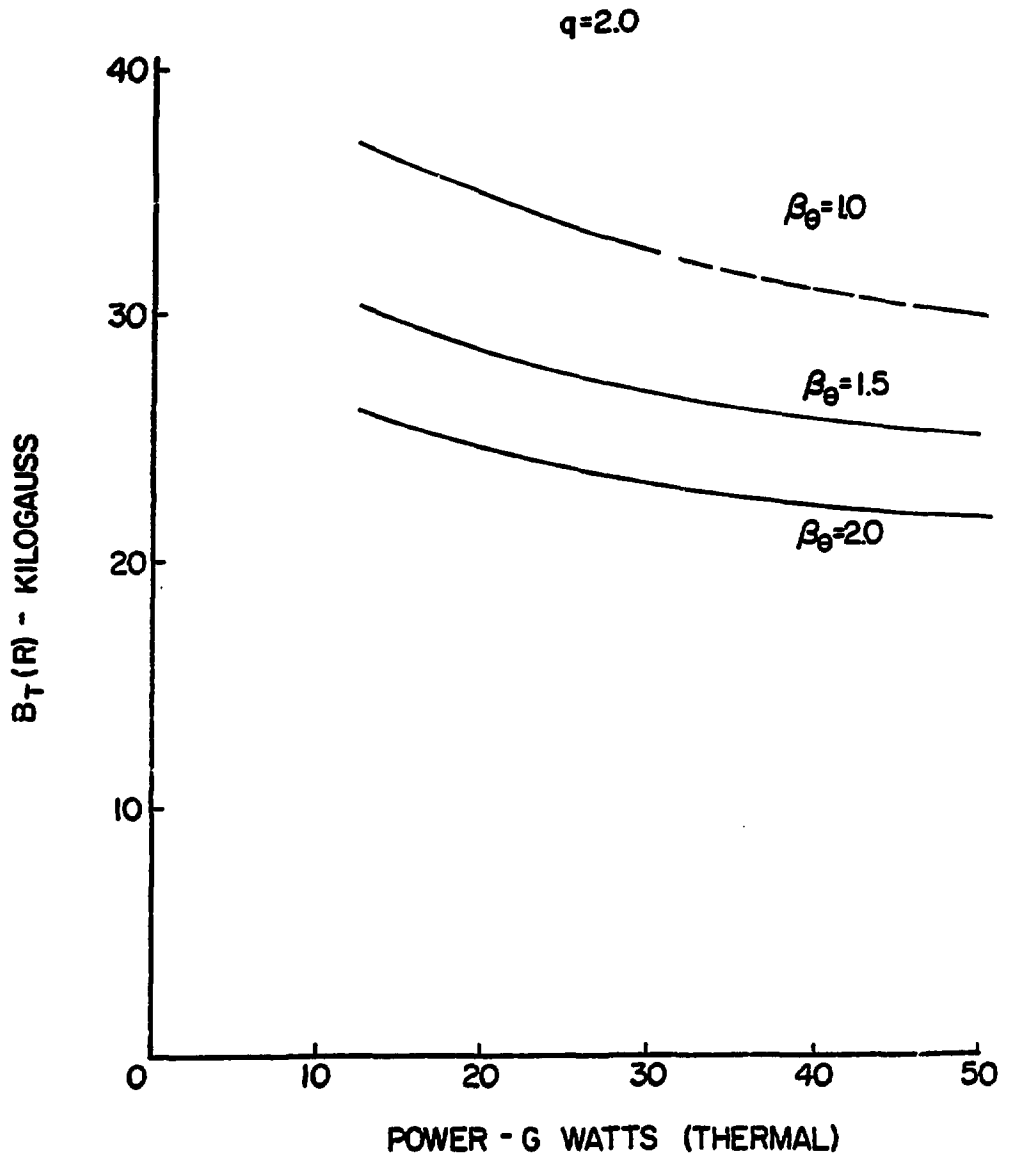

PELLET-FUELING (V_b=500 keV)

P_w=1.0 MW/m^2, F_b=20%

FIGURE 20

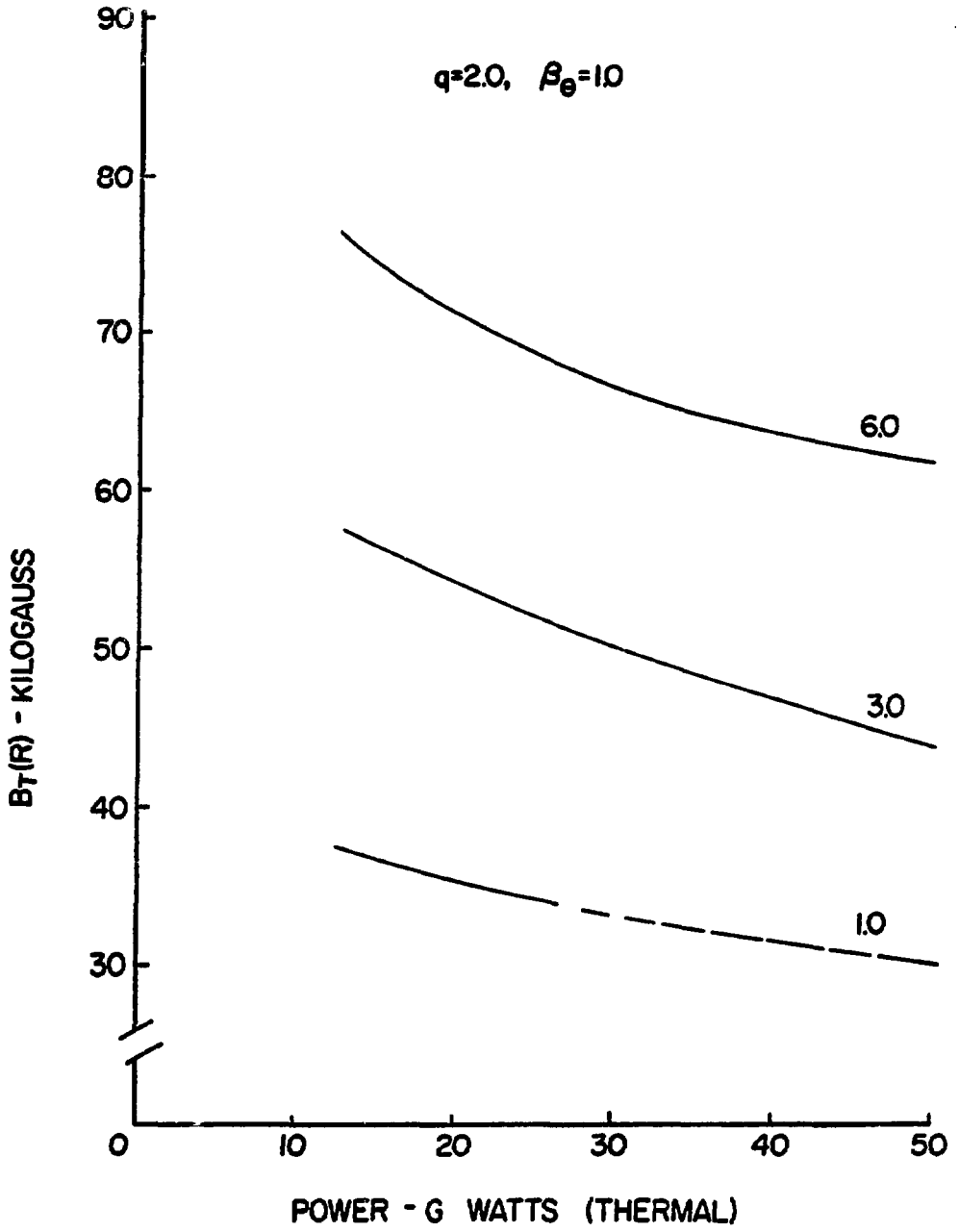

PELLET - FUELING (V_b=500 keV)
P_w VARIATION, F_b=20%

FIGURE 21

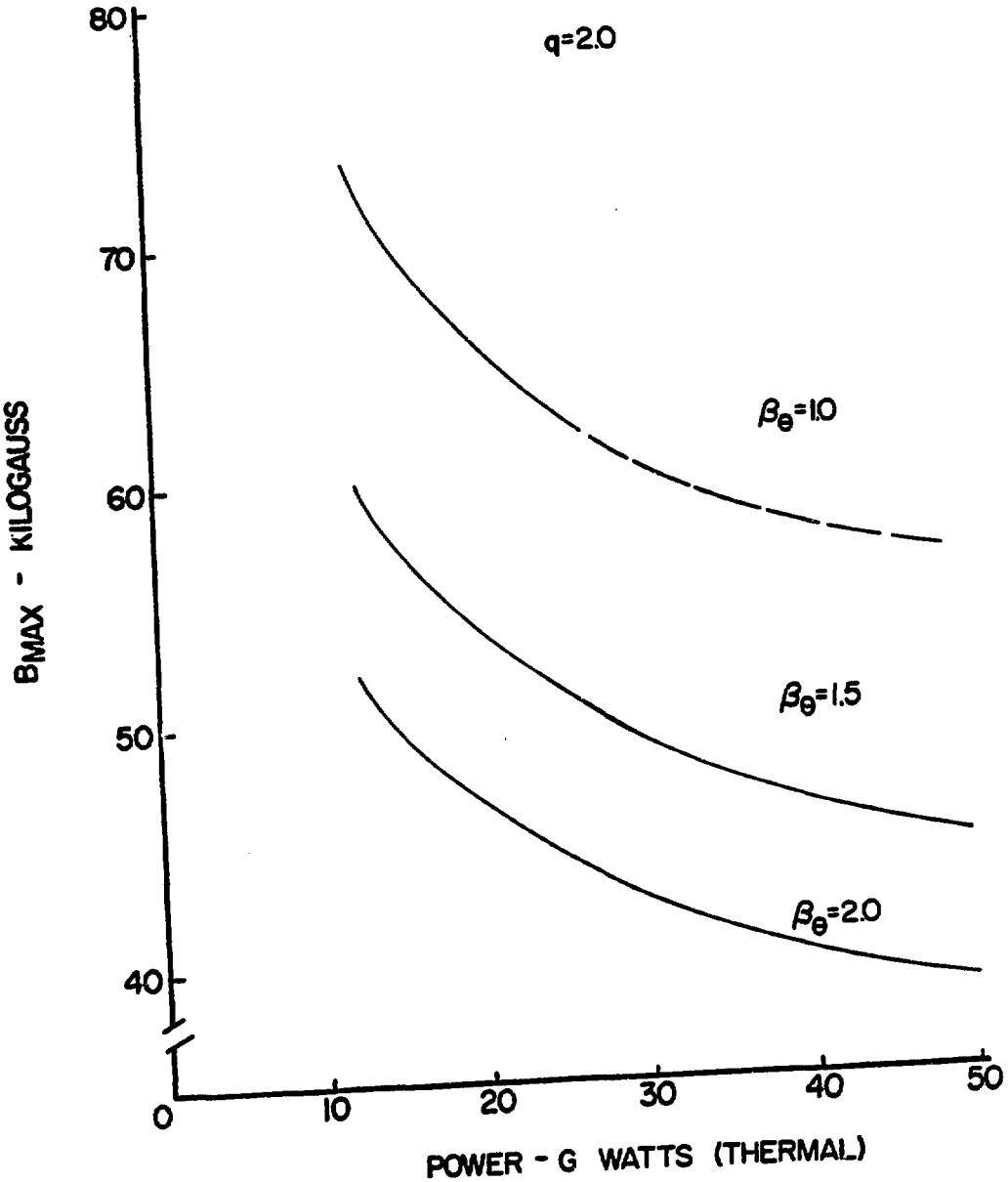

PELLET - FUELING (V_b=500 keV)
P_w = 1.0 MW/m^2, F_b=20%

FIGURE 22

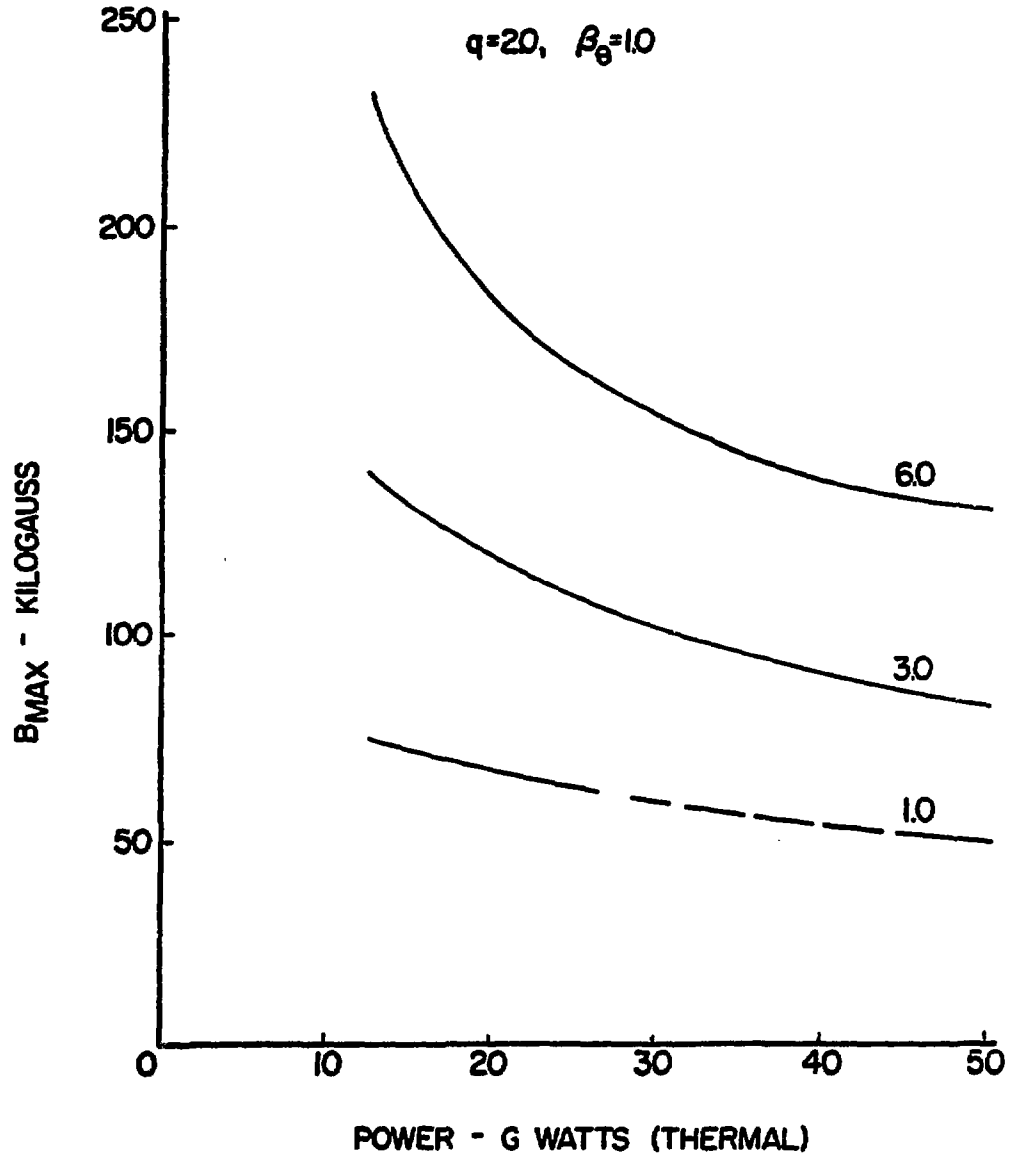

PELLET - FUELING (V_b=500 keV)
P_W VARIATION, F_b=20%

FIGURE 23

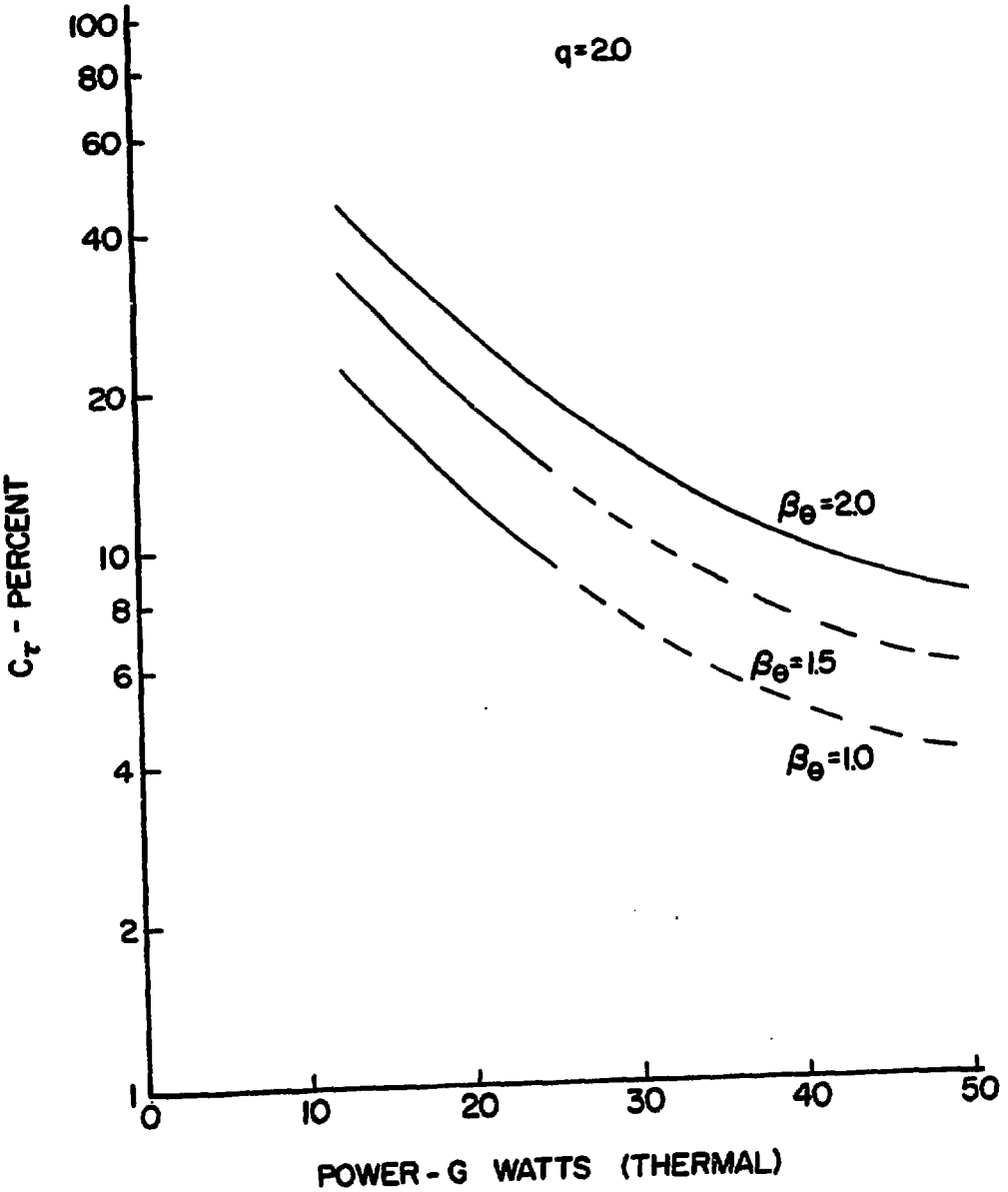

BEAM - FUELING (F_b=20%)

P_W = 1.0 MW/m^2

FIGURE 24

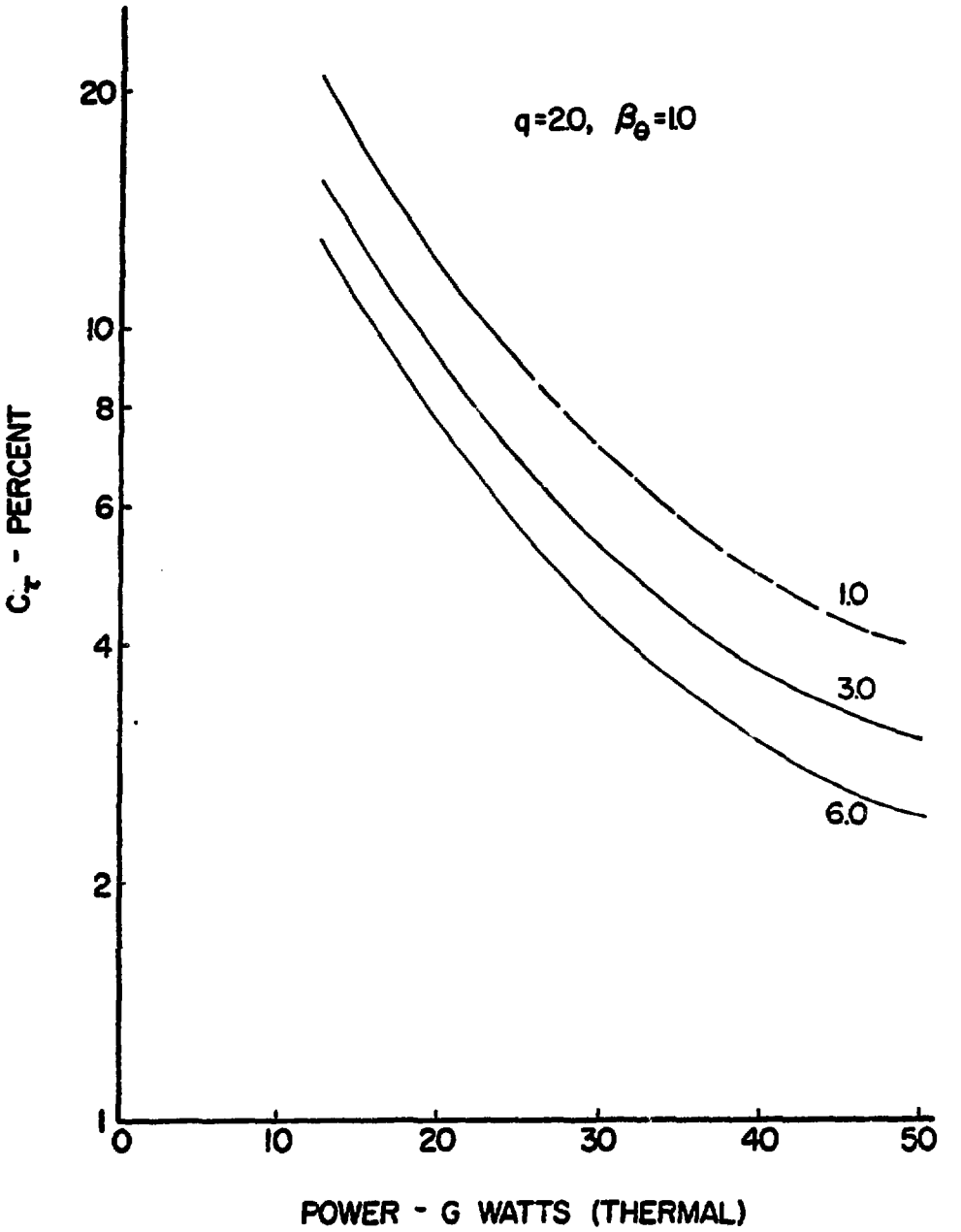

BEAM - FUELING (F_b=20%)
P_W VARIATION

FIGURE 25

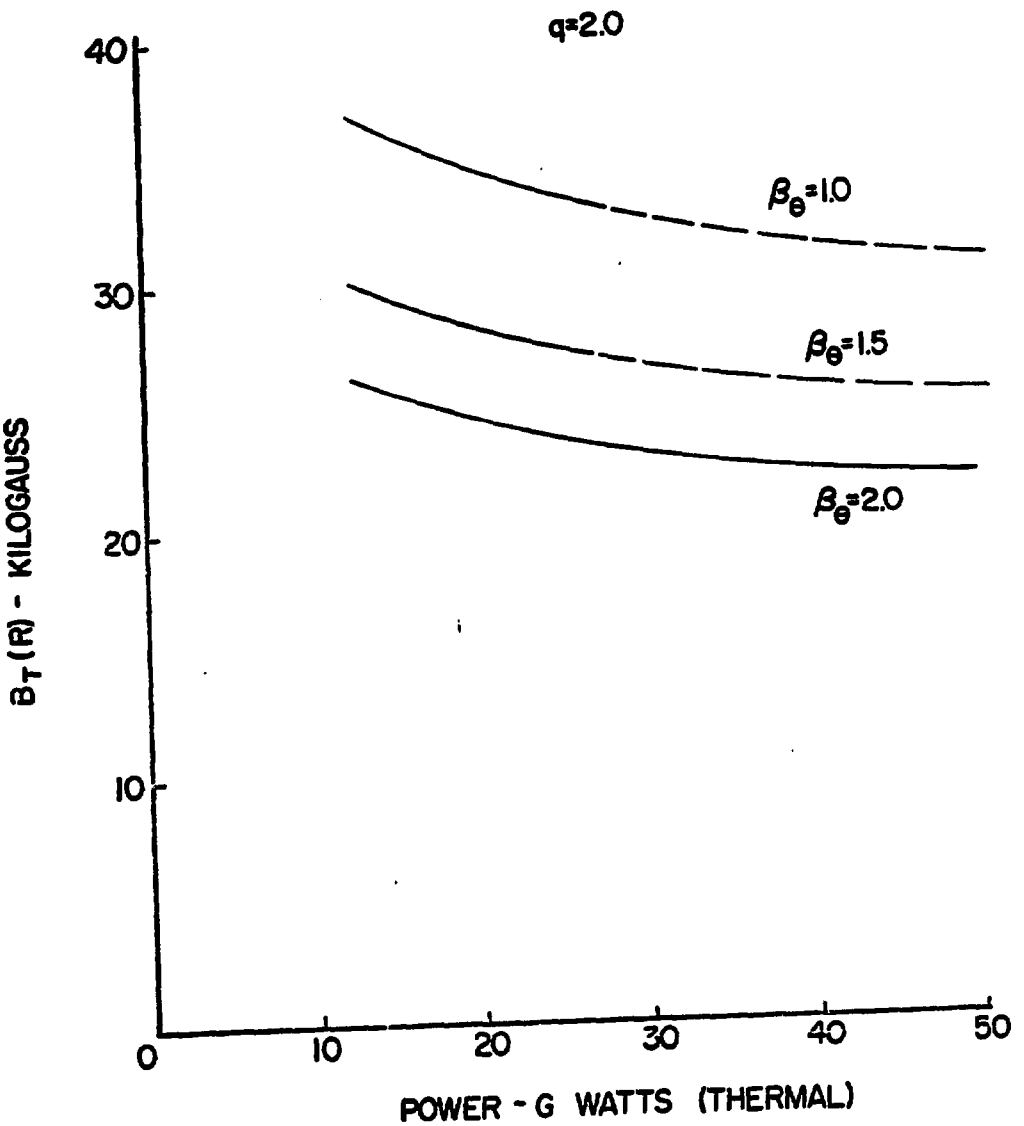

BEAM - FUELING (F_b=20%)

P_w = 1.0 MW/m^2

FIGURE 26

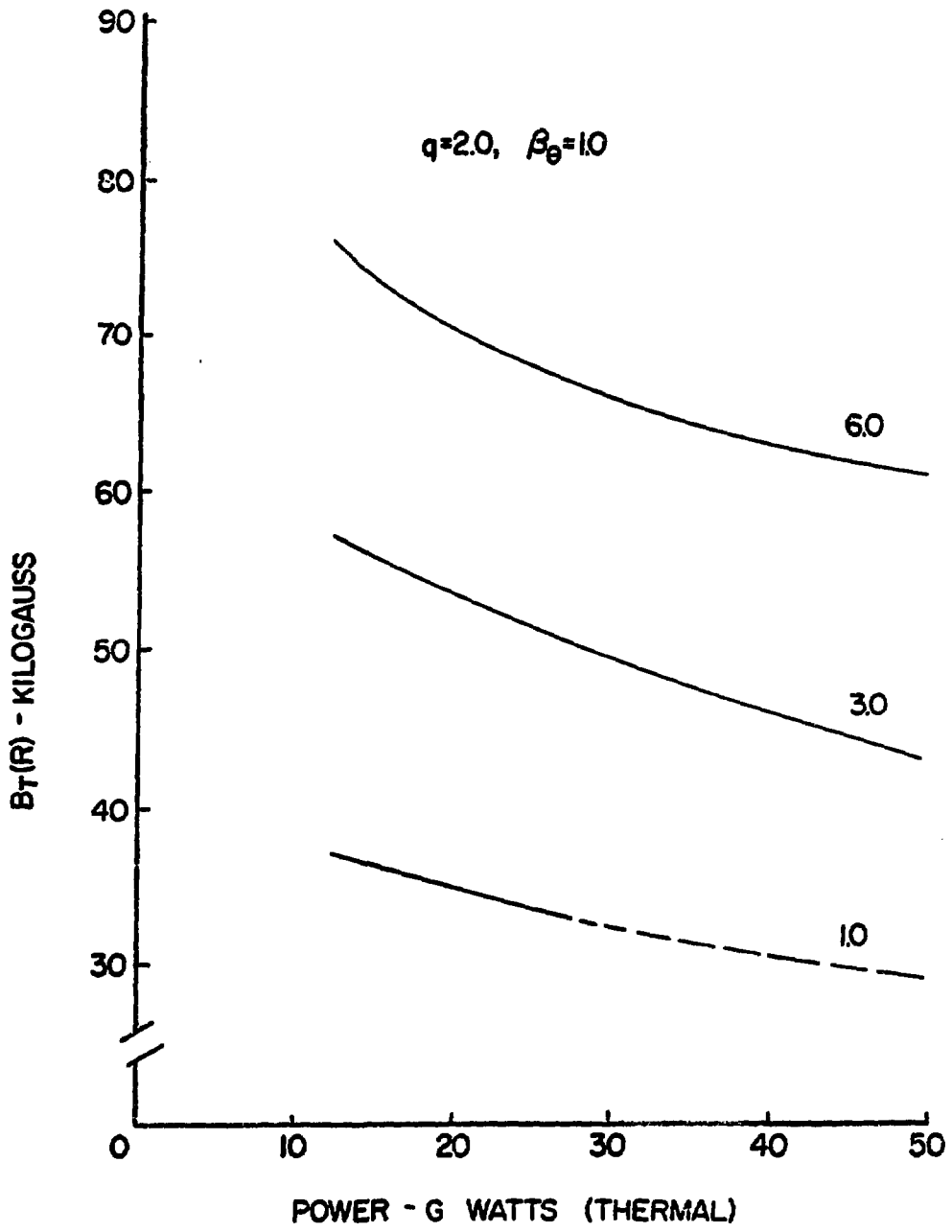

BEAM - FUELING (F_b=20%)
P_W VARIATION

FIGURE 27

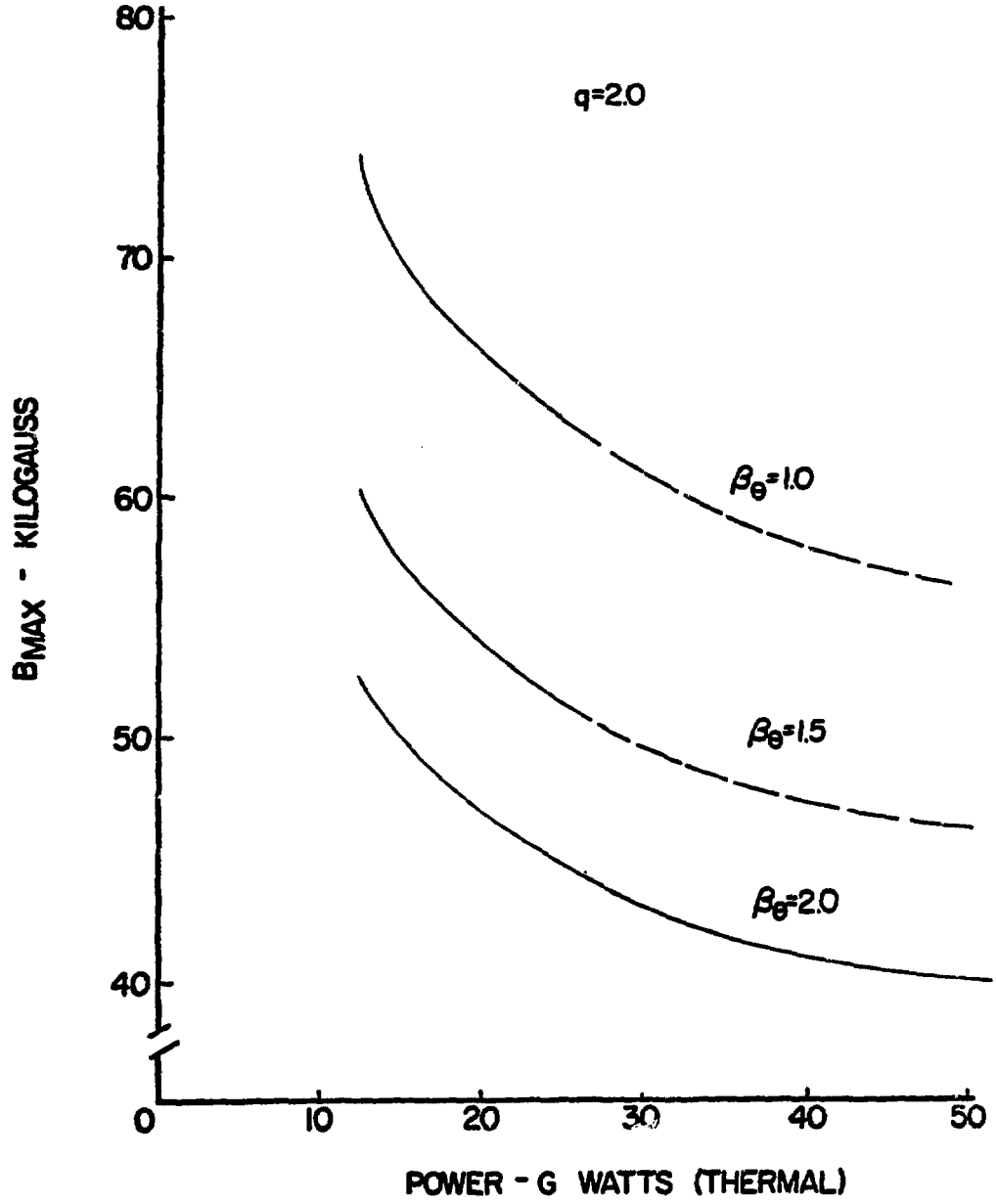

BEAM - FUELING (F_b=20%)
P_w = 1.0 MW/m^2

FIGURE 28

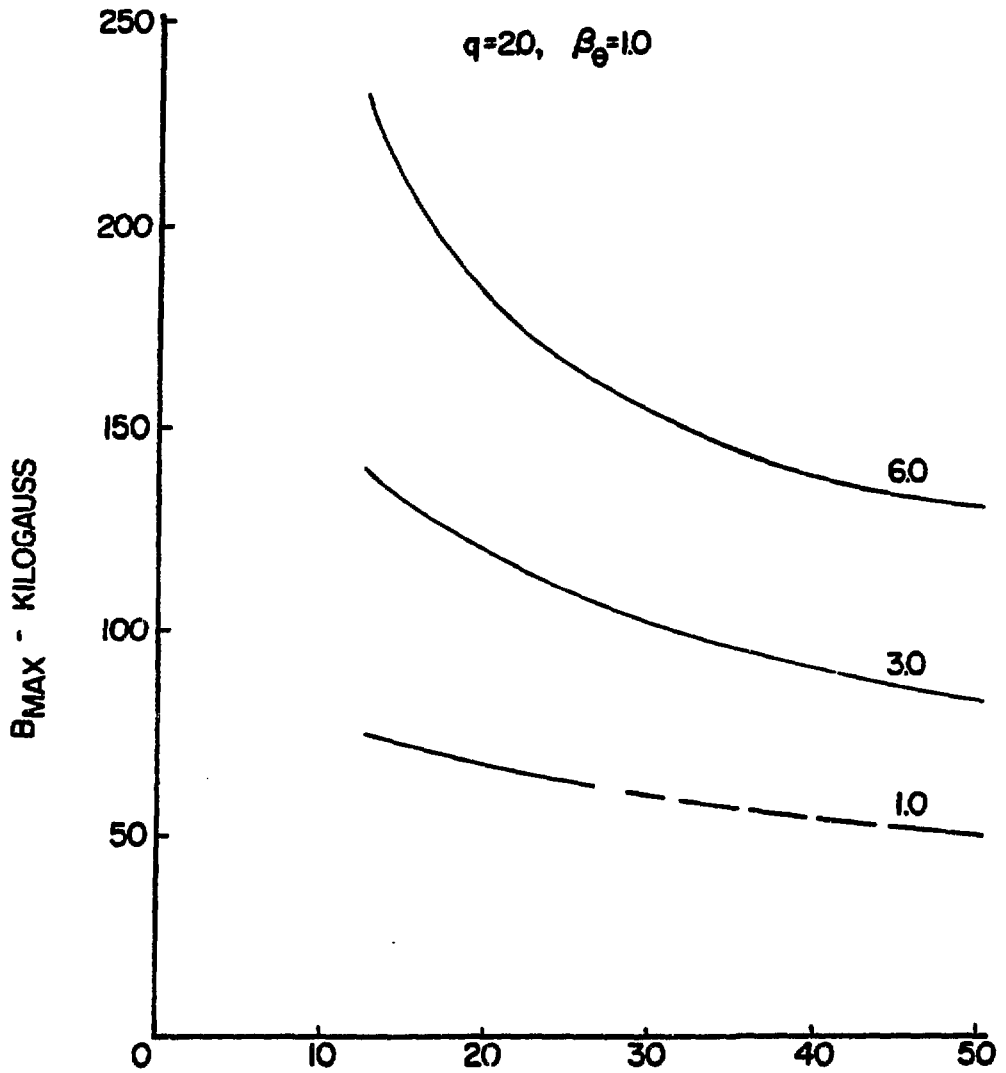

BEAM - FUELING (F_b=20%)
P_w VARIATION

FIGURE 29

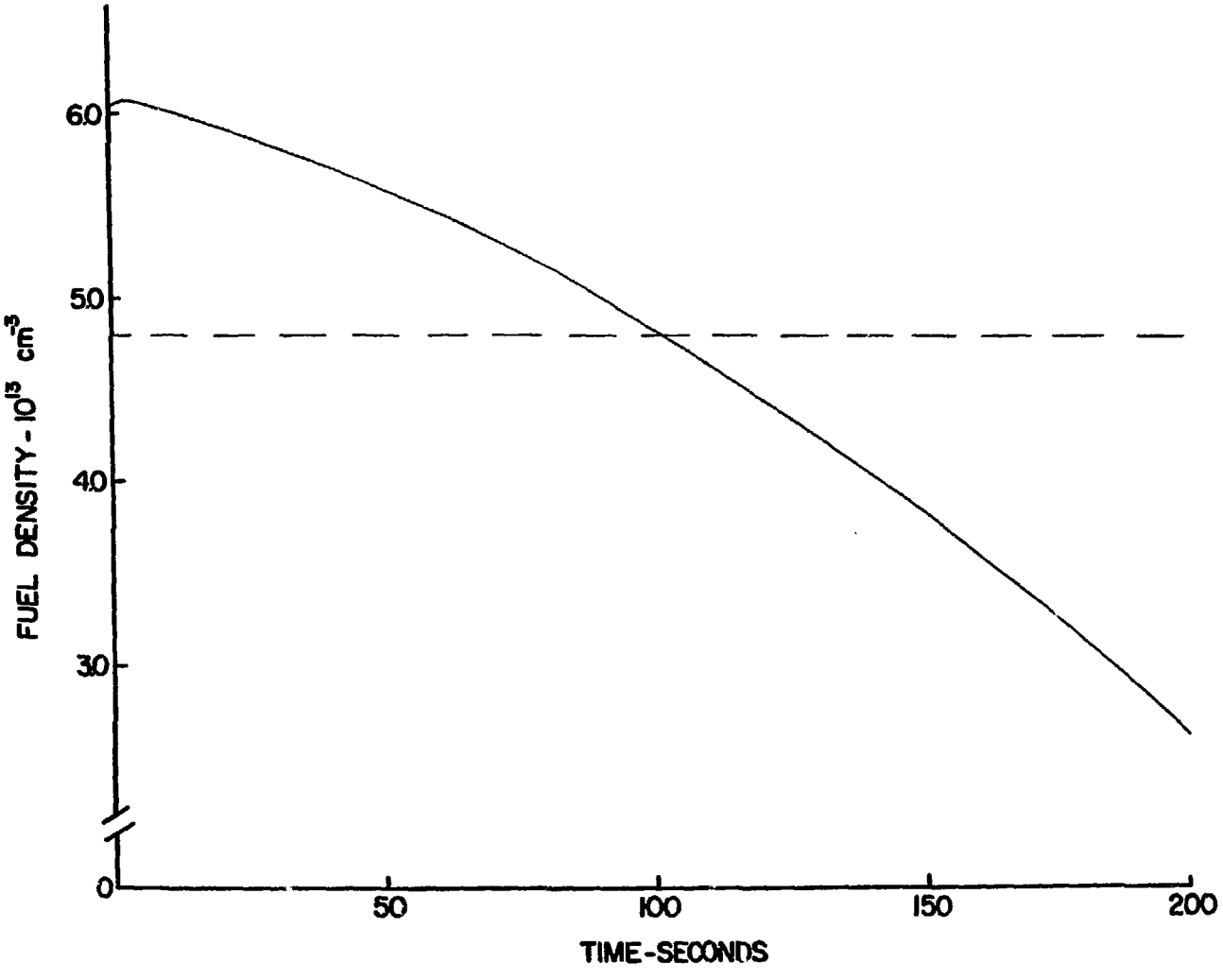

FUEL ION DENSITY FOR
200 SECOND PULSE

FIGURE 30

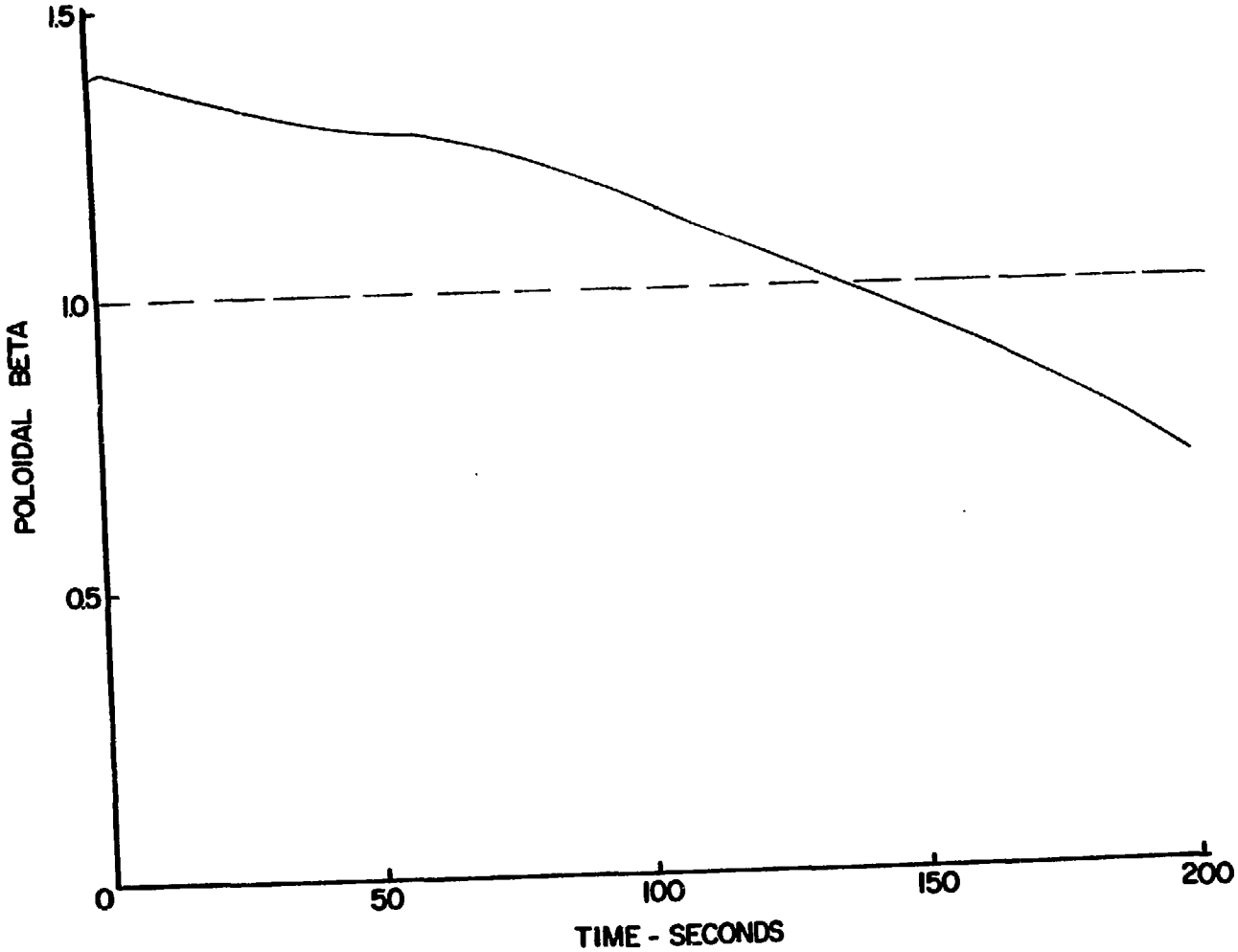

POLOIDAL BETA FOR 200
SECOND PULSE

FIGURE 31

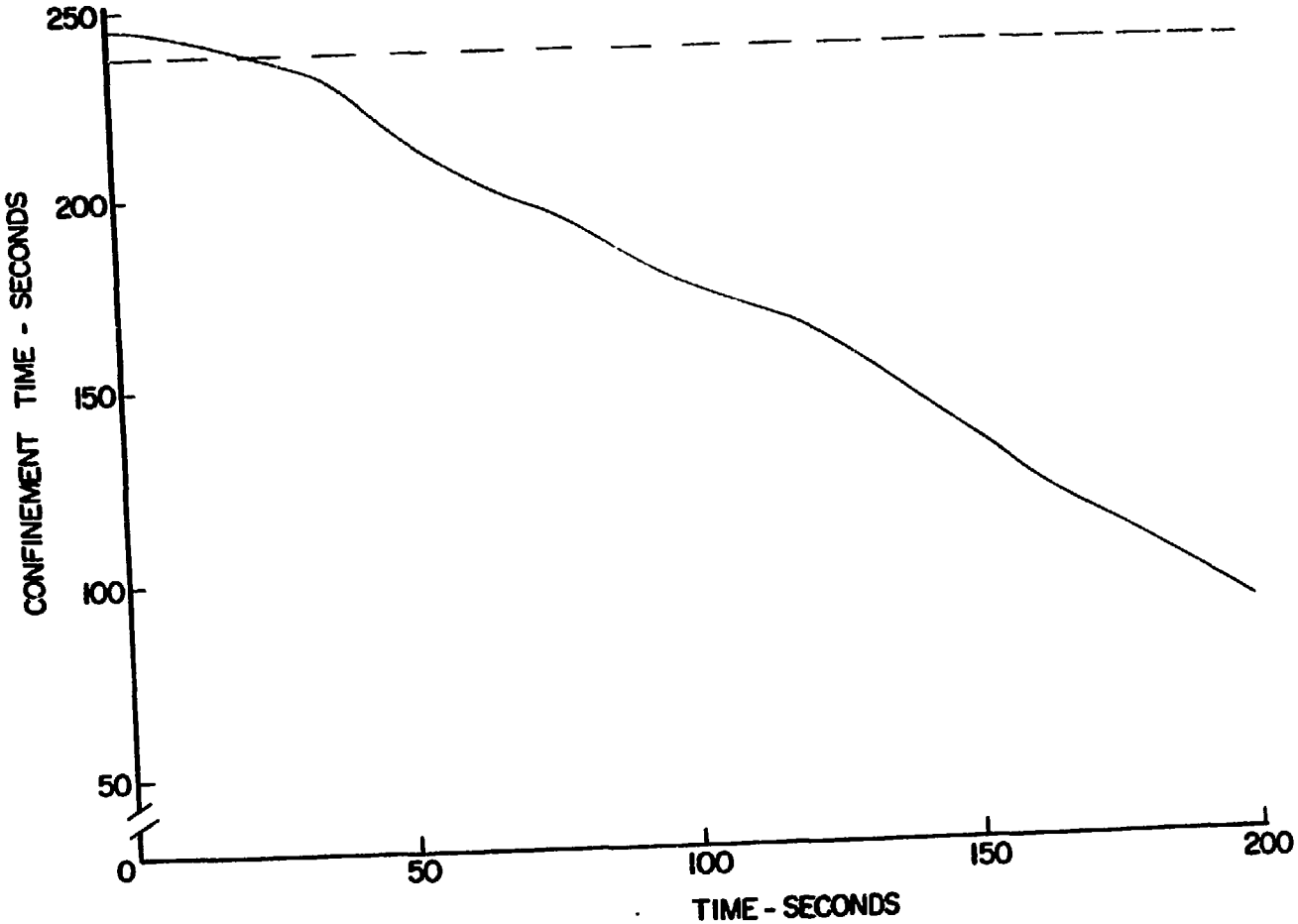

CONFINEMENT TIME FOR
200 SECOND PULSE

FIGURE 32

NOMENCLATURE

a	plasma minor radius
A	aspect ratio (= R/a)
A'	reduced aspect ratio (= A/3)
A_i	mass number of ion species i
b	bremsstrahlung coefficient, subscript identifying beam particles
b_t	reduced toroidal field (= B_t/50 kG)
B_p	poloidal magnet field
B_t	toroidal magnet field
c	mathematical constant
c_p	pulsed power fraction
c_τ	coefficient of trapped ion scaling
D	deuterium, diffusion coefficient
e	subscript identifying electrons
$\bar{E}_b$	average energy of beam particle
$\bar{E}_\alpha$	average energy of slowing-down alpha particle
E_{bo}	initial beam particle energy
$E_{\alpha o}$	initial alpha particle energy
E^b_{crit}	critical beam energy
E^α_{crit}	critical alpha particle energy
E_{fus}	total energy released in fusion reaction and subsequent events

f	subscript identifying fuel ions
f_{TCT}	per-particle probability of beam-plasma fusion while slowing down
F	factor indicating enhancement of beam energy due to beam-plasma fusion interactions
i	subscript identifying plasma ions
I	plasma current, subscript identifying impurity ions
k_s	synchrotron coefficient
k	mathematical constant
n_b	beam ion density ($= S_b \tau_{SD}^b$)
n_e	electron density
n_f	fuel ion density
n_i	ion density
n_α	alpha particle density
o	subscript identifying steady-state or initial value
p_w	wall loading
P_b	bremsstrahlung power
P_s	synchrotron power
P_t	total reactor thermal power rating
Q_α	equivalent to $E_{\alpha o}$, energy of alpha particle born in fusion reaction
r	poloidal radius variable
r_f	reflection coefficient for synchrotron radiation
r_w	first wall radius

R	plasma major radius
S	pellet source strength
S_b	beam source strength
S_t	total source strength ($= S + S_b$)
t	time variable
t_p	pulse length
T	Tritium, time-dependent temperature variable
T_e	electron temperature
T_i	ion temperature
U_{bi}	fractional multiplier to determine amount of beam energy transferred to ions
$U_{\alpha i}$	fractional multiplier to determine amount of alpha energy transferred to ions
v	relative velocity
V_b	beam particle initial energy ($= E_{bo}$)
W_{ei}	energy transfer rate from electrons to ions
Z_{eff}	effective charge of plasma ($= \Sigma\, n_i Z_i^2/n_e$)
Z_i	electronic charge of ion species i
α	subscript identifying alpha particles, control function constant
β	ratio of plasma pressure to total magnetic pressure
β_{pe}	ratio of plasma electron pressure to poloidal magnetic pressure
β_t	ratio of plasma pressure to toroidal magnetic pressure ($= \beta$)

β_θ	ratio of plasma pressure to poloidal magnetic pressure
Δt	delay time
Λ_e	electron coulomb logarithm argument
Λ_i	ion coulomb logarithm argument
σ	reaction cross section
$\langle \sigma v \rangle$	reaction probability
τ	confinement time ($= a^2/4D$)
τ'	numerical factor in slowing-down time expression
τ_B	Bohm confinement time preduction
τ_E	energy confinement time
τ_{SD}^b	beam slowing-down time
τ_{SD}^α	alpha slowing-down time

APPENDIX

STEADY-STATE RESULTS

Note:

Due to an error in the reference from which the expression for the Bohm confinement time was taken, the values of τ/τ_B presented in the tables are in error. Multiplying the tabulated values by 64 should produce the correct ratio.

Table A1: Pellet-Fueling Model, V_b = 200 keV, p_w = 1.0 MW/m^2

				Densities								Sources					
P_t	q	θ_θ	T_e (keV)	N_e (10^{13})	N_α (10^{12})	N_I (10^{12})	f_B (%)	C_τ	τ (s)	τ/τ_B	Pellet (10^{11})	Beam (10^{11})	Total (10^{11})	I (MA)	B_T (kG)	B_{max} (kG)
12.5	2	1	8.91	7.24	3.12	1.01	10.8	0.1	44.7	4.0	8.40	3.64	12.04	36.6	36.0	71.3
	2.5	1	8.92	7.47	4.81	.95	15.9	0.1	69.5	4.9	4.96	3.25	8.21	37.1	45.7	90.5
		1.5	8.91	7.25	3.25	1.00	11.2	0.1	46.5	4.0	8.02	3.59	11.61	29.9	36.8	72.8
	1.5	1	9.08	9.09	16.1	.59	39.1	1.0	237.	25.5	.95	2.38	3.33	40.9	30.2	59.8
		1.5	9.04	8.33	10.9	.74	30.3	1.0	160.	22.0	1.84	2.46	4.30	32.0	23.7	46.8
		2	9.01	7.95	8.30	.83	24.8	1.0	121.	19.6	2.69	2.57	5.26	27.1	20.0	39.6
	2	1														
		1.5	9.10	9.52	19.0	.51	43.0	1.0	278.	27.0	.64	2.38	3.02	34.1	33.7	66.6
		2	9.07	8.84	14.4	.64	36.4	1.0	211.	24.5	1.18	2.40	3.58	28.5	28.1	55.6
	2.5	1														
		1.5														
		2	9.12	9.99	22.0	.43	46.7	1.0	323.	28.4	.38	2.41	2.79	30.3	37.3	73.8
25.	1.5	1	8.95	6.07	3.34	.80	13.7	0.1	70.9	4.5	4.29	2.17	6.46	47.9	24.8	46.0
		1.5	8.92	5.93	2.27	.84	9.7	0.1	47.8	3.7	6.64	2.53	9.17	38.7	20.0	37.1
		2	8.90	5.86	1.74	.86	7.5	0.1	36.1	3.3	8.95	2.89	11.84	33.3	17.2	32.0
	2	1	8.98	6.42	5.83	.72	21.8	0.1	125.	5.8	2.16	1.90	4.06	49.2	33.9	63.0
		1.5	8.96	6.15	3.93	.78	15.8	0.1	83.8	4.9	3.54	2.07	5.61	39.4	27.1	50.4
		2	8.94	6.02	2.99	.81	12.4	0.1	63.2	4.3	4.89	2.26	7.15	33.8	23.3	43.2
	2.5	1	8.99	6.88	9.02	.62	30.2	0.1	193.	7.0	1.08	1.86	2.94	50.9	43.8	81.4
		1.5	8.98	6.45	6.06	.71	22.5	0.1	130.	5.9	2.05	1.89	3.94	40.3	34.7	64.5
		2	8.97	6.24	4.59	.76	18.0	0.1	97.9	5.2	2.94	1.99	4.93	34.4	29.6	55.0
	1.5	1														
		1.5	9.16	8.56	20.2	.30	49.4	1.0	437.	29.4	.26	1.53	1.79	46.3	23.9	44.4
		2	9.12	7.82	15.4	.43	42.7	1.0	334.	26.9	.53	1.55	2.08	38.4	19.8	36.8
	2	1.5														
		2	9.21	9.53	26.4	.16	56.1	1.0	571.	31.7	.04	1.54	1.58	42.2	29.1	54.1
50.	1.5	1	9.02	5.52	6.29	.55	26.7	0.1	197.	6.5	1.08	1.19	2.27	65.2	23.6	42.0
		1.5	8.99	5.23	4.25	.61	19.7	0.1	133.	5.5	1.79	1.29	3.08	51.9	18.8	33.4
		2	8.97	5.09	3.23	.65	15.7	0.1	100.	4.8	2.49	1.39	3.88	44.3	16.0	28.6
	2	1	9.07	6.20	10.9	.41	38.9	0.1	343.	8.0	.42	1.15	1.57	69.0	33.3	59.3
		1.5	9.03	5.68	7.40	.52	30.1	0.1	232.	6.9	.85	1.17	2.02	54.0	26.1	46.4
		2	9.01	5.43	5.61	.57	24.6	0.1	176.	6.2	1.26	1.21	2.47	45.7	22.1	39.3
	2.5	1	9.11	7.10	16.8	.25	49.3	0.1	525.	9.3	.02	1.22	1.24	73.6	44.4	79.0
		1.5	9.07	6.27	11.4	.40	39.8	0.1	357.	8.2	.38	1.15	1.53	56.6	34.1	60.8
		2	9.04	5.86	8.62	.47	33.4	0.1	271.	7.4	.67	1.15	1.82	47.5	28.6	51.0

Table A2: Pellet-Fueling Model, V_b = 200 keV, p_w = 3.0 MW/m^2

				Densities							Sources					
P_t	q	β_θ	T_e (keV)	N_e (10^{14})	N_α (10^{13})	N_I (10^{12})	f_B (%)	C_τ	τ (s)	τ/τ_B	Pellet (10^{12})	Beam (10^{12})	Total (10^{12})	I (MA)	B_T (kG)	B_{max} (kG)
12.5	1.5	1	9.12	2.37	5.11	1.08	45.9	1.0	131.	28.1	.30	1.35	1.65	36.9	48.7	117.
	2	1.5	9.14	2.50	6.00	.85	49.9	1.0	153.	29.6	.13	1.36	1.49	30.9	54.5	130.
		2	9.10	2.29	4.57	1.22	43.2	1.0	117.	27.1	.39	1.34	1.73	25.6	45.2	108.
25.	2	1	9.00	1.58	1.80	1.56	26.8	0.1	69.3	6.5	.83	1.01	1.84	43.4	53.1	111.
	2.5	1	9.02	1.72	2.79	1.26	36.1	0.1	107.	7.7	.34	1.02	1.36	45.3	69.2	144.
		1.5	9.00	1.59	1.88	1.53	27.6	0.1	72.1	6.6	.78	1.01	1.79	35.6	54.4	113.
		2	8.98	1.52	1.42	1.68	22.3	0.1	54.4	5.9	1.17	1.04	2.21	30.2	46.2	96.2
	1.5	1.5	9.21	2.24	6.18	.38	55.9	1.0	240.	31.6	.04	.85	.89	42.1	38.6	80.6
		2	9.16	2.01	4.73	.73	49.2	1.0	184.	29.3	.16	.85	1.01	34.6	31.8	66.3
50.	1.5	1	9.04	1.14	1.55	.98	31.3	0.1	125.	7.1	.31	.45	.76	59.4	33.8	63.7
		1.5	9.01	1.06	1.05	1.14	23.5	0.1	84.1	6.0	.53	.48	1.01	47.0	26.8	50.4
		2	8.99	1.03	.80	1.22	18.9	0.1	63.6	5.3	.75	.51	1.26	40.0	22.8	42.9
	2	1	9.10	1.30	2.69	.66	44.2	0.1	216.	8.7	.09	.44	.53	63.5	48.2	90.9
		1.5	9.05	1.18	1.82	.90	34.9	0.1	147.	7.6	.24	.44	.68	49.3	37.4	70.5
		2	9.03	1.11	1.38	1.03	28.9	0.1	111.	6.8	.37	.45	.82	41.6	31.6	59.4
	2.5	1.5	9.10	1.32	2.80	.63	45.1	0.1	225.	8.8	.08	.45	.53	52.2	49.5	93.3
		2	9.07	1.22	2.12	.81	38.5	0.1	171.	8.0	.18	.44	.62	43.5	41.3	77.7

Table A3: Pellet-Fueling Model, V_b = 200 keV, P_w = 6.0 MW/m^2

				Densities							Sources					
P_t	q	β_θ	T_e (keV)	N_e (10^{14})	N_α (10^{13})	N_I (10^{12})	f_B (%)	C_τ	τ (s)	τ/τ_B	Pellet (10^{12})	Beam (10^{12})	Total (10^{12})	I (MA)	B_T (kG)	B_{max} (kG)
12.5	2	1.5	9.17	4.67	12.30	1.08	53.8	1.0	102.	30.9	.06	4.23	4.29	28.8	74.4	225.
25.	2.5	1	9.03	3.12	5.79	1.91	40.4	0.1	74.1	8.3	.60	3.07	3.67	42.3	93.2	223.
		2	9.01	2.84	3.90	2.46	31.4	0.1	50.0	7.1	1.76	2.97	4.73	33.0	72.8	174.
	1.5	2	9.20	3.73	9.77	.88	53.6	1.0	126.	30.8	.25	2.52	2.77	32.7	43.2	103.
50.	1.5	1	9.06	2.42	3.91	1.78	36.2	0.1	75.9	7.7	.91	1.81	2.72	53.8	49.4	103.
		1.5	9.02	2.24	2.65	2.16	27.7	0.1	51.4	6.6	1.66	1.89	3.55	42.3	38.8	80.9
	2	1	9.13	2.86	6.77	1.01	49.5	0.1	131.	9.3	.14	1.85	1.99	58.3	71.3	149.
		1.5	9.08	2.53	4.60	1.58	40.0	0.1	89.3	8.2	.66	1.80	2.46	44.8	54.9	114.
		2	9.05	2.36	3.50	1.90	33.6	0.1	67.8	7.4	1.10	1.83	2.93	37.6	46.0	95.9
	2.5	1.5	9.14	2.90	7.04	.95	50.4	0.1	136.	9.4	.09	1.86	1.95	47.9	73.3	153.
		2	9.10	2.64	5.35	1.38	43.6	0.1	104.	8.6	.45	1.81	2.26	39.7	60.7	126.

Table A4: Pellet-Fueling Model, V_b = 350 keV, p_w = 1.0 MW/m^2

				Densities							Sources					
P_t	q	β_θ	T_e (keV)	N_e (10^{13})	N_α (10^{12})	N_I (10^{12})	f_B (%)	C_τ	τ (s)	τ/τ_B	Pellet (10^{11})	Beam (10^{11})	Total (10^{11})	I (MA)	B_T (kG)	B_{max} (kG)
12.5	2	1	9.03	7.21	3.00	1.00	10.6	0.1	43.5	3.9	10.13	2.20	12.33	36.7	36.2	71.6
	2.5	1	9.02	7.44	4.65	.95	15.5	0.1	67.9	4.8	6.62	1.96	8.38	37.2	45.9	90.7
		1.5	9.03	7.23	3.12	1.00	10.9	0.1	45.3	4.0	9.72	2.17	11.89	30.0	37.0	73.1
	1.5	1	9.14	9.04	15.8	.60	38.8	1.0	233.	25.3	1.93	1.43	3.36	40 9	30.2	59.8
		1.5	9.11	8.29	10.7	.75	30.0	1.0	158.	21.8	2.87	1.47	4.34	32.0	23.7	46.8
		2	9.09	7.91	8.08	.83	24.4	1.0	119.	19.4	3.79	1.54	5.33	27.1	20.1	39.7
	2	1	9.20	10.8	27.3	.30	52.2	1.0	403.	30.4	1.00	1.49	2.49	44.5	43.9	86.9
		1.5	9.15	9.45	18.6	.52	42.7	1.0	274.	26.9	1.63	1.43	3.06	34.1	33.6	66.5
		2	9.13	8.79	14.1	.65	36.1	1.0	208.	24.3	2.17	1.43	3.60	28.5	28.1	55.6
	2.5	1														
		1.5	9.20	11.0	28.4	.27	53.2	1.0	419.	30.7	.94	1.51	2.45	36.6	45.2	89.3
		2	9.17	9.92	21.6	.44	46.4	1.0	319.	28.2	1.37	1.44	2.81	30.2	37.2	73.7
25.	1.5	1	9.05	6.05	3.23	.80	13.4	0.1	69.3	4.4	5.29	1.31	6.60	48.1	24.8	46.2
		1.5	9.04	5.91	2.18	.84	9.4	0.1	46.4	3.7	7.88	1.53	9.41	38.9	20.1	37.3
		2	9.03	5.84	1.66	.86	7.3	0.1	35.0	3.2	10.44	1.76	12.20	33.5	17.3	32.1
	2	1	9.06	6.39	5.66	.72	21.5	0.1	122.	5.7	2.98	1.14	4.12	49.3	34.0	63.1
		1.5	9.05	6.13	3.81	.78	15.5	0.1	81.9	4.8	4.48	1.25	5.73	39.5	27.2	50.6
		2	9.05	6.00	2.88	.81	12.1	0.1	61.7	4.2	5.94	1.37	7.31	33.9	23.3	43.4
	2.5	1	9.07	6.84	8.78	.62	29.8	0.1	190.	6.9	1.86	1.11	2.97	50.9	43.9	81.5
		1.5	9.06	6.42	5.89	.71	22.2	0.1	127.	5.8	2.86	1.14	4.00	40.4	34.8	64.6
		2	9.06	6.32	4.44	.76	17.7	0.1	95.8	5.1	3.82	1.20	5.02	34.4	29.7	55.1
	1.5	1	9.28	9.93	28.9	.10	58.5	1.0	630.	32.5	.58	.93	1.51	61.1	31.5	58.6
		1.5	9.21	8.49	19.8	.31	49.2	1.0	432.	29.2	.89	.91	1.80	46.2	23.9	44.4
		2	9.17	7.77	15.1	.44	42.4	1.0	329.	26.7	1.17	.92	2.09	38.4	19.8	36.8
	2	1.5														
		2	9.26	9.45	25.9	.17	55.8	1.0	565.	31.6	.67	.92	1.59	42.2	29.0	53.9
50.	1.5	1	9.09	5.49	6.12	.55	26.4	0.1	193.	6.4	1.59	.71	2.30	65.3	23.6	42.1
		1.5	9.07	5.21	4.13	.61	19.4	0.1	130.	5.4	2.36	.77	3.13	52.0	18.8	33.5
		2	9.06	5.07	3.12	.65	15.4	0.1	98.0	4.8	3.12	.84	3.96	44.4	16.1	28.6
	2	1	9.13	6.16	10.7	.41	38.5	0.1	338.	8.0	.89	.69	1.58	68.9	33.3	59.2
		1.5	9.10	5.65	7.22	.51	29.7	0.1	228.	6.9	1.35	.70	2.05	54.0	26.1	46.4
		2	9.09	5.40	5.46	.57	24.2	0.1	172.	6.1	1.78	.73	2.51	45.8	22.1	39.3
	2.5	1	9.16	7.04	16.4	.26	49.0	0.1	519.	9.2	.51	.73	1.24	73.5	44.3	78.9
		1.5	9.13	6.23	11.1	.40	39.5	0.1	352.	8.1	.85	.69	1.54	56.6	34.1	60.8
		2	9.11	5.83	8.42	.48	33.0	0.1	266.	7.3	1.14	.69	1.83	47.5	28.6	51.0
	1.5	2	9.33	8.83	27.7	.002	62.0	1.0	881.	33.7	.38	.60	.98	58.1	21.0	37.4

Table A5: Pellet-Fueling Model, V_b = 350 keV, p_w = 3.0 MW/m^2

				Densities							Sources					
P_t	q	β_θ	T_e (keV)	N_e (10^{14})	N_α (10^{13})	N_I (10^{12})	f_B (%)	C_τ	τ (s)	τ/τ_B	Pellet (10^{12})	Beam (10^{12})	Total (10^{12})	I (MA)	B_T (kG)	B_{max} (kG)
12.5	1.5	1	9.17	2.35	5.01	1.10	45.6	1.0	129.	28.0	.83	.81	1.64	36.8	48.7	116.
	2	1	9.25	2.92	8.63	.24	59.0	1.0	222.	32.7	.38	.88	1.26	40.9	72.0	172.
		1.5	9.19	2.49	5.88	.88	49.6	1.0	152.	29.4	.69	.81	1.50	30.9	54.4	130.
		2	9.16	2.27	4.48	1.24	42.9	1.0	115.	26.9	.94	.80	1.74	25.6	45.1	108.
	2.5	1.5	9.25	2.98	8.97	.17	60.0	1.0	231.	33.0	.35	.90	1.25	33.7	74.2	177.
		2	9.21	2.63	6.83	.65	53.4	1.0	176.	30.8	.57	.83	1.40	27.5	60.6	145.
25.	2	1	9.07	1.57	1.75	1.56	26.4	0.1	68.1	6.4	1.26	.61	1.87	43.5	53.2	111.
	2.5	1	9.08	1.71	2.72	1.27	35.8	0.1	105.	7.7	.77	.61	1.38	45.3	69.2	144.
		1.5	9.07	1.58	1.82	1.54	27.2	0.1	70.9	6.5	1.21	.60	1.81	35.6	54.5	114.
		2	9.07	1.51	1.38	1.68	22.0	0.1	53.4	5.8	1.62	.62	2.24	30.2	46.3	96.4
	1.5	1.5	9.26	2.22	6.07	.41	55.6	1.0	237.	31.5	.38	.51	.89	42.0	38.6	80.4
		2	9.21	2.00	4.64	.75	49.0	1.0	182.	29.2	.50	.50	1.00	34.6	31.7	66.2
	2	2	9.31	2.52	7.92	.003	62.0	1.0	309.	33.7	.28	.52	.80	38.7	47.3	98.7
50.	1.5	1	9.11	1.13	1.51	.99	31.0	0.1	123.	7.0	.50	.27	.77	59.4	33.8	63.7
		1.5	9.08	1.06	1.02	1.14	23.2	0.1	82.6	6.0	.74	.29	1.03	47.1	26.8	50.5
		2	9.07	1.02	.77	1.23	18.6	0.1	62.3	5.3	.97	.30	1.27	40.1	22.8	43.0
	2	1	9.15	1.30	2.63	.67	43.9	0.1	213.	8.6	.28	.27	.55	63.5	48.2	90.8
		1.5	9.12	1.17	1.78	.91	34.6	0.1	145.	7.5	.42	.26	.68	49.3	37.5	70.5
		2	9.10	1.11	1.35	1.04	28.6	0.1	109.	6.7	.56	.27	.83	41.6	31.6	59.5
	2.5	1	9.20	1.51	4.03	.32	54.4	0.1	326.	9.9	.15	.29	.44	68.4	64.9	122.
		1.5	9.16	1.31	2.73	.64	44.8	0.1	222.	8.7	.26	.27	.53	52.1	49.5	93.2
		2	9.13	1.21	2.07	.82	38.1	0.1	168.	7.9	.36	.26	.62	43.5	41.3	77.7

Table A6: Pellet-Fueling Model, V_b = 350 keV, p_w = 6.0 MW/m^2

				Densities							Sources					
P_t	q	β_θ	T_e (keV)	N_e (10^{14})	N_α (10^{13})	N_I (10^{12})	f_B (%)	C_τ	τ (s)	τ/τ_B	Pellet (10^{12})	Beam (10^{12})	Total (10^{12})	I (MA)	B_T (kG)	B_{max} (kG)
12.5	2	1.5	9.22	4.64	12.06	1.13	53.5	1.0	101.	30.8	1.79	2.52	4.31	28.8	74.3	225.
	2.5	2	9.24	4.94	14.01	.68	57.2	1.0	117.	32.1	1.44	2.60	4.04	25.7	82.9	251.
25.	2.5	1	9.10	3.10	5.65	1.94	40.1	0.1	73.0	8.2	1.85	1.84	3.70	42.3	93.2	223.
		1.5	9.08	2.83	3.80	2.47	31.0	0.1	49.1	7.0	3.00	1.78	4.78	33.1	72.8	174.
	1.5	1.5	9.29	4.17	12.5	.26	60.0	1.0	163.	33.0	.96	1.52	2.48	39.9	52.8	126.
		2	9.24	3.70	9.59	.92	53.3	1.0	125.	30.7	1.28	1.50	2.78	32.6	43.2	103.
50.	1.5	1	9.12	2.41	3.83	1.80	35.8	0.1	74.8	7.7	1.66	1.08	2.74	53.8	49.4	103.
		1.5	9.09	2.23	2.59	2.17	27.4	0.1	50.5	6.5	2.46	1.13	3.59	42.3	38.9	81.0
	2	1	9.18	2.83	6.63	1.04	49.1	0.1	130.	9.3	.90	1.10	2.00	58.2	71.2	148.
		1.5	9.14	2.51	4.50	1.60	39.6	0.1	88.1	8.1	1.40	1.08	2.48	44.8	54.8	114.
		2	9.11	2.35	3.42	1.92	33.2	0.1	66.8	7.3	1.87	1.09	2.96	37.6	46.0	95.9
	2.5	1	9.23	3.39	10.2	.23	59.6	0.1	198.	10.4	.40	1.26	1.66	63.4	97.0	202.
		1.5	9.19	2.87	6.89	.98	50.1	0.1	135.	9.4	.85	1.11	1.96	47.8	73.2	153.
		2	9.15	2.62	5.24	1.40	43.3	0.1	103.	8.6	1.19	1.08	2.27	39.6	60.6	126.

Table A7: Pellet-Fueling Model, V_b = 500 keV, p_w = 1.0 MW/m^2

				Densities							Sources					
P_t	q	β_θ	T_e (keV)	N_e (10^{13})	N_α (10^{12})	N_I (10^{12})	f_B (%)	C_τ	τ (s)	τ/τ_B	Pellet (10^{11})	Beam (10^{11})	Total (10^{11})	I (MA)	B_T (kG)	B_{max} (kG)
12.5	2	1	9.11	7.19	2.91	1.00	10.4	0.1	42.7	3.8	10.95	1.61	12.56	36.8	36.3	71.8
	2.5	1	9.09	7.41	4.53	.95	15.3	0.1	66.7	4.7	7.07	1.42	8.49	37.3	46.0	90.9
		1.5	9.11	7.21	3.03	1.00	10.8	0.1	44.4	3.9	10.52	1.59	12.11	30.1	37.1	73.4
	1.5	1	9.18	8.99	15.5	.61	38.5	1.0	231.	25.2	2.35	1.03	3.38	40.9	30.2	59.8
		1.5	9.16	8.25	10.5	.75	29.7	1.0	156.	21.7	3.32	1.06	4.38	32.0	23.7	46.9
		2	9.15	7.89	7.92	.83	24.2	1.0	118.	19.3	4.27	1.11	5.38	27.2	20.1	39.7
	2	1	9.24	10.7	26.9	.31	52.0	1.0	400.	30.3	1.43	1.08	2.51	44.5	43.9	86.7
		1.5	9.20	9.40	18.2	.53	42.4	1.0	272.	26.7	2.04	1.03	3.07	34.1	33.6	66.5
		2	9.17	8.75	13.8	.65	35.8	1.0	206.	24.2	2.60	1.04	3.64	28.5	28.1	55.6
	2.5	1														
		1.5	9.24	10.9	27.9	.28	53.0	1.0	415.	30.6	1.37	1.09	2.46	36.6	45.1	89.2
		2	9.21	9.86	21.2	.45	46.2	1.0	316.	28.1	1.78	1.04	2.82	30.2	37.2	73.6
25.	1.5	1	9.13	6.03	3.15	.80	13.2	0.1	68.1	4.4	5.75	.95	6.70	48.2	24.9	46.3
		1.5	9.13	5.89	2.12	.84	9.2	0.1	45.5	3.6	8.47	1.12	9.59	39.0	20.1	37.4
		2	9.13	5.82	1.60	.85	7.1	0.1	34.2	3.2	11.18	1.29	12.47	33.6	17.4	32.3
	2	1	9.12	6.37	5.54	.72	21.2	0.1	120.	5.7	3.35	.83	4.18	49.4	34.0	63.2
		1.5	9.12	6.11	3.72	.78	15.3	0.1	80.6	4.7	4.90	.90	5.80	39.6	27.3	50.7
		2	9.13	5.98	2.80	.81	11.9	0.1	60.6	4.1	6.43	.99	7.42	34.0	23.4	43.5
	2.5	1	9.12	6.81	8.60	.62	29.5	0.1	187.	6.8	2.19	.81	3.00	51.0	43.9	81.5
		1.5	9.12	6.40	5.76	.71	21.9	0.1	125.	5.8	3.22	.82	4.10	40.4	34.8	64.7
		2	9.12	6.20	4.34	.76	17.4	0.1	94.3	5.1	4.22	.87	5.09	34.5	29.7	55.2
	1.5	1	9.31	9.87	28.5	.11	58.3	1.0	625.	32.4	.85	.67	1.52	60.9	31.5	58.5
		1.5	9.25	8.44	19.5	.32	48.9	1.0	428.	29.1	1.15	.66	1.81	46.2	23.9	44.3
		2	9.21	7.73	14.9	.44	42.2	1.0	326.	26.6	1.43	.67	2.10	38.3	19.8	36.8
	2	1.5	9.34	10.7	33.4	.003	62.1	1.0	732.	33.7	.74	.69	1.43	51.6	35.6	66.1
		2	9.29	9.39	25.6	.17	55.6	1.0	561.	31.5	.93	.67	1.60	42.1	29.0	53.9
50.	1.5	1	9.15	5.47	6.00	.55	26.1	0.1	191.	6.4	1.81	.52	2.33	65.3	23.6	42.1
		1.5	9.14	5.20	4.04	.61	19.2	0.1	128.	5.4	2.61	.56	3.17	52.1	18.8	33.5
		2	9.13	5.06	3.05	.65	15.2	0.1	96.5	4.7	3.40	.61	4.01	44.5	16.1	28.7
	2	1	9.17	6.13	10.5	.42	38.3	0.1	334.	7.9	1.09	.50	1.59	68.9	33.3	59.2
		1.5	9.15	5.63	7.08	.52	29.5	0.1	226.	6.8	1.56	.51	2.07	54.0	26.1	46.4
		2	9.14	5.38	5.35	.57	24.0	0.1	170.	6.1	2.01	.53	2.54	45.8	22.1	39.4
	2.5	1	9.21	6.99	16.1	.27	48.8	0.1	514.	9.2	.72	.52	1.24	73.4	44.3	78.8
		1.5	9.18	6.19	10.9	.40	39.2	0.1	348.	8.1	1.05	.50	1.55	56.6	34.1	60.7
		2	9.16	5.80	8.26	.48	32.8	0.1	263.	7.3	1.36	.50	1.86	47.5	28.6	51.0
	1.5	2	9.36	8.77	27.4	.009	61.9	1.0	875.	33.6	.55	.44	.99	57.9	21.0	37.3

Table A8: Pellet-Fueling Model, V_b = 500 keV, p_w = 3.0 MW/m^2

				Densities							Sources					
P_t	q	β_θ	T_e (keV)	N_e (10^{14})	N_α (10^{13})	N_I (10^{12})	f_B (%)	C_τ	τ (s)	τ/τ_B	Pellet (10^{12})	Beam (10^{12})	Total (10^{12})	I (MA)	B_T (kG)	B_{max} (kG)
12.5	1.5	1	9.21	2.34	4.93	1.12	45.4	1.0	128.	27.8	1.06	.58	1.64	36.8	48.7	116.
	2	1	9.28	2.90	8.50	.27	58.8	1.0	220.	32.7	.63	.64	1.27	40.8	71.9	172.
		1.5	9.23	2.47	5.79	.90	49.4	1.0	150.	29.3	.92	.59	1.51	30.9	54.4	130.
		2	9.20	2.26	4.40	1.26	42.6	1.0	114.	26.8	1.17	.58	1.75	25.6	45.1	108.
	2.5	1.5	9.29	2.95	8.84	.20	59.8	1.0	229.	33.0	.60	.65	1.25	33.6	74.0	177.
		2	9.25	2.62	6.73	.67	53.1	1.0	175.	30.7	.81	.60	1.41	27.5	60.5	145.
25.	2	1	9.13	1.56	1.72	1.57	26.2	0.1	67.2	6.4	1.45	.44	1.89	43.5	53.2	111.
	2.5	1	9.14	1.70	3.47	1.28	35.5	0.1	104.	7.6	.95	.44	1.39	45.3	69.3	144.
		1.5	9.13	1.57	1.79	1.55	27.0	0.1	69.9	6.5	1.39	.44	1.83	35.6	54.5	114.
		2	9.13	1.51	1.35	1.69	21.8	0.1	52.7	5.7	1.82	.45	2.27	30.3	46.3	96.6
	1.5	1.5	9.29	2.21	5.99	.42	55.4	1.0	235.	31.4	.53	.36	.89	42.0	38.5	80.3
		2	9.25	1.99	4.58	.76	48.7	1.0	180.	29.1	.65	.36	1.01	34.6	31.7	66.1
	2	2	9.34	2.50	7.82	.023	61.9	1.0	307.	33.7	.42	.37	.79	38.6	47.2	98.5
50.	1.5	1	9.16	1.12	1.48	1.00	30.7	0.1	121.	7.0	.58	.19	.77	59.5	33.9	63.8
		1.5	9.14	1.05	1.00	1.15	23.0	0.1	81.5	5.9	.83	.21	1.04	47.1	26.8	50.5
		2	9.13	1.02	.76	1.23	18.3	0.1	61.4	5.2	1.07	.22	1.29	40.2	22.9	43.1
	2	1	9.20	1.29	2.59	.68	43.6	0.1	211.	8.6	.35	.19	.54	63.4	48.2	90.7
		1.5	9.17	1.16	1.75	.92	34.3	0.1	143.	7.5	.50	.19	.69	49.3	37.5	70.6
		2	9.15	1.10	1.32	1.04	28.3	0.1	108.	6.7	.64	.20	.84	41.6	31.6	59.5
	2.5	1	9.24	1.50	3.97	.34	54.2	0.1	323.	9.8	.23	.21	.44	68.3	64.8	122.
		1.5	9.20	1.30	2.70	.65	44.6	0.1	220.	8.7	.34	.19	.53	52.1	49.4	93.1
		2	9.18	1.21	2.04	.83	37.9	0.1	167.	7.9	.44	.19	.63	43.5	41.3	77.7

Table A9: Pellet-Fueling Model, V_b = 500 keV, p_w = 6.0 MW/m^2

				Densities							Sources					
P_t	q	β_θ	T_e (keV)	N_e (10^{14})	N_α (10^{13})	N_I (10^{12})	f_B (%)	C_τ	τ (s)	τ/τ_B	Pellet (10^{12})	Beam (10^{12})	Total (10^{12})	I (MA)	B_T (kG)	B_{max} (kG)
12.5	2	1.5	9.26	4.61	1.19	1.16	53.3	1.0	99.9	30.7	2.51	1.82	4.33	28.7	74.2	224.
	2.5	2	9.28	4.91	1.38	.72	57.0	1.0	116.	32.0	2.17	1.88	4.05	25.7	82.8	251.
25.	2.5	1	9.15	3.08	5.54	1.96	39.8	0.1	72.2	8.1	2.40	1.33	3.73	42.3	93.2	223.
		1.5	9.14	2.81	3.72	2.49	30.8	0.1	48.5	7.0	3.53	1.29	4.82	33.1	72.9	174.
	1.5	1.5	9.33	4.14	1.23	.29	59.7	1.0	162.	32.9	1.39	1.10	2.49	39.8	52.7	126.
		2	9.27	3.68	.95	.95	53.1	1.0	124.	30.6	1.71	1.08	2.79	32.6	43.1	103.
50.	1.5	1	9.17	2.40	3.76	1.81	35.6	0.1	74.0	7.6	1.98	.78	2.76	53.8	49.4	103.
		1.5	9.15	2.22	2.54	2.18	27.1	0.1	49.9	6.5	2.81	.82	3.63	42.4	38.9	81.1
	2	1	9.22	2.82	6.52	1.06	48.9	0.1	128.	9.2	1.21	.80	2.01	58.1	71.1	148.
		1.5	9.18	2.50	4.43	1.62	39.4	0.1	87.2	8.1	1.72	.78	2.50	44.8	54.8	114.
		2	9.16	2.34	3.35	1.93	33.0	0.1	66.0	7.3	2.19	.79	2.98	37.6	46.0	96.0
	2.5	1	9.27	3.37	9.99	.26	59.4	0.1	196.	10.4	.75	.91	1.66	63.3	96.8	202.
		1.5	9.23	2.86	6.78	1.00	49.9	0.1	133.	9.3	1.17	.80	1.97	47.8	73.1	152.
		2	9.20	2.61	5.15	1.42	43.1	0.1	101.	8.5	1.50	.78	2.28	39.6	60.6	126.

Table A10: Pellet-Fueling Model, V_b = 1000 keV, p_w = 1.0 MW/m^2

				Densities							Sources					
p_t	q	β_θ	T_e (keV)	N_e (10^{13})	N_α (10^{12})	N_I (10^{12})	f_B (%)	C_T	τ_T (s)	τ/τ_B	Pellet (10^{11})	Beam (10^{11})	Total (10^{11})	I (MA)	B_T (kG)	B_{max} (kG)
12.5	2	1	9.28	7.15	2.72	1.00	10.0	0.1	41.1	3.8	12.09	.89	12.98	37.0	36.5	72.2
	2.5	1	9.24	7.36	4.27	.95	14.9	0.1	64.6	4.6	7.94	.79	8.73	37.5	46.2	91.3
		1.5	9.27	7.16	2.84	1.00	10.4	0.1	42.8	3.8	11.63	.88	12.51	30.3	37.3	73.8
	1.5	1	9.27	8.89	14.9	.62	38.0	1.0	226.	25.0	2.86	.56	3.42	40.8	30.2	59.7
		1.5	9.26	8.18	10.0	.76	29.2	1.0	152.	21.4	3.87	.58	4.45	32.1	23.7	46.9
		2	9.25	7.83	7.56	.84	23.7	1.0	115.	19.0	4.87	.61	5.48	27.2	20.1	39.8
	2	1	9.32	10.6	25.8	.33	51.6	1.0	393.	30.1	1.94	.59	2.53	44.3	43.7	86.4
		1.5	9.28	9.29	17.5	.54	42.0	1.0	266.	26.5	2.54	.56	3.10	34.0	33.6	66.4
		2	9.27	8.66	13.3	.66	35.4	1.0	202.	23.9	3.11	.57	3.68	28.5	28.1	55.6
	2.5	1	9.36	12.7	39.5	.024	61.9	1.0	599.	33.8	1.41	.70	2.11	48.4	59.7	118.
		1.5	9.32	10.7	26.9	.31	52.5	1.0	408.	30.5	1.88	.59	2.47	36.4	44.9	88.8
		2	9.29	9.73	20.4	.47	45.7	1.0	310.	27.9	2.28	.57	2.85	30.1	37.1	73.4
25.	1.5	1	9.27	6.00	2.96	.80	12.8	0.1	65.9	4.3	6.37	.53	6.90	48.4	25.0	46.5
		1.5	9.30	5.86	1.97	.83	8.9	0.1	43.8	3.5	9.31	.63	9.94	39.2	20.3	37.7
		2	9.34	5.79	1.48	.85	6.8	0.1	32.7	3.1	12.27	.73	13.00	33.9	17.5	32.5
	2	1	9.24	6.32	5.26	.72	20.8	0.1	117.	5.6	3.81	.46	4.27	49.5	34.1	63.4
		1.5	9.26	6.07	3.51	.78	14.9	0.1	78.1	4.6	5.45	.50	5.95	39.8	27.4	50.9
		2	9.28	5.95	2.63	.81	11.6	0.1	58.5	4.0	7.10	.55	7.65	34.2	23.5	43.7
	2.5	1	9.23	6.74	8.20	.63	29.0	0.1	183.	6.7	2.61	.44	3.05	51.0	43.9	81.6
		1.5	9.24	6.35	5.48	.72	21.5	0.1	122.	5.7	3.67	.45	4.12	40.5	34.9	64.8
		2	9.25	6.16	4.11	.76	17.0	0.1	91.6	5.0	4.73	.48	5.21	34.6	29.8	55.4
	1.5	1	9.38	9.71	27.6	.13	57.9	1.0	616.	32.4	1.16	.37	1.53	60.7	31.3	58.2
		1.5	9.32	8.33	18.8	.33	48.5	1.0	421.	29.0	1.47	.36	1.83	46.0	23.8	44.2
		2	9.29	7.64	14.3	.45	41.7	1.0	320.	26.4	1.76	.37	2.13	38.3	19.8	36.7
	2	1.5	9.40	10.5	32.3	.024	61.8	1.0	722.	33.7	1.06	.38	1.44	51.3	35.4	65.7
		2	9.36	9.25	24.7	.19	55.3	1.0	552.	31.4	1.24	.36	1.60	41.9	28.9	53.6
50.	1.5	1														
		1.5														
		2	9.27	5.03	2.88	.65	14.8	0.1	93.6	4.6	3.78	.34	4.12	44.7	16.2	28.8
	2	1														
		1.5														
		2														
	2.5	1														
		1.5														
		2														

Table A11: Pellet-Fueling Model, V_b = 1000 keV, p_w = 3.0 MW/m^2

				Densities								Sources					
P_t	q	θ_θ	T_e (keV)	N_e (10^{14})	N_α (10^{13})	N_I (10^{12})	f_B (%)	C_T	τ (s)	τ/τ_B	Pellet (10^{12})	Beam (10^{12})	Total (10^{12})	I (MA)	B_T (kG)	B_{max} (kG)
12.5	1.5	1	9.29	2.31	4.74	1.16	44.9	1.0	125.	27.6	1.34	.32	1.66	36.7	48.5	116.
	2	1	9.36	2.85	8.18	.33	58.5	1.0	217.	32.6	.93	.35	1.28	40.6	71.5	171.
		1.5	9.31	2.44	5.58	.94	49.0	1.0	148.	29.1	1.20	.32	1.52	30.8	54.2	130.
		2	9.28	2.23	4.24	1.30	42.2	1.0	112.	26.6	1.45	.32	1.77	25.6	45.0	108.
	2.5	1.5	9.36	2.90	8.51	.26	59.4	1.0	225.	32.9	.91	.35	1.26	33.4	73.6	176.
		2	9.33	2.58	6.48	.72	52.7	1.0	172.	30.5	1.09	.33	1.42	27.4	60.3	144.
25.	2	1	9.24	1.55	1.64	1.58	25.7	0.1	65.5	6.3	1.68	.24	1.92	43.6	53.3	111.
	2.5	1	9.24	1.68	2.54	1.31	35.0	0.1	102.	7.5	1.17	.24	1.41	45.3	69.2	144.
		1.5	9.24	1.56	1.71	1.56	26.5	0.1	68.2	6.4	1.62	.24	1.86	35.7	54.6	114.
		2	9.24	1.50	1.28	1.70	21.3	0.1	51.3	5.7	2.07	.25	2.32	30.4	46.4	96.8
	1.5	1.5	9.36	2.18	5.79	.46	55.1	1.0	232.	31.3	.70	.20	.90	41.8	38.4	80.0
		2	9.32	1.96	4.41	.80	48.3	1.0	177.	28.9	.82	.20	1.02	34.5	31.6	65.9
	2	2	9.40	2.46	7.56	.072	61.6	1.0	303.	33.6	.60	.20	.80	38.4	47.0	97.9
50.	1.5	1	9.25	1.11	1.42	1.01	30.2	0.1	118.	6.9	.68	.11	.79	59.5	33.9	63.8
		1.5	9.25	1.05	.95	1.16	22.5	0.1	79.5	5.8	.94	.11	1.05	47.2	26.9	50.6
		2	9.26	1.01	.72	1.23	17.9	0.1	59.7	5.1	1.20	.12	1.32	40.3	22.9	43.2
	2	1	9.28	1.27	2.48	.70	43.1	0.1	207.	8.5	.44	.11	.55	63.3	48.1	90.5
		1.5	9.26	1.15	1.68	.93	33.9	0.1	140.	7.4	.60	.11	.71	49.3	37.5	70.5
		2	9.25	1.09	1.27	1.06	27.9	0.1	106.	6.6	.74	.11	.85	41.7	31.6	59.6
	2.5	1	9.32	1.48	3.81	.37	53.7	0.1	317.	9.8	.33	.11	.44	68.0	64.5	121.
		1.5	9.28	1.29	2.58	.68	44.1	0.1	215.	8.6	.43	.11	.54	52.0	49.3	92.9
		2	9.27	1.19	1.96	.85	37.4	0.1	163.	7.8	.53	.10	.63	37.4	41.2	77.6

Table A12: Pellet-Fueling Model, V_b = 1000 keV, p_w = 6.0 MW/m^2

				Densities								Sources					
P_t	q	θ_θ	T_e (keV)	N_e (10^{14})	N_α (10^{13})	N_I (10^{12})	f_B (%)	C_T	τ(s)	τ/τ_B	Pellet (10^{12})	Beam (10^{12})	Total (10^{12})	I (MA)	B_T (kG)	B_{max} (kG)
12.5	2	1	9.38	5.39	1.68	.068	62.1	1.0	144.	33.8	2.60	1.11	3.71	38.1	98.2	297.
		1.5	9.33	4.54	1.15	1.25	52.9	1.0	98.3	30.6	3.37	1.00	4.37	28.6	73.9	224.
	2.5	2	9.35	4.83	1.33	.82	56.6	1.0	114.	31.9	3.05	1.02	4.07	25.5	82.4	249.
25.	2.5	1	9.24	3.04	5.30	2.01	39.2	0.1	70.6	8.1	3.05	.73	3.78	42.2	93.0	222.
		1.5	9.24	2.79	3.56	2.52	30.3	0.1	47.4	6.9	4.19	.71	4.90	33.1	72.9	174.
	1.5	1.5	9.39	4.08	1.19	.37	59.4	1.0	160.	32.8	1.90	.60	2.50	39.6	52.4	125.
		2	9.34	3.63	.91	1.01	52.8	1.0	122.	30.5	2.22	.59	2.81	32.5	42.9	103.
50.	1.5	1	9.26	2.37	3.61	1.84	35.1	0.1	72.5	7.5	2.38	.43	2.81	53.8	49.4	103.
		1.5	9.25	2.20	2.43	2.20	26.7	0.1	48.8	6.4	3.24	.45	3.69	42.4	38.9	81.2
	2	1	9.30	2.78	6.27	1.12	48.5	0.1	126.	9.2	1.59	.44	2.03	57.9	70.9	148.
		1.5	9.27	2.21	4.25	1.66	38.9	0.1	85.4	8.0	2.10	.43	2.53	44.8	54.8	114.
		2	9.26	2.32	3.22	1.96	32.5	0.1	64.6	7.2	2.59	.43	3.02	37.6	46.0	96.0
	2.5	1	9.35	3.30	9.59	.34	58.9	0.1	193.	10.4	1.18	.49	1.67	62.9	96.2	201.
		1.5	9.31	2.82	6.52	1.05	49.4	0.1	131.	9.3	1.55	.44	1.99	47.6	72.8	152.
		2	9.28	2.57	4.95	1.46	42.6	0.1	99.5	8.5	1.88	.43	2.31	39.5	60.5	118.

Table A13: Beam-Fueling Model, p_w = 1.0 MW/m^2 — Fixed Burn-up 20%

				Densities						Sources					
P_t	q	β_θ	T_e (keV)	N_e (10^{13})	N_α (10^{12})	N_I (10^{12})	C_τ	τ (s)	τ/τ_B	Pellet (10^{11})	Beam (10^{11})	Total (10^{11})	I (MA)	B_T (kG)	B_{max} (kG)
12.5	1.5	1	8.98	7.68	6.33	.89	.376	92.2	10.7	3.72	2.79	6.51	37.7	27.8	55.1
		1.5	8.99	7.67	6.33		.564		13.1	3.75	2.76		30.7	22.7	45.0
		2	8.99	7.67	6.33		.753		15.1	3.77	2.74		26.6	19.7	38.9
	2	1	8.96	7.68	6.34		.210		8.0	3.62	2.89		37.6	37.1	73.4
		1.5	8.98	7.68	6.33		.317		9.8	3.69	2.82		30.7	30.3	59.9
		2	8.98	7.68	6.33		.423		11.3	3.73	2.78		26.6	26.2	51.9
	2.5	1	8.94	7.68	6.36		.134		6.4	3.48	3.03		37.6	46.4	91.7
		1.5	8.96	7.68	6.34		.202		7.8	3.61	2.90		30.7	37.9	74.9
		2	8.97	7.68	6.34		.270		9.1	3.67	2.84		26.6	32.8	64.9
25.	1.5	1	8.98	6.33	5.22	.74	.159	112.	7.0	2.54	1.89	4.43	48.9	25.3	47.0
		1.5	8.99				.240		8.5	2.56	1.87		40.0	20.6	38.4
		2	8.99				.320		9.9	2.57	1.86		34.6	17.9	33.2
	2	1	8.97		5.23		.089		5.2	2.48	1.95		48.9	33.7	62.6
		1.5	8.98		5.22		.134		6.4	2.52	1.91		40.0	27.5	51.1
		2	8.99		5.22		.180		7.4	2.54	1.89		34.6	23.8	44.3
	2.5	1.5	8.97		5.23		.086		5.1	2.47	1.96		40.0	34.4	63.9
		2	8.98		5.23		.115		5.9	2.51	1.92		34.6	29.8	55.3
50.	1.5	1	8.99	5.24	4.33	.61	.068	135.	4.5	1.74	1.30	3.04	63.6	23.0	41.0
		1.5	8.99		4.32		.102		5.6	1.76	1.28		51.9	18.8	33.5
		2	8.99		4.32		.136		6.4	1.76	1.28		45.0	16.3	29.0
	2	2	8.99		4.32		.076		4.8	1.75	1.29		45.0	21.7	38.6

Table A14: Beam-Fueling Model, p_w = 3.0 MW/m^2 — Fixed Burn-up 20%

				Densities						Sources					
P_t	q	β_θ	T_e (keV)	N_e (10^{14})	N_α (10^{13})	N_I (10^{12})	C_τ	τ (s)	τ/τ_B	Pellet (10^{12})	Beam (10^{12})	Total (10^{12})	I (MA)	B_T (kG)	B_{max} (kG)
12.5	1.5	1	8.98	1.84	1.52	2.14	.279	38.5	9.2	2.13	1.61	3.74	32.6	43.1	103.
		1.5	8.98				.419		11.3	2.15	1.59		26.6	35.2	84.1
		2	8.99				.559		13.0	2.16	1.58		23.1	30.5	72.9
	2	1	8.96				.156		6.9	2.07	1.67		32.6	57.4	137.
		1.5	8.97				.235		8.5	2.12	1.62		26.6	46.9	112.
		2	8.98				.314		9.8	2.14	1.60		23.1	40.6	97.1
	2.5	1	8.93				.099		5.5	1.99	1.75		32.6	71.8	172.
		1.5	8.96				.150		6.8	2.07	1.67		26.6	58.6	140.
		2	8.97				.200		7.8	2.10	1.64		23.0	50.8	121.
25.	1.5	1	8.98	1.50	1.23	1.74	.120	47.3	6.1	1.41	1.06	2.47	42.3	38.9	81.0
		1.5	8.99				.181		7.4	1.42	1.05		34.6	31.7	66.2
		2	8.99				.242		8.6	1.43	1.04		29.9	27.5	57.3
	2	1	8.96				.067		4.5	1.38	1.09		42.3	51.8	108.
		1.5	8.98				.102		5.6	1.40	1.07		34.6	42.3	88.2
		2	8.98				.136		6.4	1.42	1.05		29.9	36.6	76.4
	2.5	1	8.94				.043		3.6	1.33	1.14		42.3	64.7	135.
		1.5	8.96				.065		4.4	1.37	1.10		34.6	52.9	110.
		2	8.97				.087		5.1	1.40	1.07		29.9	45.8	95.5
50.	1.5	1	8.98	1.04	.854	1.20	.054	68.3	4.0	.68	.51	1.19	56.8	32.3	60.9
		1.5	8.99				.081		5.0	.69	.50		46.4	26.4	49.8
		2	8.99				.108		5.7	.69	.50		40.2	22.9	43.1
	2	1	8.97				.030		3.0	.67	.52		56.8	43.1	81.2
		1.5	8.98				.045		3.7	.68	.51		46.4	35.2	66.3
		2	8.99				.060		4.3	.69	.50		40.2	30.5	57.4
	2.5	1	8.95				.019		2.4	.65	.54		56.8	53.9	101.
		1.5	8.97				.029		3.0	.67	.52		46.4	44.0	82.9
		2	8.98				.039		3.4	.68	.51		40.2	38.1	71.8

Table A15: Beam-Fueling Model, p_w = 6.0 MW/m^2 — Fixed Burn-up 20%

				Densities						Sources					
P_t	q	β_θ	T_e (keV)	N_e (10^{14})	N_α (10^{13})	N_I (10^{12})	C_τ	τ(s)	τ/τ_B	Pellet (10^{12})	Beam (10^{12})	Total (10^{12})	I (MA)	B_T (kG)	B_{max} (kG)
12.5	1.5	1	8.98	3.23	2.67	3.76	.236	21.9	8.5	6.56	4.97	11.53	29.5	57.1	173.
		1.5	8.98				.355		10.4	6.63	4.90		24.1	46.7	141.
		2	8.99				.473		12.0	6.67	4.86		20.9	40.4	122.
	2	1	8.96				.132		6.3	6.37	5.16		29.5	76.1	230.
		1.5	8.97				.199		7.8	6.52	5.01		24.1	62.2	188.
		2	8.98				.266		9.0	6.59	4.94		20.9	53.9	163.
	2.5	1	8.93				.084		5.1	6.09	5.44		29.5	95.1	288.
		1.5	8.95				.127		6.2	6.35	5.18		24.1	77.7	235.
		2	8.97				.169		7.2	6.47	5.06		20.9	67.3	204.
25.	1.5	1	8.98	2.59	2.14	3.01	.100	27.3	5.5	4.23	3.18	7.41	38.7	51.2	122.
		1.5	8.98				.150		6.8	4.27	3.14		31.6	41.8	100.
		2	8.99				.200		7.8	4.29	3.12		27.4	36.2	86.5
	2	1	8.9				.056		4.1	4.12	3.28		38.7	68.2	163.
		1.5	8.97				.084		5.1	4.21	3.20		31.6	55.7	133.
		2	8.98				.112		5.8	4.25	3.16		27.4	48.2	115.
	2.5	1	8.94				.035		3.3	3.97	3.44		38.7	85.2	204.
		1.5	8.96				.054		4.0	4.11	3.30		31.6	69.6	166.
		2	8.97				.072		4.7	4.18	3.23		27.4	60.3	144.
50.	1.5	1	8.98	2.11	1.74	2.45	.043	33.5	3.6	2.82	2.10	4.92	50.3	46.2	96.3
		1.5	8.99				.064		4.4	2.84	2.08		41.1	37.7	78.6
		2	8.99				.086		5.1	2.85	2.07		35.6	32.7	68.1
	2	1	8.97				.024		2.7	2.76	2.16		50.3	61.6	128.
		1.5	8.98				.036		3.3	2.80	2.12		41.1	50.3	105.
		2	8.98				.048		3.8	2.83	2.09		35.6	43.5	90.8
	2.5	1	8.95				.015		2.2	2.66	2.26		50.3	76.9	160.
		1.5	8.96				.023		2.6	2.75	2.17		41.1	62.8	131.
		2	8.97				.031		3.1	2.79	2.13		35.6	54.4	113.

Table A16: Pellet-Fueling Model, V_b = 200 keV, p_w = 1.0 MW/m^2 — Fixed Burn-up 20%

				Densities						Sources					
P_t	q	β_θ	T_e (keV)	N_e (10^{13})	N_α (10^{12})	N_I (10^{12})	C_τ	τ (s)	τ/τ_B	Pellet (10^{11})	Beam (10^{11})	Total (10^{11})	I (MA)	B_T (kG)	B_{max} (kG)
12.5	1.5	1	9.07	7.66	6.27	.89	.383	92.2	10.8	4.84	1.67	6.51	37.8	27.9	55.2
		1.5	9.07	7.66	6.27		.576		13.2	4.86	1.65		30.8	22.8	45.1
		2	9.08	7.66	6.26		.768		15.2	4.87	1.64		26.7	19.7	39.1
	2	1	9.05	7.66	6.28		.215		8.1	4.78	1.73		37.8	37.2	73.6
		1.5	9.06	7.66	6.27		.323		9.9	4.83	1.68		30.8	30.4	60.1
		2	9.07	7.66	6.27		.421		11.4	4.85	1.66		26.7	26.3	52.1
	2.5	1	9.03	7.67	6.29		.137		6.4	4.70	1.81		37.8	46.5	92.0
		1.5	9.05	7.66	6.28		.206		7.9	4.78	1.73		30.8	38.0	75.2
		2	9.06	7.66	6.27		.275		9.1	4.81	1.70		26.7	32.9	65.1
25.	1.5	1	9.07	6.32	5.17	.73	.163	112.	7.0	3.30	1.13	4.43	49.1	25.4	47.1
		1.5	9.07		5.17		.245		8.6	3.31	1.12		40.1	20.7	38.5
		2	9.08		5.17		.326		9.9	3.32	1.11		34.7	17.9	33.3
	2	1	9.06		5.18		.091		5.3	3.26	1.17		49.1	33.8	62.8
		1.5	9.07		5.17		.137		6.4	3.29	1.14		40.1	27.6	51.3
		2	9.07		5.17		.183		7.4	3.30	1.13		34.7	23.9	44.4
	2.5	1.5	9.06		5.18		.088		5.1	3.26	1.17		40.1	34.5	64.1
		2	9.06		5.17		.117		5.9	3.28	1.15		34.7	29.9	55.5
50.	1.5	1	9.07	5.23	4.28	.61	.069	135.	4.6	2.27	.77	3.04	63.8	23.1	41.1
		1.5	9.08				.104		5.6	2.27	.77		52.1	18.8	33.6
		2	9.08				.138		6.5	2.28	.76		45.1	16.3	29.1
	2	1.5	9.07				.058		4.2	2.26	.78		52.1	25.1	44.7
		2	9.07				.078		4.8	2.27	.77		45.1	21.8	38.7

Table A17: Pellet-Fueling Model, V_b = 200 keV, P_w = 3.0 MW/m^2 Fixed Burn-up 20%

				Densities						Sources					
P_t	q	θ_θ	T_e (keV)	N_e (10^{14})	N_α (10^{13})	N_I (10^{12})	C_τ	τ (s)	τ/τ_B	Pellet (10^{12})	Beam (10^{12})	Total (10^{12})	I (MA)	B_T (kG)	B_{max} (kG)
12.5	1.5	1	9.06	1.84	1.50	2.13	.284	38.5	9.3	2.78	.96	3.74	32.7	43.2	103.
		1.5	9.07	1.83	1.50		.427		11.4	2.79	.95		26.7	35.3	84.4
		2	9.07	1.83	1.50		.570		13.1	2.80	.94		23.1	30.6	73.1
	2	1	9.05	1.84	1.50		.159		6.9	2.74	1.00		32.7	57.6	138.
		1.5	9.06	1.84	1.50		.240		8.5	2.77	.97		26.7	47.1	113.
		2	9.07	1.84	1.50		.320		9.8	2.78	.96		23.1	40.8	97.4
	2.5	1	9.03	1.84	1.51	2.14	.101		5.5	2.69	1.05		32.7	72.0	172.
		1.5	9.05	1.84	1.50	2.13	.153		6.8	2.74	1.00		26.7	58.8	141.
		2	9.06	1.84	1.50	2.13	.204		7.9	2.76	.98		23.1	50.9	122.
25.	1.5	1	9.07	1.49	1.22	1.73	.123	47.3	6.1	1.84	.63	2.47	42.5	39.0	81.3
		1.5	9.07			1.73	.185		7.5	1.85	.62		34.7	31.8	66.4
		2	9.07			1.73	.246		8.6	1.85	.62		30.0	27.6	57.5
	2	1	9.05			1.74	.069		4.6	1.82	.65		42.5	52.0	108.
		1.5	9.06			1.73	.104		5.6	1.83	.64		34.7	42.4	88.5
		2	9.07			1.73	.138		6.5	1.84	.63		30.0	36.8	76.6
	2.5	1	9.03		1.23	1.74	.044		3.6	1.79	.68		42.5	64.9	135.
		1.5	9.05		1.22	1.74	.066		4.5	1.81	.66		34.7	53.0	111.
		2	9.06		1.22	1.73	.088		5.2	1.83	.64		30.0	45.9	95.8
50.	1.5	1	9.07	1.03	.85	1.20	.055	68.3	4.1	.89	.30	1.19	57.0	32.4	61.1
		1.5	9.07				.082		5.0	.89	.30		46.5	26.5	49.9
		2	9.08				.110		5.8	.89	.30		40.3	22.9	43.2
	2	1	9.06				.031		3.0	.88	.31		57.0	43.3	81.5
		1.5	9.07				.046		3.7	.88	.31		46.5	35.3	66.5
		2	9.07				.062		4.3	.89	.30		40.3	30.6	57.6
	2.5	1	9.04				.020		2.4	.86	.33		57.0	54.1	102.
		1.5	9.06				.030		3.0	.88	.31		46.5	44.1	83.2
		2	9.06				.039		3.4	.88	.31		40.3	38.2	72.0

Table A18: Pellet-Fueling Model, V_b = 200 keV, p_w = 6.0 MW/m^2 — Fixed Burn-up 20%

				Densities						Sources					
P_t	q	β_θ	T_e (keV)	N_e (10^{14})	N_α (10^{13})	N_I (10^{12})	C_τ	τ (s)	τ/τ_B	Pellet (10^{17})	Beam (10^{12})	Total (10^{12})	I (MA)	B_T (kG)	B_{max} (kG)
12.5	1.5	1	9.06	3.22	2.64	3.75	.241	21.9	8.5	8.56	2.97	11.53	29.6	57.3	173.
		1.5	9.07				.362		10.5	8.60	2.93		24.2	46.8	142.
		2	9.07				.483		12.1	8.62	2.91		20.9	40.5	123.
	2	1	9.04				.135		6.4	8.44	3.09		29.6	76.4	231.
		1.5	9.06				.203		7.8	8.53	3.00		24.2	62.4	189.
		2	9.06				.271		9.0	8.59	2.96		20.9	54.0	163.
	2.5	1	9.02	3.23	2.65		.086		5.1	8.27	3.26		29.6	95.5	289.
		1.5	9.04	3.23	2.64		.129		6.3	8.43	3.10		24.2	78.0	236.
		2	9.05	3.22	2.64		.173		7.2	8.50	3.03		20.9	67.5	204.
25.	1.5	1	9.06	2.59	2.12	3.01	.102	27.3	5.5	5.51	1.90	7.41	38.8	51.3	123.
		1.5	9.07	2.58	2.11		.153		6.8	5.54	1.87		31.7	41.9	100.
		2	9.07	2.58	2.11		.204		7.8	5.55	1.86		27.5	36.3	86.8
	2	1	9.05	2.59	2.12		.057		4.2	5.45	1.96		38.8	68.4	164.
		1.5	9.06	2.59	2.12		.086		5.1	5.50	1.91		31.7	55.9	134.
		2	9.07	2.59	2.12		.115		5.9	5.52	1.89		27.5	48.4	116.
	2.5	1	9.03	2.59	2.12		.036		3.3	5.35	2.06		38.8	85.5	204.
		1.5	9.05	2.59	2.12		.055		4.1	5.44	1.97		31.7	69.8	167.
		2	9.06	2.59	2.12		.073		4.7	5.48	1.93		27.4	60.5	145.
50.	1.5	1	9.07	2.11	1.72	2.45	.044	33.5	3.6	3.66	1.26	4.92	50.5	46.3	96.6
		1.5	9.07		1.72		.066		4.5	3.68	1.24		41.2	37.8	78.9
		2	9.07		1.72		.088		5.1	3.69	1.23		35.7	32.8	68.3
	2	1	9.05		1.73		.024		2.7	3.63	1.29		50.5	61.8	129.
		1.5	9.06		1.72		.037		3.3	3.66	1.26		41.2	50.4	105.
		2	9.07		1.72		.049		3.9	3.67	1.25		35.7	43.7	91.1
	2.5	1	9.04		1.73		.016		2.2	3.57	1.35		50.5	77.2	161.
		1.5	9.05		1.73		.024		2.7	3.62	1.30		41.2	63.0	131.
		2	9.06		1.72		.031		3.1	3.65	1.27		35.7	54.6	114.

Table A19: Pellet-Fueling Model, V_b = 350 keV, p_w = 1.0 MW/m^2 Fixed Burn-up 20%

				Densities						Sources					
P_t	q	β_θ	T_e (keV)	N_e (10^{13})	N_α (10^{12})	N_I (10^{12})	C_τ	τ(s)	τ/τ_B	Pellet (10^{11})	Beam (10^{11})	Total (10^{11})	I (MA)	B_T (kG)	B_{max} (kG)
12.5	1.5	1	9.13	7.65	6.22	.89	.389	92.2	10.8	5.30	1.21	6.51	37.9	28.0	55.4
		1.5	9.13		6.22		.584		13.2	5.32	1.19		30.9	22.9	45.2
		2	9.14		6.22		.780		15.3	5.33	1.18		26.8	19.8	39.2
	2	1	9.12		6.23		.218		8.1	5.26	1.25		37.9	37.3	73.8
		1.5	9.13		6.22		.328		9.9	5.29	1.22		30.9	30.5	60.3
		2	9.13		6.22		.438		11.5	5.31	1.20		26.8	26.4	52.2
	2.5	1	9.10		6.24		.139		6.5	5.20	1.31		37.8	46.6	92.3
		1.5	9.12		6.23		.209		7.9	5.26	1.25		30.9	38.1	75.3
		2	9.12		6.23		.280		9.2	5.28	1.23		26.8	33.0	65.3
25.	1.5	1	9.13	6.31	5.13	.73	.165	112.	7.0	3.61	.82	4.43	49.2	25.4	47.2
		1.5	9.14		5.13		.248		8.6	3.62	.81		40.2	20.8	38.6
		2	9.14		5.13		.331		10.0	3.63	.80		34.8	18.0	33.4
	2	1	9.12		5.14		.093		5.3	3.59	.84		49.2	33.9	63.0
		1.5	9.13		5.13		.139		6.5	3.61	.82		40.2	27.8	51.4
		2	9.13		5.13		.186		7.5	3.62	.81		34.8	24.0	44.5
	2.5	1	9.10		5.15		.059		4.2	3.55	.88		49.2	42.4	78.7
		1.5	9.12		5.14		.089		5.2	3.58	.85		40.2	34.6	64.3
		2	9.13		5.14		.119		6.0	3.60	.83		34.8	30.0	55.7
50.	1.5	1	9.13	5.23	4.25	.61	.070	135.	4.6	2.48	.56	3.04	63.9	23.1	41.2
		1.5	9.14	5.22			.105		5.6	2.49	.55		52.2	18.9	33.6
		2	9.14	5.22			.141		6.5	2.49	.55		45.2	16.4	29.1
	2	1.5	9.13	5.23			.059		4.2	2.48	.56		52.2	25.2	44.8
		2	9.14	5.23			.079		4.9	2.48	.56		45.2	21.8	38.8
	2.5	2	9.13	5.23			.050		3.9	2.47	.57		45.2	27.3	48.5

Table A20: Pellet-Fueling Model, V_b = 350 keV, p_w = 3.0 MW/m^2 — Fixed Burn-up 20%

				Densities						Sources					
P_t	q	β_θ	T_e (keV)	N_e (10^{14})	N_α (10^{13})	N_I (10^{12})	C_τ	τ (s)	τ/τ_B	Pellet (10^{12})	Beam (10^{12})	Total (10^{12})	I (MA)	B_T (kG)	B_{max} (kG)
12.5	1.5	1	9.13	1.83	1.49	2.13	.289	38.5	9.3	3.04	.70	3.74	32.8	43.3	104.
		1.5	9.13				.434		11.4	3.05	.69		26.8	35.4	84.6
		2	9.13				.579		13.2	3.06	.68		23.2	30.6	73.3
	2	1	9.11				.162		7.0	3.02	.72		32.8	57.8	138.
		1.5	9.12				.243		8.6	3.04	.70		26.8	47.2	113.
		2	9.13				.325		9.9	3.05	.69		23.2	40.9	97.7
	2.5	1	9.09		1.50		.103		5.6	2.98	.76		32.8	72.2	173.
		1.5	9.11		1.49		.155		6.8	3.01	.73		26.8	59.0	141.
		2	9.12		1.49		.207		7.9	3.03	.71		23.2	51.1	122.
25.	1.5	1	9.13	1.49	1.21	1.73	.125	47.3	6.1	2.01	.46	2.47	42.6	39.1	81.5
		1.5	9.13				.187		7.5	2.02	.45		34.8	31.9	66.5
		2	9.14				.250		8.7	2.02	.45		30.1	27.6	57.6
	2	1	9.12				.070		4.6	2.00	.47		42.6	52.1	109.
		1.5	9.13				.105		5.6	2.01	.46		34.8	42.5	88.7
		2	9.13				.140		6.5	2.02	.45		30.1	36.8	76.8
	2.5	1	9.10		1.22		.045		3.7	1.98	.49		42.6	65.1	136.
		1.5	9.12		1.21		.067		4.5	2.00	.47		34.8	53.2	111.
		2	9.12		1.21		.090		5.2	2.01	.46		30.1	46.0	96.0
50.	1.5	1	9.13	1.03	.84	1.20	.056	68.3	4.1	.97	.22	1.19	57.1	32.5	61.3
		1.5	9.14				.084		5.0	.97	.22		46.6	26.6	50.0
		2	9.14				.111		5.8	.97	.22		40.4	23.0	43.3
	2	1	9.12				.031		3.1	.96	.23		57.1	43.4	81.7
		1.5	9.13				.047		3.8	.97	.22		46.6	35.4	66.7
		2	9.13				.063		4.3	.97	.22		40.4	30.7	57.8
	2.5	1	9.11				.020		2.4	.95	.24		57.1	54.2	102.
		1.5	9.12				.030		3.0	.96	.23		46.6	44.3	83.4
		2	9.13				.040		3.5	.97	.22		40.4	38.3	72.2

Table A21: Pellet-Fueling Model, V_b = 350 keV, p_w = 6.0 MW/m^2 Fixed Burn-up 20%

				Densities						Sources					
P_t	q	β_θ	T_e (keV)	N_e (10^{14})	N_α (10^{13})	N_I (10^{12})	C_τ	τ (s)	τ/τ_B	Pellet (10^{12})	Beam (10^{12})	Total (10^{12})	I (MA)	B_T (kG)	B_{max} (kG)
12.5	1.5	1	9.12	3.22	2.62	3.74	.244	21.9	8.6	9.38	2.15	11.53	29.7	57.4	174.
		1.5	9.13				.367		10.5	9.42	2.11		24.2	46.9	142.
		2	9.13				.490		12.1	9.43	2.10		21.0	40.6	123.
	2	1	9.11				.137		6.4	9.30	2.23		29.7	76.6	232.
		1.5	9.12				.206		7.9	9.36	2.17		24.2	62.5	189.
		2	9.13				.275		9.1	9.39	2.14		21.0	54.2	164.
	2.5	1	9.09		2.63	3.75	.087		5.1	9.17	2.36		29.7	95.7	290.
		1.5	9.11		2.62	3.74	.131		6.3	9.29	2.24		24.2	78.2	237.
		2	9.12		2.62	3.74	.176		7.3	9.34	2.19		21.0	67.7	205.
25.	1.5	1	9.13	2.58	2.10	3.00	.103	27.3	5.6	6.04	1.37	7.41	38.9	51.4	123.
		1.5	9.13				.155		6.8	6.06	1.35		31.8	42.0	100.
		2	9.13				.207		7.9	6.07	1.34		27.5	36.4	87.0
	2	1	9.11				.058		4.2	5.99	1.42		38.9	68.6	164.
		1.5	9.12				.087		5.1	6.03	1.38		31.8	56.0	134.
		2	9.13				.116		5.9	6.05	1.36		27.5	48.5	116.
	2.5	1	9.10		2.11		.037		3.3	5.92	1.49		38.9	85.7	205.
		1.5	9.11		2.10		.056		4.1	5.99	1.42		31.8	70.0	167.
		2	9.12		2.10		.074		4.7	6.02	1.39		27.5	60.6	145.
50.	1.5	1	9.13	2.10	1.71	2.44	.044	33.5	3.6	4.01	.91	4.92	50.6	46.4	96.8
		1.5	9.13			2.44	.067		4.5	4.02	.90		41.3	37.9	79.0
		2	9.13			2.44	.089		5.2	4.03	.89		35.8	32.8	68.5
	2	1	9.12			2.45	.025		2.7	3.99	.93		50.6	61.9	129.
		1.5	9.13			2.45	.037		3.4	4.01	.91		41.3	50.5	105.
		2	9.13			2.44	.050		3.9	4.02	.90		35.8	43.8	91.3
	2.5	1	9.10		1.72	2.45	.016		2.2	3.94	.98		50.6	77.4	161.
		1.5	9.12		1.71	2.45	.024		2.7	3.98	.94		41.3	63.2	132.
		2	9.12		1.71	2.45	.032		3.1	4.00	.92		35.8	54.7	114.

Table A22: Pellet-Fueling Model, V_b = 500 keV, p_w = 1.0 MW/m^2 Fixed Burn-up 20%

				Densities						Sources					
P_t	q	β_θ	T_e (keV)	N_e (10^{13})	N_α (10^{12})	N_I (10^{12})	C_T	τ (s)	τ/τ_B	Pellet (10^{11})	Beam (10^{11})	Total (10^{11})	I (MA)	B_T (kG)	B_{max} (kG)
12.5	1.5	1	9.25	7.62	6.08	.89	.400	92.2	10.9	5.85	.66	6.51	38.0	28.1	55.6
		1.5	9.25				.600		13.4	5.86	.65		31.0	22.9	45.4
		2	9.25				.801		15.4	5.86	.65		26.9	19.9	39.3
	2	1	9.24				.224		8.2	5.82	.69		38.0	37.5	74.1
		1.5	9.25				.337		10.0	5.84	.67		31.0	30.6	60.5
		2	9.25				.450		11.6	5.85	.66		26.9	26.5	52.4
	2.5	1	9.23				.143		6.5	5.79	.72		38.0	46.8	92.7
		1.5	9.24				.215		8.0	5.82	.69		31.0	38.2	75.7
		2	9.24				.287		9.2	5.84	.67		26.9	33.1	65.5
25.	1.5	1	9.25	6.28	5.01	.73	.170	112.	7.1	3.98	.45	4.43	49.4	25.5	47.4
		1.5	9.25				.255		8.7	3.99	.44		40.3	20.8	38.7
		2	9.26				.340		10.0	3.99	.44		34.9	18.0	33.5
	2	1	9.24				.095		5.3	3.97	.46		49.4	34.0	63.2
		1.5	9.25				.143		6.5	3.98	.45		40.3	27.8	51.6
		2	9.25				.191		7.5	3.98	.45		34.9	24.1	44.7
	2.5	1	9.23	6.29	5.02		.061		4.3	3.95	.48		49.4	42.5	79.0
		1.5	9.24	6.28	5.01		.091		5.2	3.97	.46		40.3	34.7	64.5
		2	9.25	6.28	5.01		.122		6.0	3.98	.45		34.9	30.1	55.9
50.	1.5	1	9.25	5.20	4.15	.61	.072	135.	4.6	2.73	.31	3.04	64.2	23.2	41.4
		1.5	9.25				.108		5.7	2.74	.30		52.4	19.0	33.8
		2	9.26				.144		6.5	2.74	.30		45.4	16.4	29.2
	2	1	9.24				.040		3.5	2.72	.32		64.2	31.0	55.1
		1.5	9.25				.061		4.3	2.73	.31		52.4	25.3	45.0
		2	9.25				.081		4.9	2.74	.30		45.4	21.9	39.0
	2.5	1	9.23	5.21	4.16		.026		2.8	2.71	.33		64.2	38.7	68.9
		1.5	9.24	5.21	4.15		.039		3.4	2.72	.32		52.4	31.6	56.3
		2	9.25	5.20	4.15		.052		3.9	2.73	.31		45.4	27.4	48.7

Table A23: Pellet-Fueling Model, V_b = 500 keV, p_w = 3.0 MW/m^2 Fixed Burn-up 20%

				Densities						Sources					
P_t	q	β_θ	T_e (keV)	N_e (10^{14})	N_α (10^{13})	N_I (10^{12})	C_T	τ (s)	τ/τ_B	Pellet (10^{12})	Beam (10^{12})	Total (10^{12})	I (MA)	B_T (kG)	B_{max} (kG)
12.5	1.5	1	9.25	1.82	1.46	2.13	.297	38.5	9.4	3.36	.38	3.74	32.9	43.5	104.
		1.5	9.25	1.82			.446		11.5	3.36	.38		26.9	35.5	84.9
		2	9.25	1.82			.595		13.3	3.37	.37		23.3	30.8	73.6
	2	1	9.24	1.83			.166		7.0	3.34	.40		32.9	58.0	139.
		1.5	9.24	1.82			.250		8.6	3.35	.39		26.9	47.4	113.
		2	9.25	1.82			.334		10.0	3.36	.38		23.3	41.0	98.1
	2.5	1	9.22	1.83			.106		5.6	3.32	.42		32.9	72.5	173.
		1.5	9.23	1.83			.160		6.9	3.34	.40		26.9	59.2	142.
		2	9.24	1.83			.213		8.0	3.35	.39		23.3	51.3	123.
25.	1.5	1	9.25	1.48	1.18	1.73	.128	47.3	6.2	2.22	.25	2.47	42.8	39.2	81.8
		1.5	9.25				.193		7.6	2.22	.25		34.9	32.0	66.8
		2	9.25				.257		8.7	2.22	.25		30.2	27.7	57.8
	2	1	9.24				.072		4.6	2.21	.26		42.8	52.3	109.
		1.5	9.25				.108		5.7	2.22	.25		34.9	42.7	89.0
		2	9.25				.144		6.6	2.22	.25		30.2	37.0	77.1
	2.5	1	9.23				.046		3.7	2.20	.27		42.8	65.4	136.
		1.5	9.24				.069		4.5	2.21	.26		34.9	53.4	111.
		2	9.24				.092		5.2	2.22	.25		30.2	46.2	96.4
50.	1.5	1	9.25	1.03	.82	1.20	.057	68.3	4.1	1.07	.12	1.19	57.4	32.7	61.5
		1.5	9.25				.086		5.1	1.07	.12		46.8	26.7	50.2
		2	9.25				.114		5.8	1.07	.12		40.6	23.1	43.5
	2	1	9.24				.032		3.1	1.06	.13		57.4	43.5	82.0
		1.5	9.25				.048		3.8	1.07	.12		46.8	35.5	67.0
		2	9.25				.064		4.4	1.07	.12		40.6	30.8	58.0
	2.5	1	9.23				.020		2.5	1.06	.13		57.4	54.4	103.
		1.5	9.24				.031		3.0	1.07	.12		46.8	44.4	83.7
		2	9.25				.041		3.5	1.07	.12		40.6	38.5	72.5

Table A24: Pellet-Fueling Model, V_b = 500 keV, p_w = 6.0 MW/m^2 Fixed Burn-up 20%

				Densities						Sources					
P_t	q	β_θ	T_e (keV)	N_e (10^{14})	N_α (10^{13})	N_I (10^{12})	C_τ	τ(s)	τ/τ_B	Pellet (10^{12})	Beam (10^{12})	Total (10^{12})	I (MA)	B_T (kG)	B_{max} (kG)
12.5	1.5	1	9.24	3.21	2.56	3.74	.251	21.9	8.6	10.35	1.18	11.53	29.8	57.7	175.
		1.5	9.25				.377		10.6	10.37	1.16		24.3	47.1	143.
		2	9.25				.503		12.2	10.38	1.15		21.1	40.8	123.
	2	1	9.23				.141		6.5	10.30	1.23		29.8	76.9	233.
		1.5	9.24				.212		7.9	10.34	1.19		24.3	62.8	190.
		2	9.24				.283		9.2	10.36	1.17		21.1	54.4	165.
	2.5	1	9.22				.090		5.2	10.23	1.30		29.8	96.1	291.
		1.5	9.23				.135		6.3	10.30	1.23		24.3	78.5	238.
		2	9.24				.181		7.3	10.33	1.20		21.1	68.0	206.
25.	1.5	1	9.25	2.57	2.05	3.00	.106	27.3	5.6	6.66	.75	7.41	39.1	51.7	123.
		1.5	9.25				.159		6.9	6.67	.74		31.9	42.2	101.
		2	9.25				.213		8.0	6.68	.73		27.6	36.5	87.3
	2	1	9.24				.060		4.2	6.63	.78		39.1	68.9	165.
		1.5	9.24				.089		5.2	6.65	.76		31.9	56.2	134.
		2	9.25				.119		6.0	6.66	.75		27.6	48.7	116.
	2.5	1	9.22				.038		3.4	6.59	.82		39.1	86.1	206.
		1.5	9.23				.057		4.1	6.63	.78		31.9	70.3	168.
		2	9.24				.076		4.8	6.65	.76		27.6	60.9	146.
50.	1.5	1	9.25	2.09	1.67	2.44	.046	33.5	3.7	4.42	.50	4.92	50.8	46.6	97.2
		1.5	9.25				.068		4.5	4.43	.49		41.5	38.1	79.4
		2	9.25				.091		5.2	4.43	.49		35.9	33.0	68.7
	2	1	9.24				.026		2.8	4.41	.51		50.8	62.2	130.
		1.5	9.25				.038		3.4	4.42	.50		41.5	50.8	106.
		2	9.25				.051		3.9	4.43	.49		35.9	44.0	91.6
	2.5	1	9.23				.016		2.2	4.38	.54		50.8	77.7	162.
		1.5	9.24				.025		2.7	4.41	.51		41.5	63.4	132.
		2	9.25				.033		3.1	4.42	.50		35.9	54.9	115.

Table A25: Pellet-Fueling Model, V_b = 1000 keV, p_w = 1.0 MW/m^2

				Densities								Source				
P_t	q	β_θ	T_e (keV)	N_e (10^{13})	N_α (10^{12})	N_I (10^{12})	f_B (%)	C_τ	τ(s)	τ/τ_B	S (10^{11})	V_b (keV)	I (MA)	B_T (kG)	B_{max} (kG)
12.5	2	1	9.07	7.27	3.48	.98	10.4	0.1	42.8	3.8	12.52	28.0	36.8	36.3	71.8
	2.5	1	8.96	7.52	5.19	.93	15.7	0.1	68.5	4.8	8.31	51.5	37.2	45.9	90.8
		1.5	9.05	7.29	3.60	.98	10.8	0.1	44.7	3.9	12.04	29.7	30.1	37.1	73.3
	1.5	1	9.07	9.14	16.4	.58	39.1	1.0	237.	25.5	3.33	131.	41.0	30.3	59.9
		1.5	9.03	8.39	11.3	.73	30.3	1.0	160.	21.9	4.29	95.2	32.1	23.7	46.9
		2	9.02	8.01	8.70	.81	24.7	1.0	121.	19.5	5.27	74.6	27.2	20.1	39.7
	2	1	9.15	10.9	27.9	.29	52.5	1.0	408.	30.5	2.48	202.	44.6	44.0	87.0
		1.5	9.09	9.56	19.2	.51	43.0	1.0	279.	27.0	3.02	148.	34.2	33.7	66.7
		2	9.05	8.89	14.8	.63	36.5	1.0	212.	24.5	3.57	119.	28.6	28.2	55.7
	2.5	1.5	9.16	11.1	28.9	.26	53.5	1.0	424.	30.8	2.43	209.	36.7	45.2	89.5
		2	9.11	10.0	22.2	.43	46.7	1.0	324.	28.4	2.78	167.	30.3	37.3	73.9
25.	1.5	1	9.04	6.11	3.65	.79	13.4	0.1	69.0	4.4	6.62	36.5	48.2	24.9	46.3
		1.5	9.14	5.95	2.56	.82	9.1	0.1	45.0	3.6	9.68	21.3	39.0	20.2	37.5
	2	1	8.99	6.46	6.15	.71	21.7	0.1	124.	5.8	4.08	69.6	49.4	34.0	63.2
		1.5	9.02	6.19	4.25	.77	15.5	0.1	82.2	4.8	5.70	44.6	39.6	27.3	50.6
		2	9.07	6.06	3.28	.80	12.0	0.1	61.0	4.1	7.37	31.5	34.0	23.4	43.5
	2.5	1	8.98	6.92	9.31	.61	30.2	0.1	194.	6.9	2.93	110.	51.0	43.9	81.6
		1.5	8.98	6.50	6.39	.70	22.4	0.1	129.	5.9	3.95	72.6	40.4	34.8	64.6
		2	9.00	6.29	4.91	.75	17.8	0.1	96.7	5.1	4.98	53.3	34.5	29.7	55.2
	1.5	1	9.24	10.0	29.4	.091	58.7	1.0	636.	32.6	1.51	209.	61.2	31.6	58.7
		1.5	9.16	8.58	20.4	.30	49.5	1.0	437.	29.4	1.79	164.	46.3	23.9	44.5
		2	9.11	7.86	15.7	.42	42.8	1.0	334.	26.9	2.07	138.	38.5	19.9	36.9
	2	2	9.21	9.53	26.5	.16	56.1	1.0	571.	31.7	1.58	195.	42.2	29.1	54.1
50.	1.5	1	9.02	5.56	6.55	.54	26.7	0.1	197.	6.5	2.28	83.3	65.4	23.7	42.1
		1.5	9.02	5.27	4.52	.60	19.6	0.1	131.	5.4	3.10	57.0	52.0	18.8	33.5
		2	9.04	5.12	3.49	.64	15.4	0.1	98.2	4.7	3.95	42.2	44.5	16.1	28.7
	2	1	9.06	6.23	11.1	.40	38.9	0.1	344.	8.0	1.56	135.	69.1	33.3	59.4
		1.5	9.02	5.72	7.66	.50	30.1	0.1	232.	6.9	2.02	96.6	54.1	26.1	46.5
		2	9.01	5.46	5.88	.56	24.5	0.1	175.	6.1	2.48	74.9	45.8	22.1	39.4
	2.5	1	9.11	7.10	16.8	.25	49.3	0.1	526.	9.3	1.23	197.	73.6	44.4	79.0
		1.5	9.06	6.30	11.6	.39	39.8	0.1	357.	8.2	1.53	140.	56.7	34.2	60.9
		2	9.03	5.90	8.87	.47	33.4	0.1	271.	7.4	1.82	110.	47.6	28.7	51.1

Table A26: Pellet-Fueling Model, V_b = 1000 keV, p_w = 3.0 MW/m^2

				Densities							Source				
P_t	q	δ_0	T_e (keV)	N_e (10^{14})	N_α (10^{13})	N_I (10^{12})	f_B (%)	C_τ	τ (s)	τ/τ_B	S (10^{12})	V_b (keV)	I (MA)	B_T (kG)	B_{max} (kG)
12.5	1.5	1	9.11	2.38	5.16	1.07	46.0	1.0	131.	28.1	1.63	158.	36.9	48.8	117.
	2	1	9.21	2.94	8.72	.23	59.3	1.0	224.	32.9	1.26	243.	40.9	72.1	172.
		1.5	9.14	2.51	6.03	.85	49.9	1.0	154.	29.6	1.15	178.	31.0	54.6	130.
		2	9.10	2.30	4.64	1.21	43.2	1.0	117.	27.1	1.73	146.	25.7	45.2	108.
	2.5	1.5	9.22	2.99	9.06	.15	60.2	1.0	232.	33.2	1.24	252.	33.7	74.2	177.
		2	9.17	2.66	6.97	.62	53.6	1.0	178.	30.9	1.15	200.	27.6	60.7	145.
25.	2	1	8.99	1.59	1.88	1.53	26.8	0.1	69.3	6.5	1.84	89.6	43.5	53.3	111.
	2.5	1	9.00	1.73	2.84	1.24	36.2	0.1	107.	7.7	1.36	139.	45.3	69.3	145.
		1.5	8.99	1.60	1.95	1.51	27.6	0.1	72.2	6.6	1.79	93.2	35.7	54.5	114.
		2	8.99	1.53	1.49	1.65	22.3	0.1	54.2	5.8	2.22	70.1	30.3	46.3	96.5
	1.5	1.5	9.21	2.24	6.19	.38	55.9	1.0	240.	31.6	.884	190.	42.1	38.7	80.6
		2	9.15	2.02	4.78	.72	49.3	1.0	184.	29.3	1.00	162.	34.7	31.8	66.3
50.	1.5	1	9.03	1.14	1.60	.97	31.3	0.1	125.	7.1	.757	100.	59.5	33.9	63.9
		1.5	9.01	1.07	1.10	1.12	23.5	0.1	83.8	6.0	1.01	70.6	47.1	26.8	50.5
		2	9.02	1.03	.848	1.20	18.7	0.1	62.9	5.3	1.27	53.5	40.2	22.9	43.1
	2	1	9.09	1.31	2.72	.65	44.2	0.1	217.	8.7	.537	158.	63.6	48.3	91.0
		1.5	9.04	1.18	1.87	.89	35.0	0.1	147.	7.5	.678	115.	49.4	37.5	70.7
		2	9.02	1.12	1.44	1.02	28.9	0.1	111.	6.8	.820	90.9	41.7	31.6	59.6
	2.5	1	9.15	1.52	4.09	.31	54.7	0.1	330.	9.9	.434	230.	68.5	65.0	122.
		1.5	9.09	1.33	2.82	.63	45.2	0.1	225.	8.8	.525	163.	52.3	49.6	93.4
		2	9.06	1.23	2.17	.80	38.5	0.1	171.	8.0	.616	130.	43.6	41.3	77.9

Table A27: Pellet-Fueling Model, V_b = 1000 keV, p_w = 6.0 MW/m^2

				Densities							Source				
P_t	q	β_θ	T_e (keV)	N_e (10^{14})	N_α (10^{13})	N_I (10^{12})	$\bar{f}_B$ (%)	C_τ	τ (s)	τ/τ_B	S (10^{12})	V_b (keV)	I (MA)	B_T (kG)	B_{max} (kG)
12.5	2	1.5	9.17	4.68	12.3	1.08	53.8	1.0	102.	30.9	4.29	197.	28.8	74.4	225.
	2.5	2	9.20	4.98	14.2	.64	57.4	1.0	118.	32.2	4.02	221.	25.8	83.1	251.
25.	2.5	1	9.02	3.13	5.86	1.89	40.5	0.1	74.2	8.2	3.66	160.	42.4	93.3	223.
		1.5	9.00	2.86	4.02	2.42	31.4	0.1	50.1	7.1	4.72	109.	33.1	72.9	174.
	1.5	1.5	9.26	4.20	12.7	.22	60.1	1.0	164.	33.1	2.47	208.	40.0	52.9	126.
		2	9.19	3.74	9.81	.87	53.6	1.0	126.	30.8	2.77	178.	32.7	43.3	103.
50.	1.5	1	9.05	2.44	4.01	1.75	36.2	0.1	76.1	7.7	2.72	118.	53.9	49.5	103.
		1.5	9.02	2.26	2.76	2.12	27.7	0.1	51.3	6.6	3.56	85.5	42.4	38.9	81.1
	2	1	9.13	2.86	6.80	1.01	49.5	0.1	131.	9.3	1.99	183.	58.3	71.3	149.
		1.5	9.07	2.54	4.69	1.56	40.0	0.1	89.5	8.2	2.46	135.	44.9	55.0	115.
		2	9.04	2.38	3.60	1.87	33.6	0.1	67.9	7.4	2.93	108.	37.7	46.1	96.1
	2.5	1	9.20	3.40	10.2	.22	59.8	0.1	199.	10.5	1.65	268.	63.4	97.0	202.
		1.5	9.13	2.90	7.06	.94	50.4	0.1	136.	9.4	1.95	189.	47.9	73.3	153.
		2	9.09	2.65	5.42	1.36	43.7	0.1	104.	8.6	2.25	152.	39.7	60.8	127.

Table A28: Beam-Fueling Model, p_w = 1.0 MW/m^2 — Fixed Burn-up 20%

				Densities						Source				
P_t	q	β_θ	T_e (keV)	N_e (10^{13})	N_α (10^{12})	N_I (10^{12})	C_T	τ (s)	τ/τ_B	S (10^{11})	V_b (keV)	I (MA)	B_T (kG)	B_{max} (kG)
12.5	1.5	1	9.00	7.74	6.77	.88	.379	92.2	10.7	6.51	60.3	37.8	27.9	55.3
		1.5	9.01				.569		13.1		58.9	30.9	22.8	45.1
		2	9.02				.760		15.1		58.3	26.7	19.8	39.1
	2	1	8.98				.212		8.0		63.9	37.8	37.2	73.6
		1.5	9.00				.319		9.8		61.1	30.8	30.4	60.2
		2	9.01				.426		11.3		59.8	26.7	26.3	52.1
	2.5	1	8.95				.134		6.4		69.1	37.7	46.5	92.0
		1.5	8.98				.203		7.8		64.3	30.8	38.0	75.2
		2	8.99				.272		9.1		62.0	26.7	32.9	65.1
25.	1.5	1	9.01	6.38	5.59	.72	.161	112.	7.0	4.43	59.8	49.1	25.4	47.1
		1.5	9.01				.242		8.5		58.6	40.1	20.7	38.5
		2	9.02				.323		9.8		58.1	34.7	17.9	33.3
	2	1	8.99				.090		5.2		63.0	49.1	33.8	62.8
		1.5	9.00				.136		6.4		60.6	40.1	27.6	51.3
		2	9.01				.181		7.4		59.4	34.7	23.9	44.5
	2.5	1.5	8.98				.086		5.1		63.4	40.1	34.5	64.1
		2	9.00				.115		5.9		61.4	34.7	29.9	55.5
50.	1.5	1	9.01	5.29	4.63	.60	.068	135.	4.5	3.04	59.5	63.8	23.1	41.1
		1.5	9.02				.103		5.6		58.4	52.1	18.9	33.6
		2	9.02				.137		6.4		57.9	45.1	16.3	29.1
	2	2	9.01				.077		4.8		59.1	45.1	21.8	38.8

Table A29: Beam-Fueling Model, $p_w = 3.0$ MW/m^2 — Fixed Burn-up 20%

				Densities						Source				
P_t	q	β_θ	T_e (keV)	N_e (10^{14})	N_α (10^{13})	N_I (10^{12})	C_τ	τ(s)	τ/τ_B	S (10^{12})	V_b (keV)	I (MA)	B_T (kG)	B_{max} (kG)
12.5	1.5	1	9.00	1.85	1.62	2.10	.281	38.5	9.2	3.74	60.5	32.7	43.3	103.
		1.5	9.01				.423		11.3		59.0	26.7	35.3	84.4
		2	9.01				.564		13.0		58.4	23.1	30.6	73.1
	2	1	8.98				.157		6.9		64.4	32.7	57.6	138.
		1.5	8.99				.237		8.4		61.4	26.7	47.1	113.
		2	9.00				.316		9.8		60.0	23.1	40.8	97.5
	2.5	1	8.94			2.11	.100		5.5		70.1	32.7	72.0	172.
		1.5	8.97			2.10	.151		6.7		64.8	26.7	58.8	141.
		2	8.99			2.10	.202		7.8		62.4	23.1	51.0	122.
25.	1.5	1	9.00	1.51	1.32	1.71	.122	47.3	6.0	2.47	60.1	42.5	39.0	81.3
		1.5	9.01				.183		7.4		58.8	34.7	31.9	66.4
		2	9.02				.244		8.6		58.2	30.1	27.6	57.5
	2	1	8.98				.068		4.5		63.5	42.5	52.0	108.
		1.5	9.00				.102		5.6		60.8	34.7	42.5	88.5
		2	9.01				.137		6.4		59.6	30.1	36.8	76.7
	2.5	1	8.95				.043		3.6		68.4	42.4	64.9	135.
		1.5	8.98				.065		4.4		63.9	34.7	53.0	111.
		2	8.99				.087		5.1		61.7	30.0	45.9	95.8
50.	1.5	1	9.01	1.04	.914	1.18	.054	68.3	4.0	1.19	59.6	57.0	32.5	61.2
		1.5	9.01				.081		4.9		58.5	46.6	26.5	49.9
		2	9.02				.109		5.7		58.0	40.3	23.0	43.3
	2	1	8.99				.030		3.0		62.6	57.0	43.3	81.5
		1.5	9.00				.046		3.7		60.3	46.6	35.3	66.6
		2	9.01				.061		4.3		59.2	40.3	30.6	57.7
	2.5	1	8.96			1.19	.019		2.4		66.9	57.0	54.0	102.
		1.5	8.99			1.19	.029		3.0		62.9	46.5	44.2	83.2
		2	9.00			1.18	.039		3.4		61.1	40.3	38.3	72.1

Table A30: Beam-Fueling Model, $P_w = 6.0$ MW/m^2 — Fixed Burn-up 20%

				Densities						Source				
P_t	q	β_θ	T_e (keV)	N_e (10^{14})	N_α (10^{13})	N_I (10^{12})	C_T	τ (s)	τ/τ_B	S (10^{12})	V_b (keV)	I (MA)	B_T (kG)	B_{max} (kG)
12.5	1.5	1	9.00	3.26	2.85	3.69	.238	21.9	8.5	11.53	60.7	29.6	57.3	173.
		1.5	9.01			3.69	.358		10.4		59.2	24.2	46.8	142.
		2	9.01			3.69	.478		12.0		58.4	21.0	40.6	123.
	2	1	8.97			3.70	.133		6.3		64.8	29.6	76.4	231.
		1.5	8.99			3.69	.200		7.8		61.6	24.2	62.4	189.
		2	9.00			3.69	.268		9.0		60.2	20.9	54.1	164.
	2.5	1	8.94			3.70	.084		5.1		70.7	29.6	95.4	289.
		1.5	8.97			3.70	.128		6.2		65.2	24.2	78.0	236.
		2	8.99			3.69	.171		7.2		62.7	20.9	67.4	204.
25.	1.5	1	9.00	2.61	2.29	2.96	.101	27.3	5.5	7.41	60.2	38.8	51.3	123.
		1.5	9.01				.151		6.7		58.9	31.7	41.9	100.
		2	9.01				.202		7.8		58.2	27.5	36.3	86.8
	2	1	8.98				.056		4.1		63.8	38.8	68.4	164.
		1.5	9.00				.085		5.1		61.0	31.7	55.9	134.
		2	9.00				.113		5.8		59.8	27.5	48.4	116.
	2.5	1	8.95			2.97	.036		3.3		70.0	38.8	85.4	204.
		1.5	8.98			2.96	.054		4.0		64.2	31.7	69.8	167.
		2	8.99			2.96	.072		4.7		62.0	27.5	60.5	145.
50.	1.5	1	9.00	2.13	1.86	2.41	.043	33.5	3.6	4.92	59.8	50.5	46.3	96.6
		1.5	9.01				.065		4.4		58.6	41.2	37.8	78.9
		2	9.02				.087		5.1		58.0	35.7	32.8	68.3
	2	1	8.98				.024		2.7		63.0	50.5	61.8	129.
		1.5	9.00				.036		3.3		60.5	41.2	50.4	105.
		2	9.01				.049		3.8		59.4	35.7	43.7	91.1
	2.5	1	8.96			2.42	.015		2.2		67.5	50.4	77.1	161.
		1.5	8.98			2.41	.023		2.6		63.3	41.2	63.0	131.
		2	8.99			2.41	.031		3.1		61.3	35.7	54.6	114.